CR-174914
FR-18683-2
JANUARY 1987

NASA

BREADBOARD RL10-IIB LOW THRUST OPERATING MODE FINAL TEST REPORT

CONTRACTS NAS3-24238
NAS3-22902

Prepared for
National Aeronautics and Space Administration
Lewis Research Center
21000 Brookpark Road, Cleveland, Ohio 44135

Prepared by
Pratt & Whitney
Government Products Division
P.O. Box 2691, West Palm Beach, Florida 33402

UNITED TECHNOLOGIES

6085M
Printed in the United States of America

CR-174914
FR-18683-2
JANUARY 1987

NASA

BREADBOARD RL10-IIB LOW THRUST OPERATING MODE FINAL TEST REPORT

CONTRACTS NAS3-24238
NAS3-22902

Prepared for
National Aeronautics and Space Administration
Lewis Research Center
21000 Brookpark Road, Cleveland, Ohio 44135

Prepared by
Pratt & Whitney
Government Products Division
P.O. Box 2691, West Palm Beach, Florida 33402

UNITED TECHNOLOGIES PRATT&WHITNEY

1. Report No. NASA CR-174914	2. Government Accession No.	3. Recipient's Catalog No.

4. Title and Subtitle
Report of Preliminary Low-Thrust Testing of the RL10-IIB Breadboard Engine

5. Report Date
January 1987

6. Performing Organization Code

7. Author(s)
Thomas D. Kmiec
Donald E. Galler

8. Performing Organization Report No.
FR-18683-2

10. Work Unit No.

9. Performing Organization Name and Address
Pratt & Whitney Government Products Division
P.O. Box 109600
West Palm Beach, Florida 33410-9600

11. Contract or Grant No. NAS 3-22902
NAS 3-24238

13. Type of Report and Period Covered
Topical, 24 Feb thru 29 Feb 1984

12. Sponsoring Agency Name and Address
National Aeronautics and Space Administration
Lewis Research Center
21000 Brookpark Rd
Cleveland, Ohio 44135

14. Sponsoring Agency Code

15. Supplementary Notes
Program Technical Monitor: Richard L. DeWitt
RL10 Program Manager: James A. Burkhart

16. Abstract

Cryogenic space engines require a cooling process to condition engine hardware to operating temperature before start. This can be accomplished most efficiently by burning propellants that would otherwise be dumped overboard after cooling the engine. The resultant low thrust operating modes are called Tank Head Idle and Pumped Idle.

During February 1984, Pratt & Whitney conducted a series of tests demonstrating operation of the RL10 rocket engine at low thrust levels using a previously untried hydrogen/oxygen heat exchanger.

This report describes the initial testing of the RL10-IIB Breadboard Low Thrust Engine. The testing demonstrated operation at both tank head idle and pumped idle modes.

17. Key Words (Suggested by Author(s))	18. Distribution Statement
RL10 Rocket Liquid Rocket Multi-Mode Thrust, Low Thrust Cryogenic Rocket	

19. Security Classif. (of this report)	20. Security Classif. (of this page)	21. No. of Pages	22. Price*
UNCLASSIFIED	UNCLASSIFIED	80	

*For sale by the National Technical Information Service, Springfield, Virginia 22161

PREFACE

During February 1984, Pratt & Whitney (P&W) conducted a series of tests demonstrating operation of the RL10 Hydrogen/Oxygen Rocket Engine at reduced thrust levels using a unique and previously untried Hydrogen/Oxygen heat exchanger concept to simplify the engine and improve performance at low thrust. Although this initial test series was limited in scope, the concept was proven; an important step has been taken for Advanced Space Vehicles.

Space engines using cryogenic propellants require a cooling process to condition the engine to operating temperature before start. This process has previously been accomplished by flowing propellants through the engine and overboard, an extremely inefficient method. As an alternative, the concept demonstrated herein permits burning of these propellants, whether supplied as gases, liquid/gas mixtures or liquids, while providing significant useful thrust for settling propellants to the vehicle tank exit; (typically space vehicles are operating at a zero gravity condition). Auxiliary propulsion systems are currently required to perform this function. This low thrust level is called the tank head idle operating mode.

Following a period of conditioning at tank head idle, the engine is thermally ready to start; however, high performance rocket engine propellant pumps require net positive suction pressure to prevent cavitation. This is currently accomplished by low performance auxiliary boost pumps or vehicle tank pressurization systems using a pressurizing gas such as helium. The improved scheme permits operation at a low thrust level of approximately 10 percent (called pumped idle) with liquid propellants but net positive suction head is not required because the pumps are operating at low speed. In this mode the engine can supply propellants at pressure and temperature conditions which can be used to pressurize the vehicle tanks, thus eliminating the boost pumps or auxiliary pressurizing system. The engine may be operated in this mode as required for vehicle maneuvering, deployment of payloads where low "g" is desired to minimize payload structural impacts, or for tank pressurization prior to acceleration to full thrust.

The test series demonstrated operation at both tank head and pumped idle modes. The heat exchanger eliminates an active engine control system and improves engine performance by optimizing propellant injection velocities into the combustion chamber.

CONTENTS

SECTION I
INTRODUCTION

This report describes the initial testing of the RL10-IIB Breadboard Low Thrust engine. The background for engine configuration can be found in Reference 1, "Design and Analysis Report for the RL10-IIB Breadboard Low Thrust Engine," 12 December 1984. This testing was accomplished in February 1984 under contract NAS3-22902.

SECTION II
OBJECTIVE

The objective of this test series was to establish the feasibility of the Oxidizer Heat Exchange (OHE) at Tank Head Idle (THI) and 10 percent thrust Pumped Idle (PI) operating conditions. The transient operation at start and from THI to PI was also to be evaluated. Information from this test series will be used to provide input for improved designs prior to further low thrust testing.

SECTION III
CONFIGURATION

The configuration of the RL10-IIB breadboard engine was intended to be as described in Reference 1, however, fabrication problems with portions of the OHE made modifications necessary. The OHE was designed to limit heat transfer to the oxidizer during THI and PI to avoid unstable boiling which would occur if the liquid oxygen was heated rapidly. A system which incorporated two low heat transfer rate stages (i.e., stages 1 and 2) and one high rate unit (i.e., stage 3) was designed. Problems with the braze of the low rate units made them unavailable in time to support the required test date. An alternate approach, which employed only the high rate unit (i.e. stage 3), was selected. To damp flow oscillations expected as a result of unstable boiling in the high heat transfer rate third stage, a damper volume was installed in the flowline downstream of the unit. The final engine configuration is shown in Figure 1.

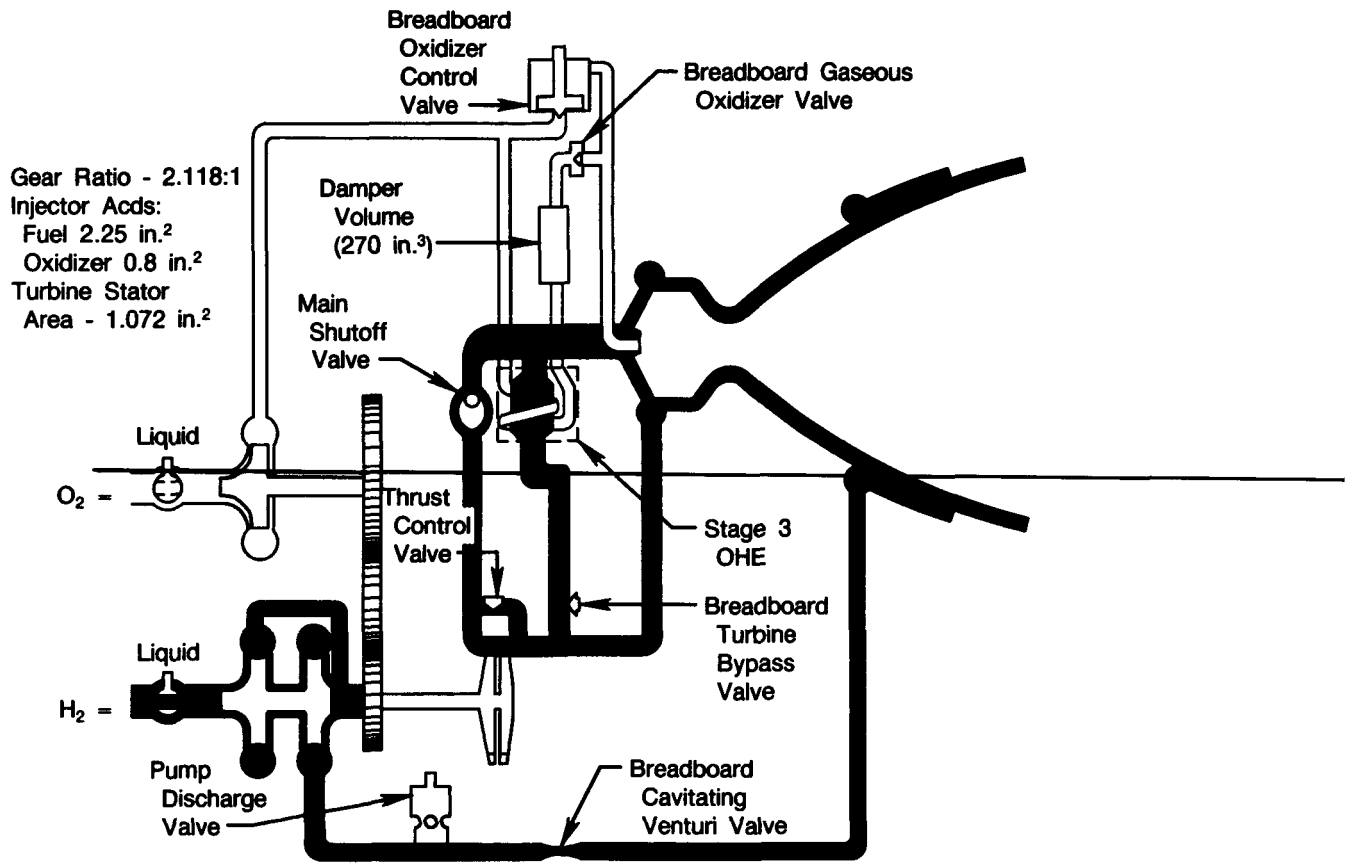

Figure 1. Breadboard RL10-IIB Engine Flow Schematic

The engine was an RL10A-3-3A model with the following major changes:

1. Oxidizer Heat Exchanger (OHE) added
2. Four hydraulically actuated valves added

    a. Gaseous Oxidizer Valve (GOV)
    b. Oxidizer Control Valve (OCV)
    c. Cavitating Venturi Valve (CVV)
    d. Turbine Bypass Valve (TBV)

3. Pump gear ratio changed
4. Single bearing idler gear incorporated
5. Injector with higher flow faceplate
6. Dual ignition systems with a Torch Igniter
7. Reduced area turbine stators
8. No Interstage Cooldown Valve
9. Modified Pump Discharge Valve

The engine buildup was completed on 17 February 1984 and was sent to Test Stand E-6 for testing. Photos taken of the engine prior to sending it to the test stand are shown in Figures 2 through 5. A description of the engine components can be found in Appendix A, and the Oxidizer Heat Exchanger in Appendix B.

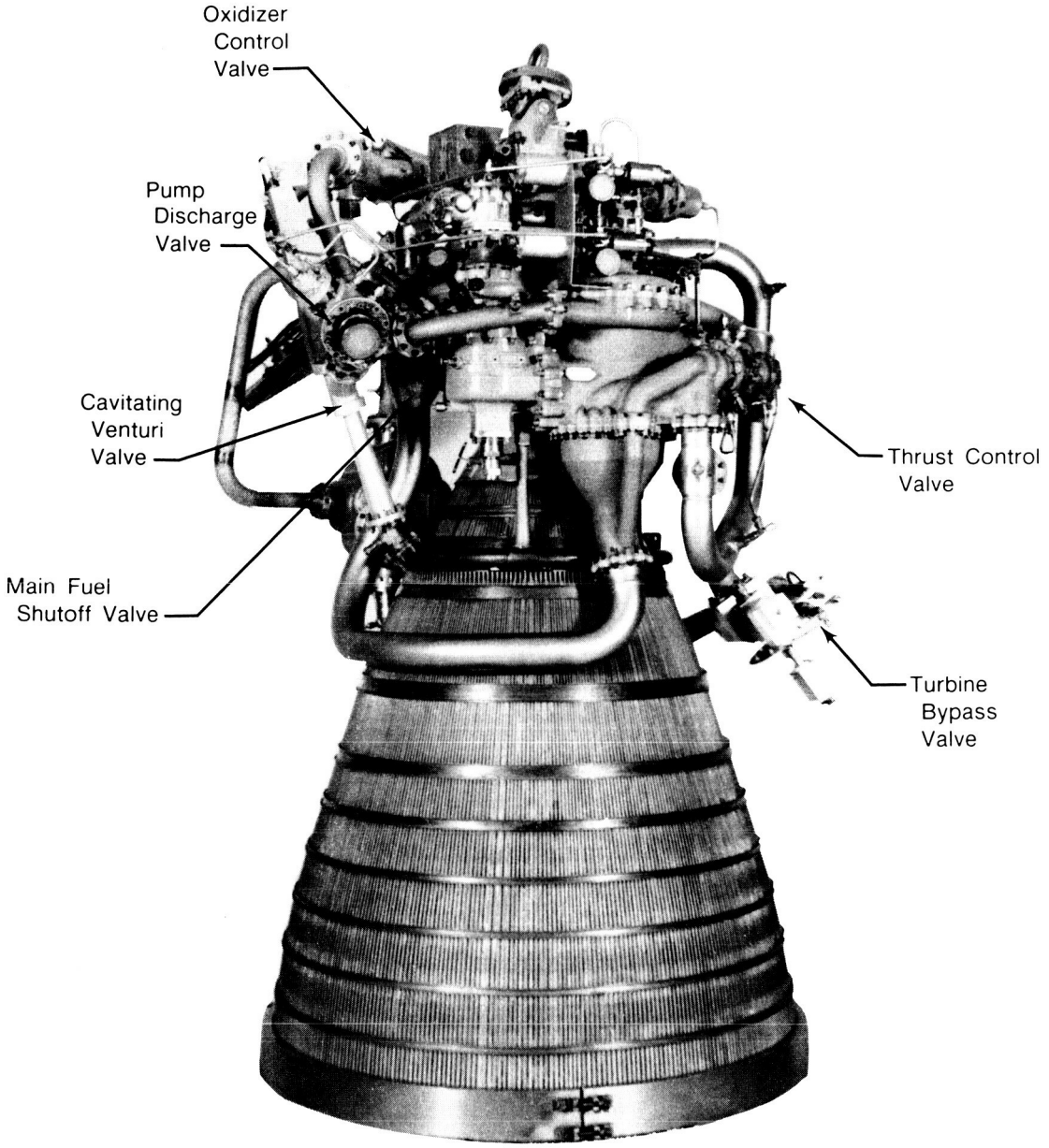

Figure 2. Breadboard Engine XR201-1 View 1

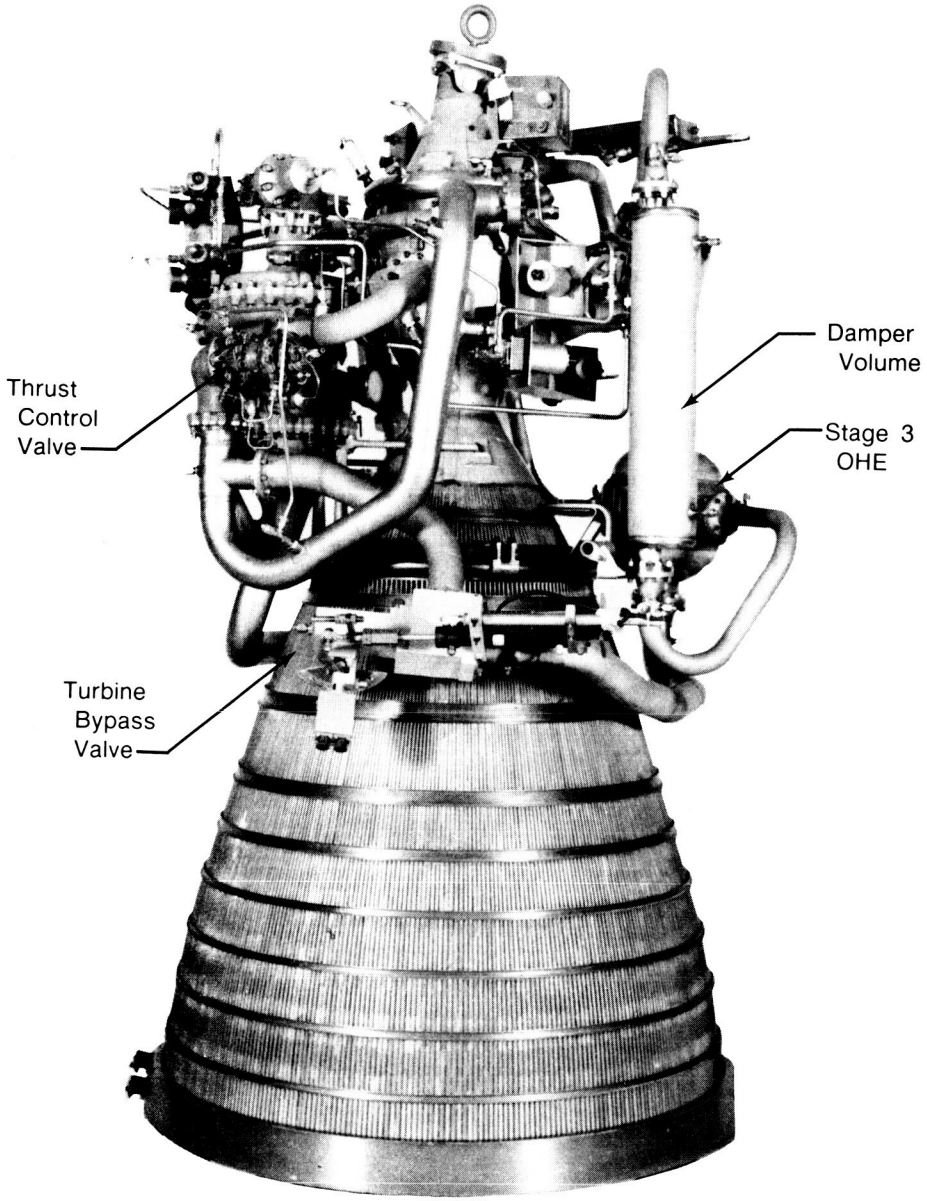

FD 311717

Figure 3. Breadboard Engine XR201-1 View 2

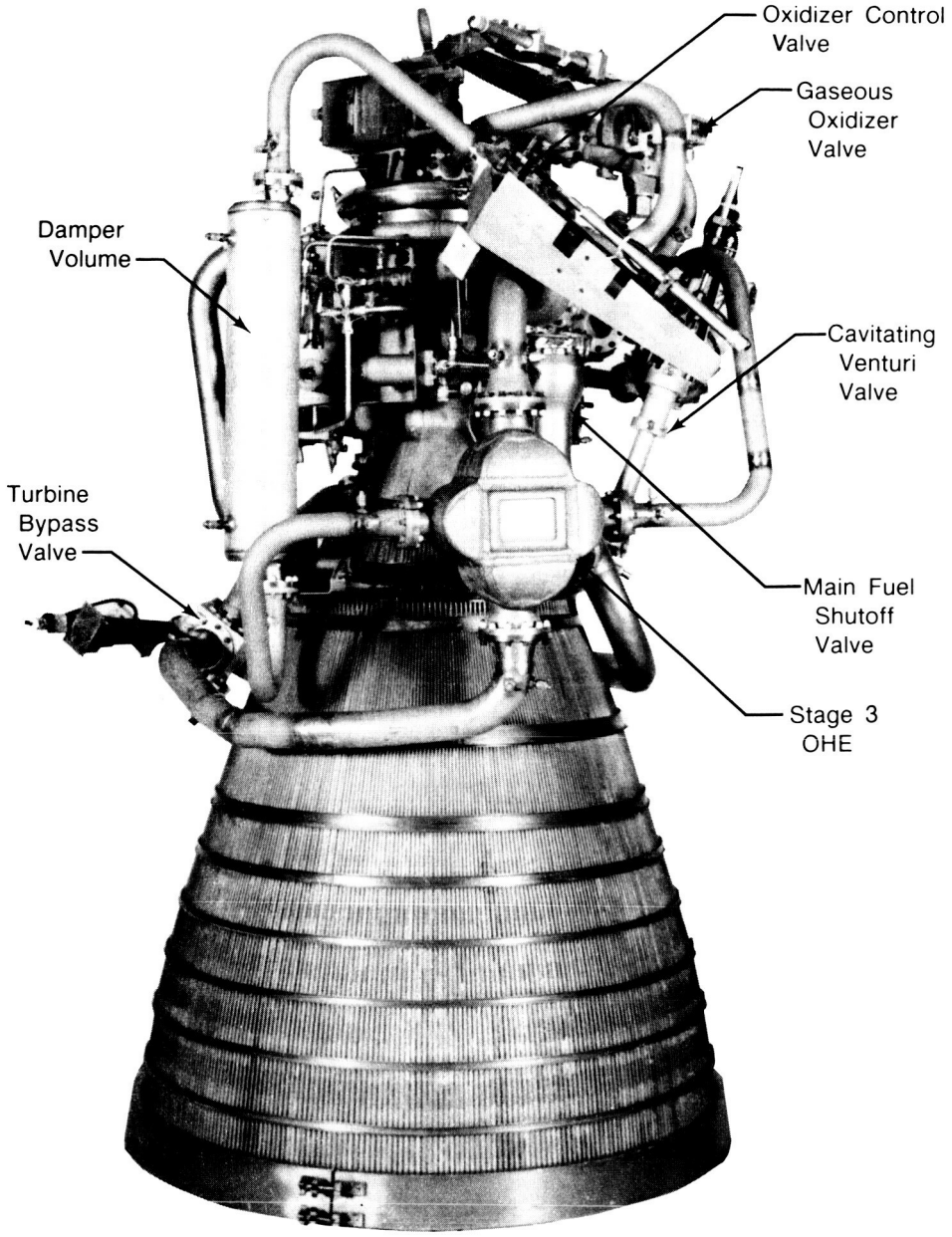

FD 311718

Figure 4. Breadboard Engine XR201-1 View 3

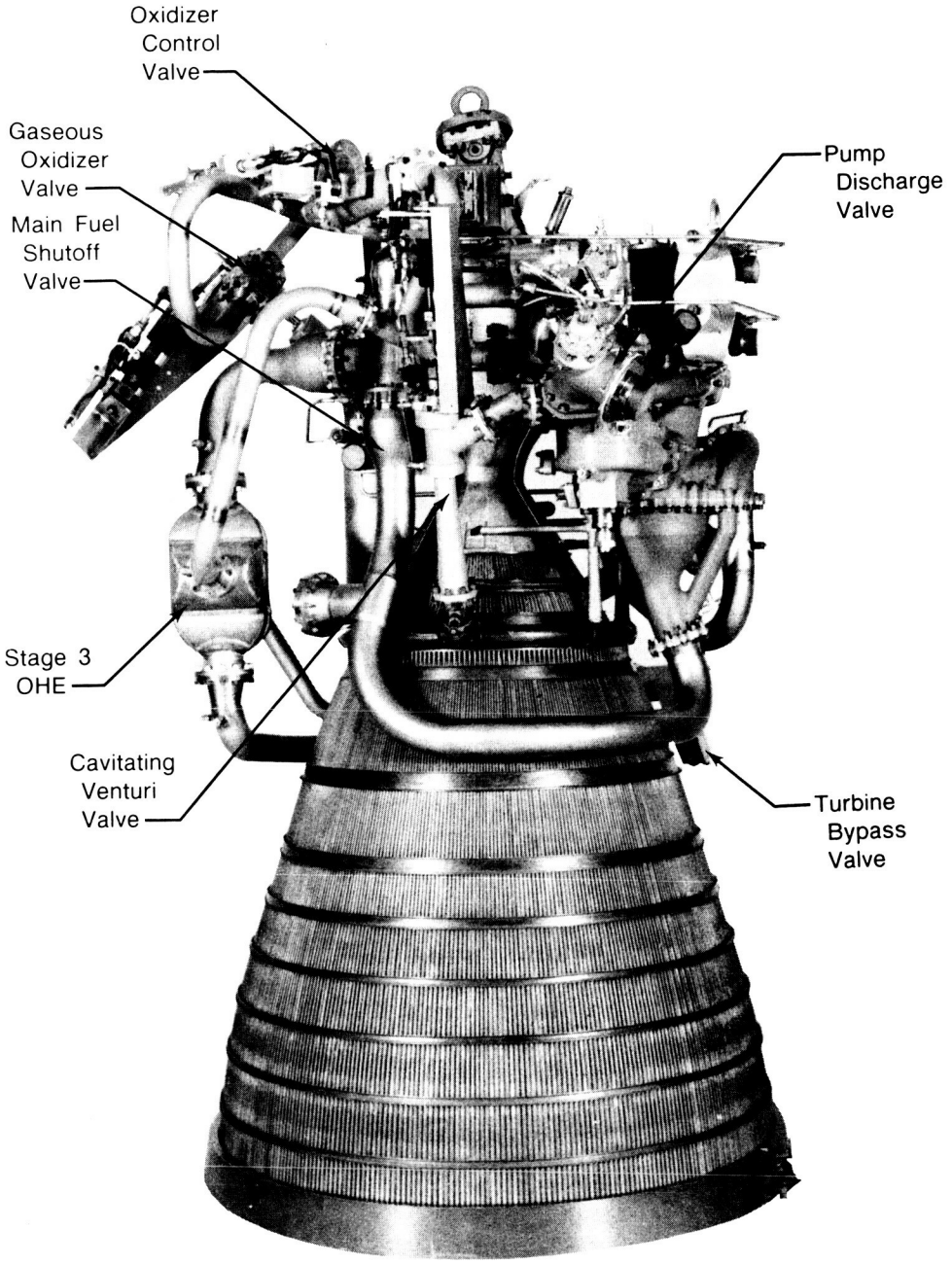

Figure 5. Breadboard Engine XR201-1 View 4

SECTION IV
TESTING ACTIVITY OVERVIEW

Engine XR201-1 was sent to Test Stand E-6 on 17 February 1984. Photos of the engine mounted in the test stand are shown in Figures 6 and 7. Testing commenced on 24 February and fifteen firings were accomplished before the testing activity was completed on 29 February.

During this test series, 1651.2 seconds of run time were accumulated at Tank Head Idle (THI). The THI starts were approximately as predicted (see Section VI) although a change in the Gaseous Oxidizer Valve setting was required to accommodate the OHE characteristics. Fourteen starts were made with liquid at both pump inlets, and one start was accomplished with gas at both inlets. A detailed description of the objective and results of each run can be found in Appendix C.

Transition to Pumped Idle (PI) was successfully accomplished during six firings. A total of 1342.1 seconds were accumulated at PI. The transition to PI, however, required modifications to a preplanned valve sequence to account for OHE characteristics encountered.

The facility operated as expected during the testing. The hydraulic control system installed for the RL10-IIB breadboard testing provided good control and allowed flexibility for valve positioning and PI transition scheduling. The design flight representative point inlet pressures of 20 psia were not run during this test series. Instead, engine operation was investigated with the propellant inlet conditions achievable on the E-6 test stand (Fuel Pump Inlet Pressure (FPIP) = 25 psia, Oxidizer Pump Inlet Pressure (OPIP) = 33 psia). Installation of an oxidizer tank at the engine level prior to the next test series will eliminate the excess head pressure which prevented setting low inlet pressures during this series.

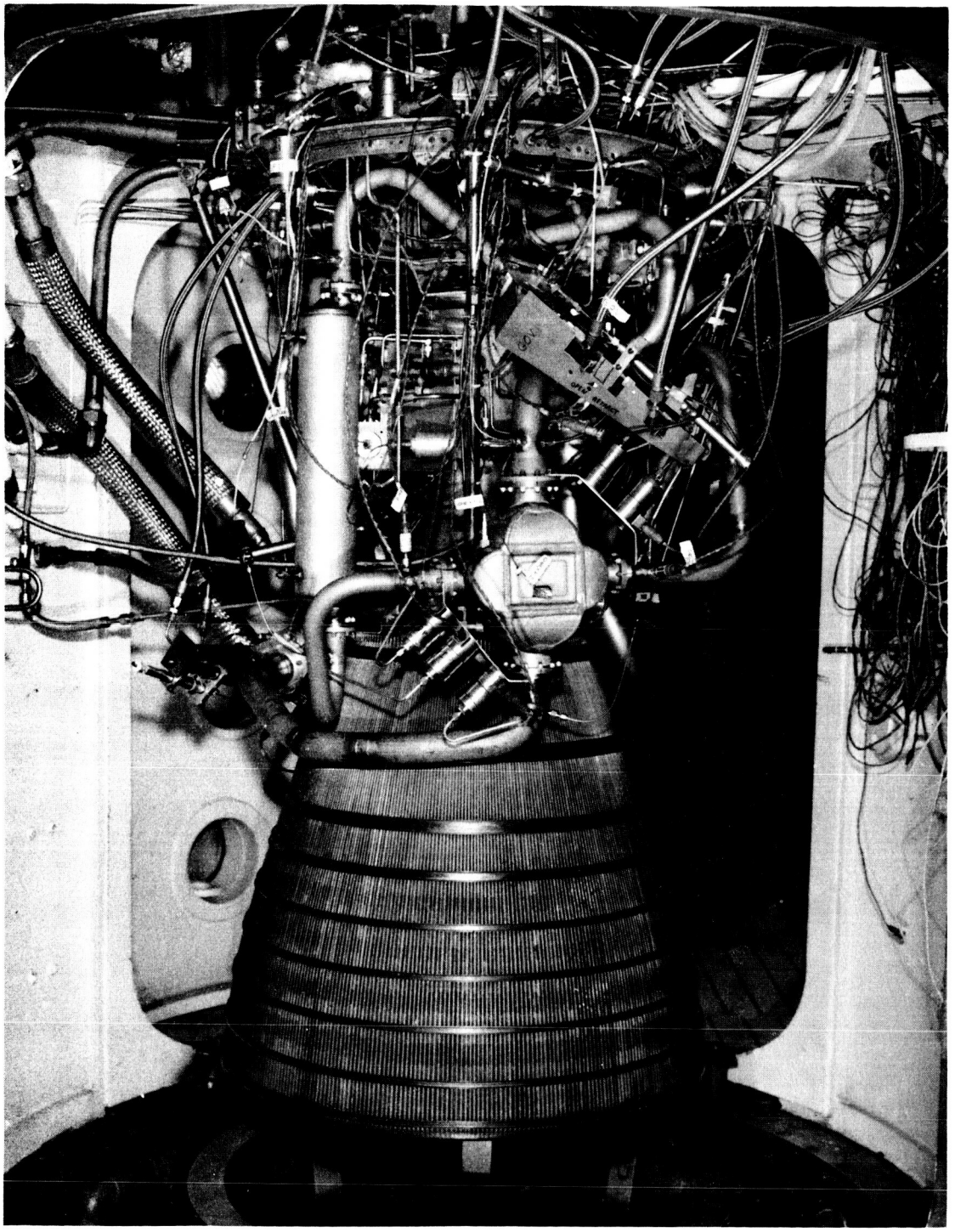

FE 357307-2

Figure 6. Breadboard Engine XR201-1 in Test Stand E-6

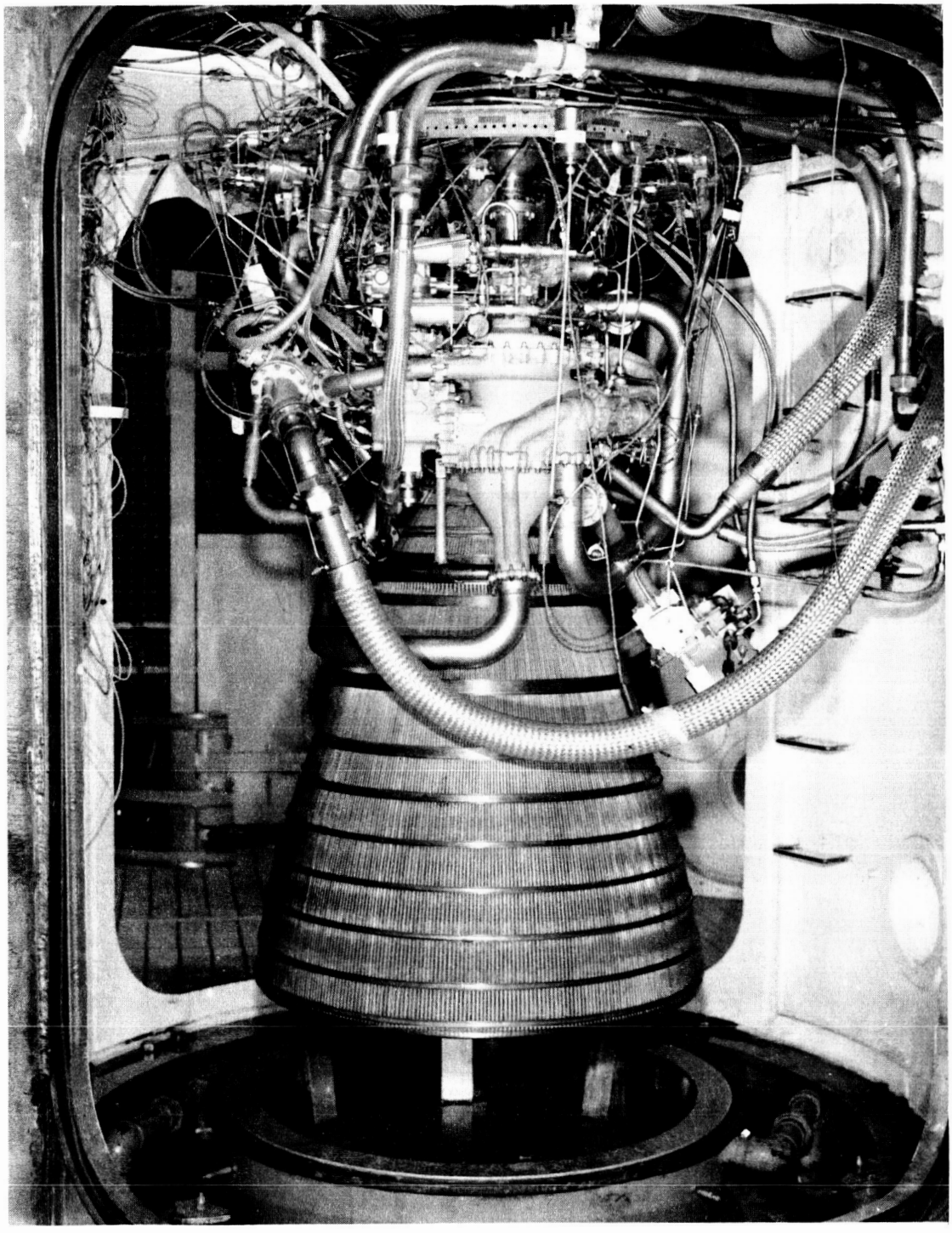

FE 357307-4

Figure 7. Breadboard Engine XR201-1 in Test Stand E-6

SECTION V
OVERALL TEST RESULTS

SUMMARY

Chamber/nozzle heat transfer at the low thrust levels was characterized and oxidizer heat exchanger performance (e.g., heat transfer and pressure losses) was calculated. Heat exchanger induced flow oscillations were examined both with and without a downstream damper volume installed. The start transient and the transient from THI thrust to PI thrust were defined. Engine performance and pump operation were calculated at pumped idle. The following summarizes the RL10-IIB Breadboard Demonstrator engine initial test results.

1. Chamber/nozzle heat transfer was significantly higher than predicted at low mixture ratios. At a mixture ratio of 6.0, heat transfer was 5 percent higher than predicted while at 4.0 mixture ratio it was approximately 40 percent higher.

2. Oxidizer heat exchanger performance was not as expected with heat transfer 10 percent to 50 percent below predicted values. Additionally, the fuel side pressure losses were five to nine times higher than predicted and the oxidizer side pressure losses were up to six times higher than predicted.

3. The heat exchanger induced chamber pressure oscillations were ± 1.0 psi during THI operation (Pc $\approx$ 9 psia), but this level is unlikely to be of significance in a vehicle system. At PI thrust (Pc $\approx$ 40 psia), with the volume installed, oscillations were intermittent and low in amplitude (± 2 psi). With the volume removed, the oscillations became regular and increased in amplitude (± 6 psi).

4. Specific impulse at PI thrust was within 2.5 percent of predicted. (Specific impulse at THI could not be accurately determined due to inaccurate thrust measurements at this level, and because the nozzle was not flowing full.)

5. The high fuel pressure loss of the OHE caused the turbopumps to prematurely begin rotation during the THI to PI transition.

6. The higher flow injector faceplate caused uneven hydrogen flow distribution resulting in poor propellant mixing and local hot spots at the injector face.

Detailed discussion of the test results and analysis can be found in Appendix D.

SECTION VI
COMPUTER SIMULATION ANALYSIS SYNOPSIS

PRE-TEST

Prior to this initial test series of the RL10-IIB Preliminary Breadboard Demonstrator Engine, an analysis effort was undertaken to accurately predict engine operation with only the Stage 3 OHE. This analysis was used as the basis for proceeding with the proposed test program. Both the steady state and transient computer simulations as described in Ref. 1 were modified to include the hardware conditions to be used during the test (RL10A-3-3A thrust chamber/nozzle, stage 3 OHE, high propellant pump inlet pressures, etc.). Also, based on the oxygen side pressure oscillations experienced during 1975 testing of a breadboard heat exchanger, and on Reference 2, a computer program was written and used to predict oscillations which would occur with the Stage 3 OHE.

The computer simulation was used to predict the transients to THI and PI and to set the breadboard valve positions for the first engine firings. It was also used to establish the valve sequencing that was used for the first attempted transitions to PI.

From the oscillation prediction program described in Appendix E, it was recommended that the volume be installed downstream of the OHE. The prediction indicated that this would damp the oscillations to an acceptable level.

POST-TEST

After the test data analysis for engine XR201-1 was completed, the results were incorporated into both the steady state and transient computer simulation to improve their usefulness as prediction tools for future testing.

The correlations which were established during the testing were incorporated into the computer simulation and cycle analysis was performed. With these modifications, the predicted steady state parameters agreed closely with those measured at THI. At PI, the fuel side prediction agreed closely with the test data, but the oxidizer side differed slightly.

The transient simulations were also modified based on actual test results. The predicted transient from start to THI does not compare well with the actual test results due to the difficulty of simulating the heat input to the pumps. It is felt that the prediction would be closer to the actual if an insulating blanket was installed to limit this heat input. The transient from THI to PI predicted with the modified program, however, did agree closely with the actual test results. The transient was simulated with both the original valve schedule and the final valve schedule, and both agreed well with the test results.

The computer simulation appears to be an effective tool in the prediction of both steady state and transient performance, although the THI transient prediction needs further modification to account for heat input to the pumps. The data generated during this test series provided correlations which were useful in modifying the programs to provide accurate predictions. These programs will be useful in predicting required valve areas and system performance for future test runs.

Further discussion of the programs and specific modifications to them can be found in Appendix E. This appendix also addresses the program used to predict the oscillations due to boiling in the OHE.

SECTION VII
CONCLUSIONS

1. The Oxidizer Heat Exchanger is effective for providing acceptable engine performance at low thrust levels without an active control system.

    a. The Stage 3 Oxidizer Heat Exchanger provided acceptable stability at Tank Head Idle.

    b. The Stage 3 Oxidizer Heat Exchanger with a downstream volume provided acceptable stability at Pumped Idle.

2. The high fuel pressure drop at the Oxidizer Heat Exchanger needs to be reduced to provide better THI to PI transient control.

3. Modifications to the computer simulation analysis program, based on test results, improved its usefulness as a prediction tool for further work.

4. Test stand modifications made to support this test series were effective in providing flexibility for testing.

SECTION VIII
RECOMMENDATIONS

1. Switch to a lower flow injector faceplate for the next test series to provide better distribution of hydrogen and help eliminate the center hot spot on the injector.

2. The heat exchangers tested should be flowed and physically examined to determine why heat transfer was lower and pressure losses were higher than predicted. The prediction programs should then be modified as required.

3. The high pressure loss of the OHE needs to be lowered to the original design specification to provide better THI to PI transient control.

REFERENCES

1. FR-18046-3 (CR-174857), *Design and Analysis Report for the RL10-IIB Breadboard Low Thrust Engine,* 12 December 1984.

2. R. S. Thurston and J. D. Rogers, *Advances in Cryogenic Engineering, Vol. 12,* Plenum Press, New York (1967), p.438.

APPENDIX A
COMPONENT AND ENGINE CONFIGURATION

The majority of the components were obtained from engines used during RL10 low thrust testing which was conducted during the 1960s. The following sections describe the components used in the buildup of the breadboard RL10-IIB demonstrator engine XR201-1.

FUEL PUMP AND TURBINE ASSEMBLY

The Fuel Pump and Turbine was baseline RL10A-3-3A. The majority of the parts were obtained from development engine P641904 which was built as an RL10A-3-7 in 1967. This assembly included the following:

1. A new gear was provided to increase the Oxidizer Pump speed. The shaft assembly was obtained by installing the new gear onto an existing shaft. The gear ratio (Fuel Pump to Oxidizer Pump) was changed from 2.500:1 for RL10A-3-3A Bill-of-Material (B/M) to 2.118:1.

2. The lower 1st Turbine Stator flow area was obtained by installing 10 additional plugs into a reduced area stator. This stator had an area reduction of 10 percent from the RL10A-3-3A B/M prior to installing the plugs. Water flows on G-13 test bench showed an effective area of 1.072 $in.^2$ or a total reduction of 22 percent from the B/M RL10A-3-3A.

3. The 2nd stator also had a reduced area. This stator was obtained from development engine FX141-45, which was built as an RL10A-3-7 in 1966, and had an effective area of 1.471 $in.^2$ versus 1.9 $in.^2$ for the RL10A-3-3A.

4. The exit stator was also from FX141-45 and included a cone shaped exit shroud designed to reduce the discharge housing pressure losses.

Turbopump build, rotor balance, pressure test and seal flows were accomplished per standard RL10 procedures.

OXIDIZER PUMP AND GEARBOX ASSEMBLY

The Oxidizer Pump and Gearbox Assembly were baseline RL10A-3-3A with most parts obtained from P641904. The following describes the major differences:

1. A new gear was provided to incorporate the 2.118:1 gear ratio. An existing shaft was utilized, a new gear installed, and the bearing seat machined. This shaft assembly also incorporated a short accessory drive coupling to allow installation of a speed transducer at the accessory pad.

2. A single bearing idler gear was used per layout L-238361. The new gear was required to incorporate the ratio change. The single bearing feature, tested during the 1960s, was used to reduce gear wear due to housing misalignment.

3. The elbow housing was modified to accept the single bearing configuration and the 2.118:1 idler gear.

The pump was built and seals were flow tested per standard RL10 procedures.

TURBOPUMP ASSEMBLY

The turbopump assembly consisted of the above Fuel Pump and Oxidizer Pump and was assembled per B/M RL10A-3-3A procedures.

FUEL VENT VALVE

The Fuel Vent Valve (FVV) is based on the RL10A-3-3A Pump Discharge Cooldown Valve. The only purpose of this valve, however, is to provide venting of fuel following engine shutdown. The valve ports are enlarged to provide additional flow area, since there is no Interstage Cooldown Valve. The effective vent flow area for this valve is 0.510 $in.^2$, compared to 0.300 $in.^2$ for the RL10A-3-3A valve. Because the valve is required to open rapidly at shutdown from any thrust level, the signal pressure for opening is provided by helium, rather than hydrogen from the fuel pump discharge. This latter pressure would be insufficient to provide the required boost at Tank Head Idle or Pumped Idle shutdown. A calibration was performed on this valve prior to installing it on the engine. This valve was obtained from engine P641904.

TURBINE BYPASS VALVE

The Turbine Bypass Valve (TBV) was obtained from P641904. The valve was cleaned and a gaseous nitrogen flow calibration was performed prior to installation on the engine. The effective area versus valve position is shown in Figure A-1.

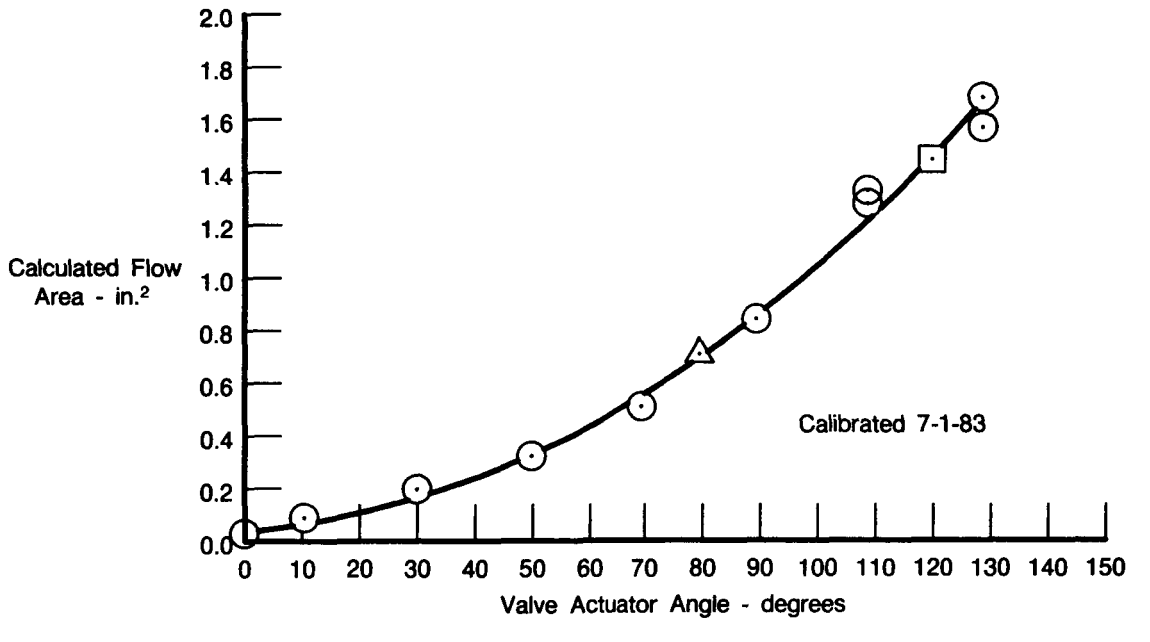

Figure A-1. Turbine Bypass Valve S/N CKD 1188

OXIDIZER CONTROL VALVE

The Oxidizer Control Valve was obtained from P641904. This valve was cleaned and a liquid nitrogen calibration was performed on G-1 test stand. The effective area versus valve position is shown in Figure A-2.

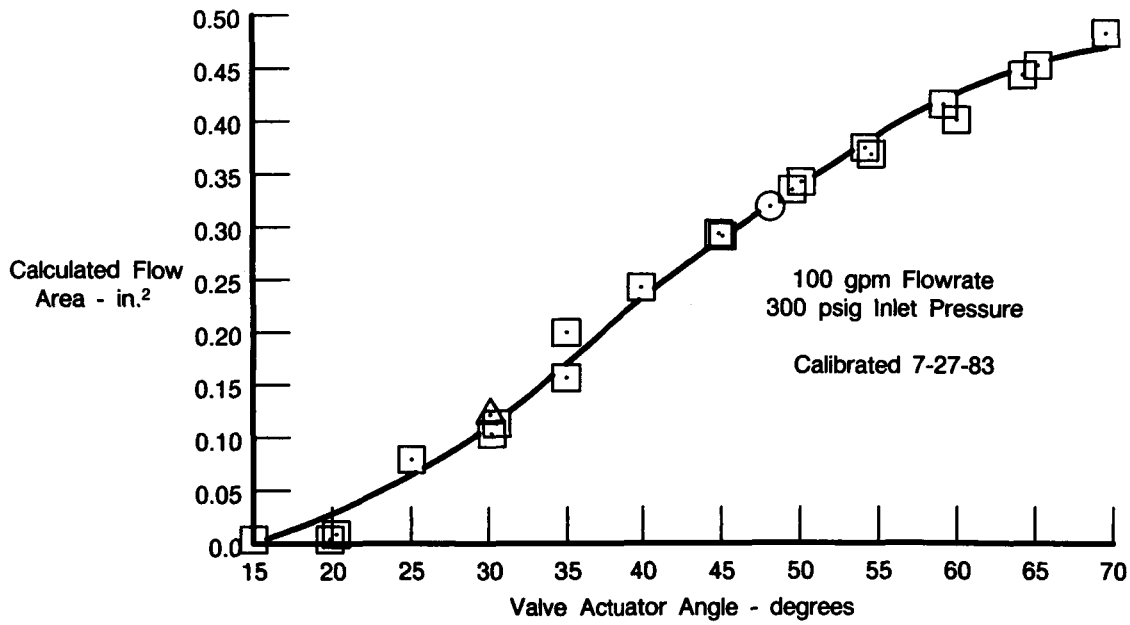

Figure A-2. Oxidizer Control Valve S/N 600090

CAVITATING VENTURI VALVE

The Cavitating Venturi Valve (CVV) was obtained from P641904. Calibration data from 1967 was available and no new calibration was performed. The effective area versus valve position is shown in Figure A-3.

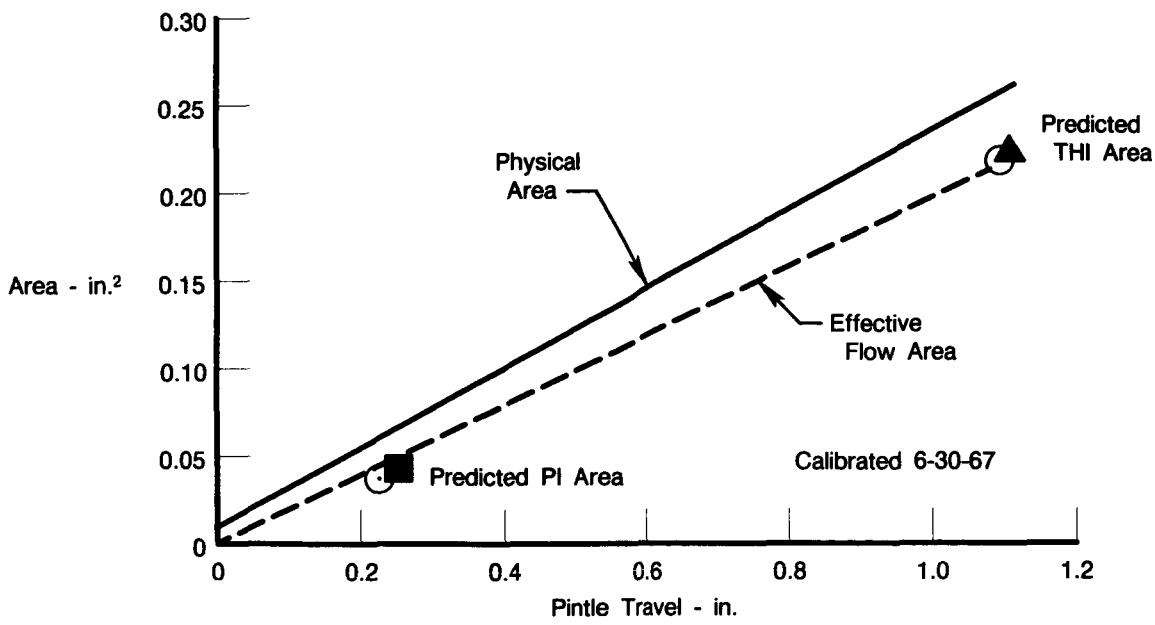

Figure A-3. Cavitating Venturi Area S/N B54X-012

GASEOUS OXIDIZER VALVE

The Gaseous Oxidizer Valve (GOV), was obtained from RL10 Used Stores. Similar valves had been used in the 1960s as throttle valves for oxidizer and fuel. Calibration curves were available for this valve and a new calibration was not performed. The effective area versus valve position curve that was used is shown in Figure A-4.

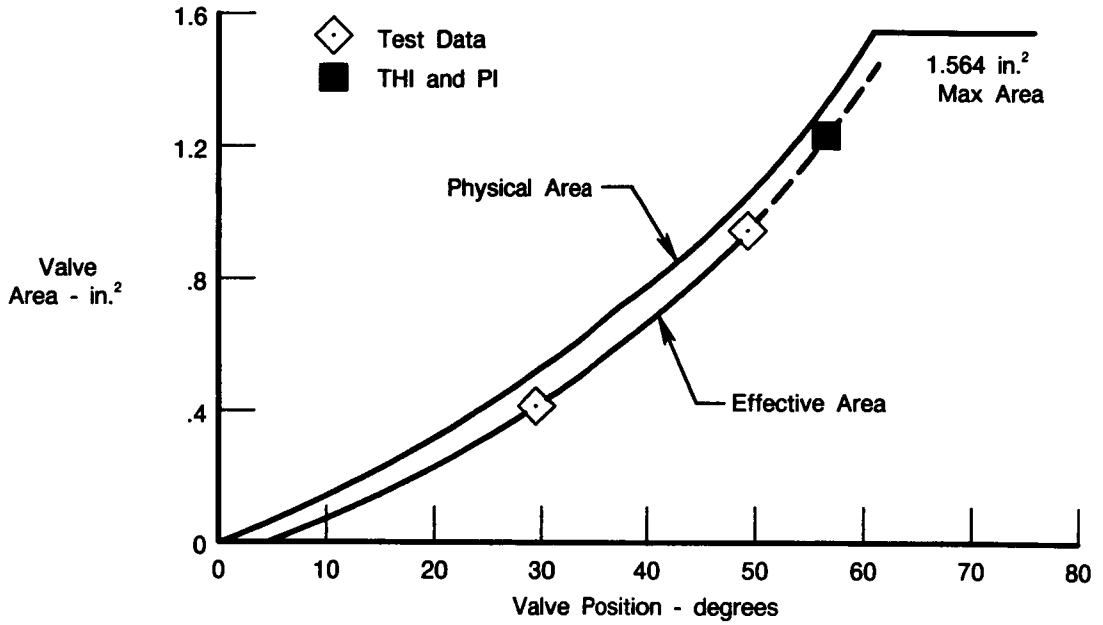

Figure A-4. Gaseous Oxidizer Valve S/N CKD 1311

IGNITION SYSTEM

The system used to ignite the propellants consisted of two spark ignition systems, each similar to that used for the RL10A-3-3A integrated with a torch igniter housing. Hydrogen and oxygen are supplied to the torch igniter housing and this mixture is then ignited by the spark igniters. The resulting "torch" then ignites the propellants in the combustion chamber. The spark ignition systems and torch igniter housing were obtained from engine P641904. This system was developed in the 1960s to provide reliability as well as redundancy for safe repeatable propellant ignition in the combustion chamber.

CHAMBER

The chamber is a "hook tube" design which is intended to reduce the chance of creating tube socket leaks by locating these joints away from the combustion area. This is the same joint design that will be used for the new primary nozzle for the RL10-IIB. The difference between this joint design and the RL10A-3-3A is shown in Figure A-5. The chamber had no silver throat insert as is used on the RL10A-3-3A.

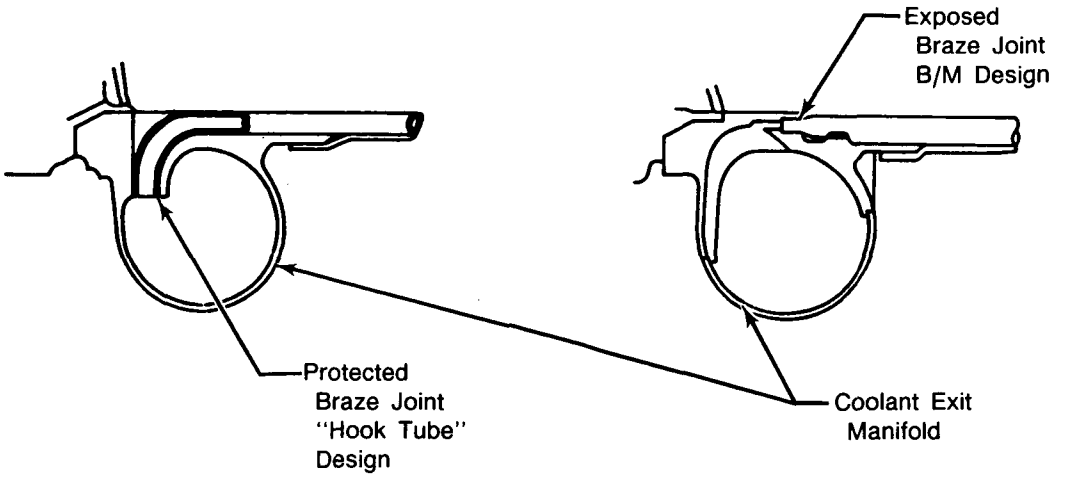

Figure A-5. Thrust Chamber Exit Manifold Differences

INJECTOR

The injector for this build was obtained from P641904 and had a new rigimesh faceplate installed for this testing. It was baseline RL10A-3-3A except that the rigimesh had a 250 scfm flow instead of the 120 scfm flow for the RL10A-3-3A. This was done to provide more coolant flow through the face with the low differential pressures at THI and PI. The injector also had a provision for installation of the torch igniter sleeve and a flame detector probe. Gaseous nitrogen flows indicated an effective area of 0.760 $in.^2$ for the oxidizer side and 3.048 $in.^2$ for the fuel side. The hydrogen side effective area for the RL10A-3-3A is 2.25 $in.^2$

THRUST CONTROL

The thrust control was RL10A-3-3A configuration, but was not required to be functional for the THI and PI thrust levels. Because of this, a chamber pressure sensing line was not connected to it, nor was the restrictor assembly connected to the engine. A line from turbine upstream pressure was connected to the servo supply fitting to prevent any differential pressure across the bypass valve allowing the internal spring to keep it closed during engine operation.

MISCELLANEOUS COMPONENTS

The solenoid valves, shutoff valves, and inlet valves were all RL10A-3-3A configuration. All completed calibrations prior to engine installation. A prelaunch cooldown valve was installed on the engine, but was used only to provide a path for coolant flow from the fuel pump to the gearbox during engine operation.

PLUMBING

Plumbing from engine P641904 was used where possible. New large plumbing was fabricated by piecing together bends and flanges. All new welds were X rayed and fluorescent penetrant inspected. All new tubes were pressure checked to 1000 psig.

HYDRAULIC ACTUATORS

Hydraulic actuators were installed to control the position of the four breadboard valves. The actuators included linear position pots to supply a signal for the control system. Brackets for the TBV, OCV, and CVV were obtained from engine P641904. The GOV bracket was obtained from storage.

GIMBAL

The gimbal was obtained from FX141-45 and included bracketing to allow mounting of the two spark ignition systems.

OXIDIZER HEAT EXCHANGER

Only the last stage of the originally intended three-stage heat exchanger was used in this test series. This high heat transfer rate unit employed a crossflow design. A description of this unit and discussion of its fabrication can be found in Appendix B.

DAMPER VOLUME

A volume of approximately 270 $in.^3$ was installed downstream of the OHE on the oxidizer side. The intent of the volume was to damp oscillations induced by unstable boiling of the liquid oxygen in the high heat transfer Stage 3 heat exchanger.

APPENDIX B
OXIDIZER HEAT EXCHANGER

The stage 3 Oxidizer Heat Exchanger unit (OHE) used for this test series was an aluminum, cross flow unit designed for high heat transfer and low pressure drop. The flow passages were created by chemically etching grooves into aluminum panels. These panels were then stacked in a cross flow arrangement and brazed together to form the heat exchanger core. Fluxless aluminum brazing was used to avoid entrapment of any salts that would be expected if the less difficult dip braze method was used. A description of the core, as designed, is shown in Figure B-1.

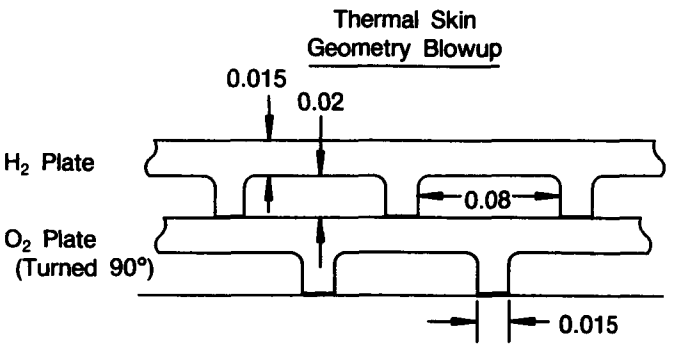

Geometry

	H_2 Plate	O_2 Plate
No. Plates	87.0	86.0
Passage Diameter, in.	0.0336	0.0336
Flow Area, in.^{2}	6.475	5.180
Heat Transfer Area, ft^2	21.3	
Core Weight, lb	19.3	

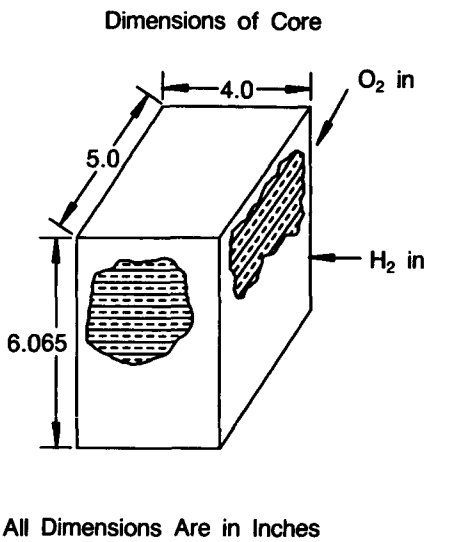

FDA 308207

Figure B-1. Stage 3 OHE Core Design Features

Two Stage 3 units were fabricated, however, both were found to have considerable cross circuit leakage. This was due to a leak path created by diffusion of silicon from the braze filler material into the aluminum alloy parent material. An attempt to eliminate this leakage was made by welding passages closed on each face. This procedure did eliminate many of major leaks, but numerous smaller leaks remained. It was felt that continuing weld repair would result in an unusable unit, due to extensive blockage.

A method was developed to impregnate the cores with a sealant to fill the paths created by the diffusion. Dura-Seal, Type C was selected for use since it was the only sealant that could be found that was compatible with liquid oxygen. The sealant was introduced into the oxidizer circuit while the hydrogen circuit was evacuated. After the oxidizer circuit was filled, it was pressurized to 100 psig with gaseous nitrogen. This pressure/vacuum was held for one hour. Additionally, heat lamps were placed on either side to warm the core and allow further penetration of the sealant. A schematic for the impregnation rig is shown in Figure B-2. This technique was successful in virtually eliminating the numerous small leaks caused by silicon diffusion. The remaining larger leaks were repaired by injecting the sealant into individual core passages to plug them.

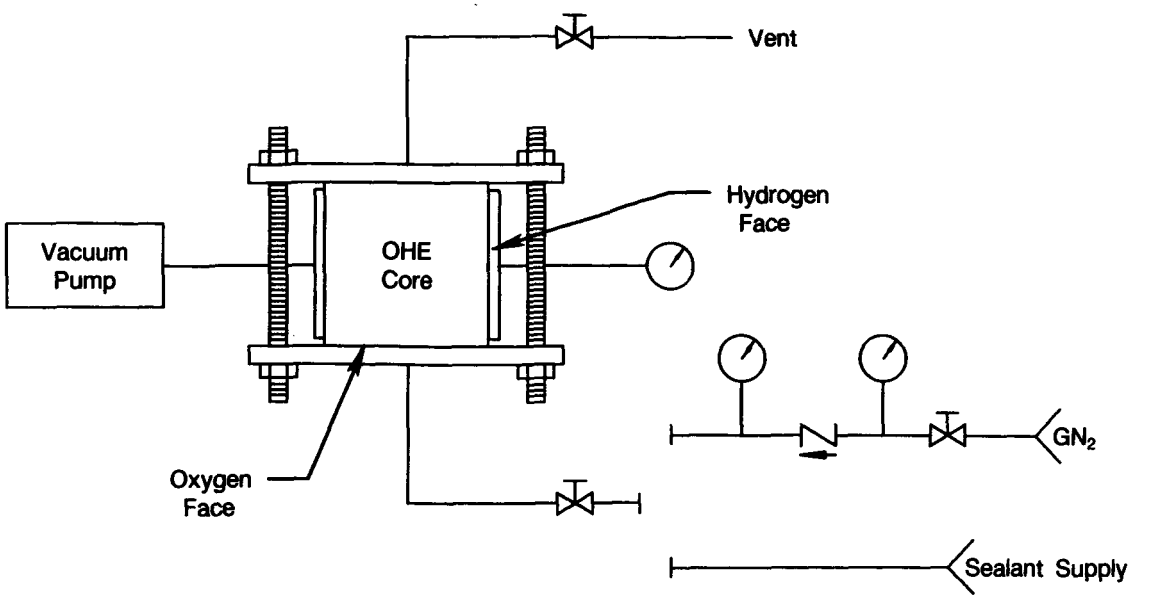

Figure B-2. OHE Core Impregnation Rig Schematic

This impregnation/injection method was used for both cores. The assembled heat exchangers were then impregnated a second time following installation of the manifolds. Serial number 002 was selected for initial test since it had the least weld repair and the fewest plugged passages. Cross circuit leakage on this unit was reduced from 2300 sccm of gaseous helium at 50 psid to virtually zero.

The units were proof tested to 200 psig rather than the target design proof pressure of 1500 psig because of concerns with the structural integrity of the braze joints due to the extensive silicon diffusion.

Photographs of the Stage 3 OHE are shown in Figure B-3.

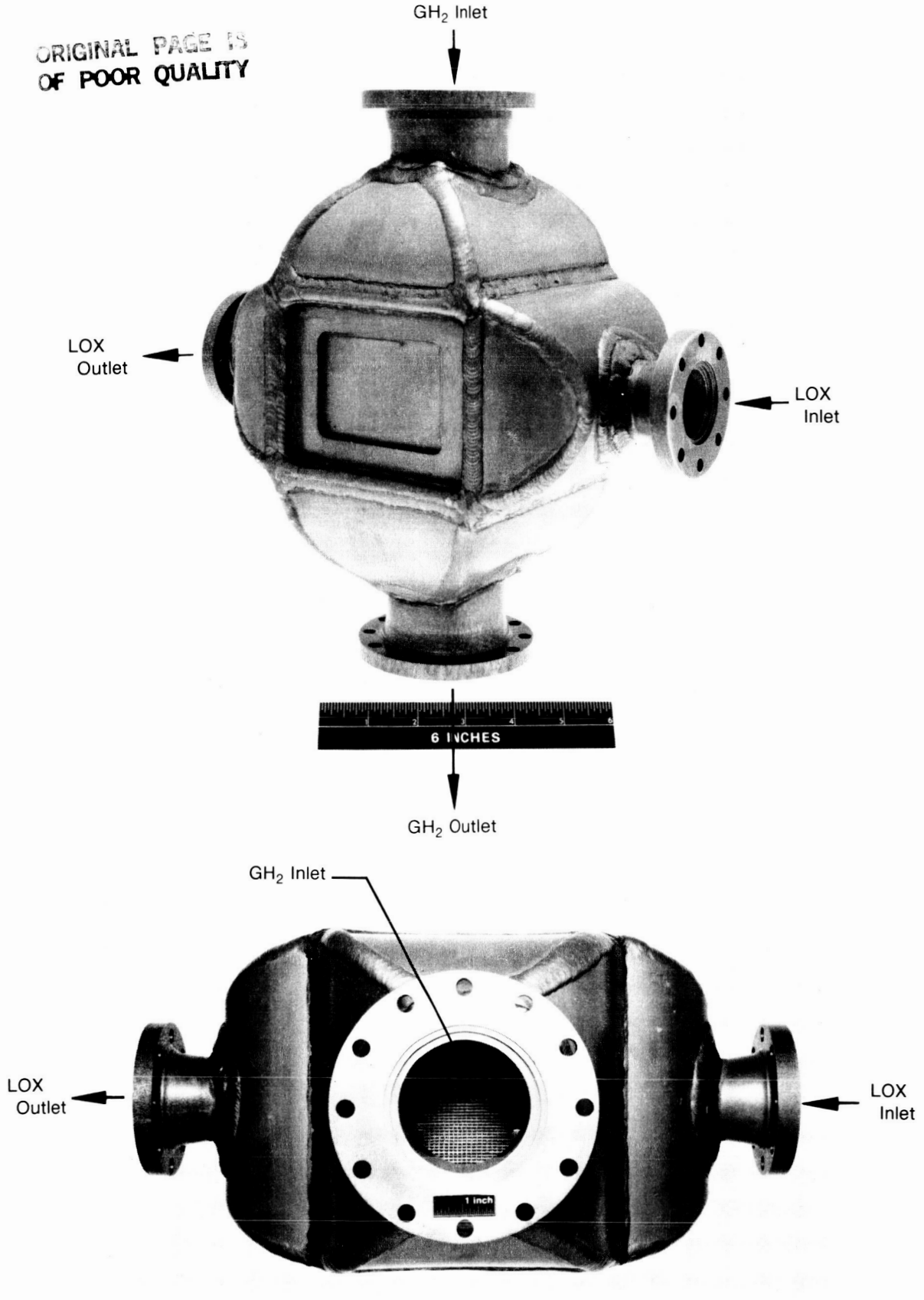

FD 311720
FD 311721

Figure B-3. Stage 3 Oxidizer Heat Exchanger

APPENDIX C
ENGINE RUN SUMMARY

Engine XR201-1 completed fifteen firings during this test program. A test summary is shown in Table C-1. A description of each run follows:

The objective of test No. 1.01 was to start and run at THI. A total of 162.0 seconds were accumulated at THI prior to a false automatic abort due to a malfunction of the "watchdog" timer which monitors the hydraulic valve scheduler. Adjustment of the Gaseous Oxidizer Valve (GOV), to reduce the mixture ratio and decrease the combustion temperature, was started prior to the abort. Post-run inspection showed discoloration of the injector face and several chamber leaks in the thrust chamber coolant tubes and between the tubes probably due to the high mixture ratio at engine start. This run demonstrated that the engine would start and run with the OHE, but indicated a need for a change in the GOV preset position due to the OHE characteristics.

The objective of test No. 2.01 was to evaluate THI operation at various mixture ratios. There was a false Flame Detector abort after 24.2 seconds of run time. The GOV area at start was reduced for this run to lower the mixture ratio and avoid further damage to the injector and chamber. An engine start was again accomplished, but it appeared that the GOV area needed further reduction due to high hydrogen temperature indicated at the chamber jacket discharge.

The objective of test No. 3.01 was the same as for test 2.01. A diffuser pressure abort occurred at 2.9 seconds. It appeared that the engine had late ignition causing a pressure spike in the diffuser to trigger the abort. The GOV area at start was again reduced, and this may have caused the late light.

The objective of test No. 4.01 was the same as for test 2.01. A THI run for 331.3 seconds duration was accomplished. The GOV was returned to the starting position of run 2.01 to avoid the late ignition. During this run, mixture ratio excursions were performed using the GOV and the fuel inlet pressure. The run was terminated due to depletion of steam required for the test stand ejector. The test demonstrated acceptable THI stability with the Stage 3 OHE unit over a range of various mixture ratios. The high jacket discharge temperature experienced during the short 2.01 test was seen again; however, this appears to have been a transient rise only and the temperature dropped to an acceptable range during steady state operation.

The objective of test No. 5.01 was to demonstrate a transition to PI. A total of 133.4 seconds were accumulated at THI prior to attempting the transition to PI. The pumps oversped during the transition causing a high OHE oxidizer inlet pressure abort. During the transition, the Turbine Bypass Valve (TBV) was closed and held closed momentarily to provide a temporary high turbine differential pressure to overcome the breakaway torque. The overspeed appeared to be due to leaving the TBV closed too long during the transition.

The objective of test No. 6.01 was to demonstrate a transition to PI. A total of 129.5 seconds were accumulated at THI, prior to attempting the transition. As during test 5.01, there was an overpressure abort due to pump overspeed. The closed dwell time for the TBV had been reduced to 0.100 second from 0.200 second during run 5.01. The GOV was opened during THI in an attempt to increase combustion chamber pressure, increasing turbine backpressure to reduce the overspeed when the transition to PI was attempted. This test indicated that another change in the valve schedule was necessary.

Table C-1. XR201-1 Test Summary

Run No.	Date	Hot Time (sec)	ACCUM Hot Time (sec)	THI Time (sec)	PI Time (sec)	Run Summary	Valve Areas — ACD (in^2) THI GOV Initial/Final	THI DCV	THI CVV	THI TBV	PI GOV Initial/Final	PI TBV	PI CVV Initial/Final
1.01	2-24-84	162.0	162.0	162.0	0	Achieved THI start. Had false "watchdog timer" abort while closing the GOV to reduce O/F.	0.50/0.53	0	0.22	1.400	N/A	N/A	N/A
2.01	2-25-84	24.2	186.2	24.2	0	Achieved THI start. Had false flame detector abort prior to making any engine control adjustments.	0.34	0	0.22	1.400	N/A	N/A	N/A
3.01	2-26-84	2.9	189.1	2.9	0	Had high diffuser pressure abort due to spike in diffuser pressure Possibly due to late light.	0.20	0	0.22	1.400	N/A	N/A	N/A
4.01	2-27-84	331.3	520.4	331.3	0	Achieved THI start. Performed mixture ratio excursion with GOV and fuel inlet pressure. S/D due to steam depletion.	0.30/0.18	0	0.22	1.400	N/A	N/A	N/A
5.01	2-27-84	136.3	656.7	133.4	2.9	Achieved THI start. Had high heat exchanger 0_2 inlet pressure abort due to pump overspeed during transition to PI.	0.30/0.20	0	0.22	1.400	0.20	1.40	0.05
6.01	2-27-84	131.1	787.8	129.5	1.6	Achieved THI start Reduced TBV closed time during PI transition from 0.200 to 0.100 sec and manually opened to GOV prior to PI transition. Had same overspeed and abort as 5.01.	0.30/0.34	0	0.22	1.400	0.34	1.40	0.05
7.01	2-28-84	92.2	880.0	90.3	1.9	Achieved THI start, closed TBV to 35% with no hold during PI transition. GOV same as 6.01. Had overspeed and abort same as 6.01.	0.30/0.34	0	0.22	1.400	0.34	1.40	0.05
8.01	2-28-84	131.4	1011.4	105.0	26.4	Achieved THI start. Did not close TBV during PI transition. GOV same as 7.01. FVV opened prior to PI transition. Had overspeed and OHE overpressure abort when FVV was closed.	0.30/0.34	0	0.22	1.400	0.34	1.40	0.05
9.01	2-28-84	89.9	1101.3	85.9	4.0	Achieved THI start. Repeated 8.01 PI transition, had flame detector abort at 4.0 sec into PI, possibly due to lower CVV area.	0.30/0.34	0	0.22	1.400	0.34	1.40	0.038

Table C-1. XR201-1 Test Summary (Continued)

Run No.	Date	Hot Time (sec)	ACCUM Hot Time (sec)	THI Time (sec)	PI Time (sec)	Run Summary	Valve Areas — ACD (in^2) THI GOV Initial/Final	THI DCV	THI CVV	THI TBV	PI GOV Initial/Final	PI TBV	PI CVV Initial/Final
10.01	2-29-84	600.1	1701.4	86.9	513.2	Achieved THI start and transition to PI. CVV area increased to 8.01 level. FVV opened prior to PI transition, closed control valve down-stream of FVV to 6% after PI was achieved, then did GOV and CVV excursions.	0.30/0.34	0	0.22	1.400	0.34/0.36	1.40	0.05/0.034
11.01	2-29-84	219.5	1920.9	94.9	124.6	Achieved THI start and transition to PI. FVV opened prior to PI transition. Adjusted CVV while closing control valve downstream of FVV. Had fuel pump stall when control valve was completely closed.	0.30/0.34	0	0.22	1.400	0.34/0.36	1.40	0.05/0.025
12.01	2-29-84	161.6	2082.5	90.3	71.3	Achieved THI start. Transitioned to PI. FVV opened prior to PI transition. Set CVV at larger area than for 11.01 prior to closing FVV downstream control valve. Had fuel pump stall when FVV was closed.	0.30/0.34	0	0.22	1.4	0.34/0.36	1.40	0.05/0.043
13.01	2-29-84	340.5	2423.0	79.1	261.4	Achieved THI start. Transitioned to PI. FVV opened prior to PI transition. Opened GOV to raise Pc and lower rpm prior to closing FVV downstream control valve. Achieved PI with FVV closed, had fuel pump stall while reducing CVV area.	0.30/0.34	0	0.22	1.4	0.34/0.94	1.40	0.05/0.021
14.01	2-29-84	35.0	2458.0	35.0	0	Achieved THI start with gaseous propellants. Had flame detector abort at 35 sec.	0.30	0	0.22	1.4	N/A	N/A	N/A
15.01	2-29-84	535.3	2993.3	200.5	334.8	Achieved THI start and transitioned to PI same as 13.01. Performed mixture ratio excursions at both thrust levels.	0.30/0.34	0	0.22	1.4	0.34/0.91	1.40	0.05/0.038
				Σ=1651.2	Σ=1342.1								

6083M

The objective of test No. 7.01 was to demonstrate a transition to PI. A total of 90.3 seconds were accumulated at THI prior to the attempting the transition. The same overspeed and abort occurred as in tests 5.01 and 6.01. During this transition, the TBV was only partially closed, then immediately reopened, with no dwell time. The GOV was opened during THI as in test 6.01. This test indicated the TBV need not be closed at all since the high OHE pressure drop created a high turbine differential pressure to provide the necessary breakaway torque.

The objective of test No. 8.01 was to demonstrate a transition to PI. A total of 105.0 seconds were accumulated at THI prior to the transition. A successful transition to PI was accomplished by opening the Fuel Vent Valve (FVV) prior to the transition to reduce fuel flow through the engine. Additionally, the TBV was left open during the transition. Pump overspeed and the resulting overpressure abort occurred when the two-position FVV was closed after 26.4 seconds of PI. The test indicated that a transition to PI could be accomplished, however, a change in valve positions would be necessary to maintain PI due to the OHE characteristics.

The objective of test No. 9.01 was to demonstrate operation at PI. A total of 85.9 seconds were accumulated at THI prior to attempting the transition. Prior to this run a control valve was installed in the FVV stand dump line to allow slow reduction of the overboard flow in an attempt to eliminate the pump overspeed that occurred when the FVV was closed during test 8.01. Additionally, the Cavitating Venturi Valve (CVV) flow area during the transient to PI was reduced to cause higher pump backpressure. A flame detector abort occurred at 4.0 seconds into PI probably due to lower fuel flow resulting from the reduced CVV area. This test indicated that a change in the CVV area during the transition to PI was necessary to allow transition as during run 8.01.

The objective of test No. 10.01 was to demonstrate operation at PI. A total of 86.9 seconds were accumulated at THI prior to a 513.2 second run period at PI. The transition to PI was made by leaving the FVV open, the TBV open, and the CVV set at the area used for test 8.01. The control valve downstream of the FVV was closed to 6 percent of its area to increase chamber pressure following the transition. After achieving an acceptable chamber pressure, GOV and CVV excursions were performed. This test demonstrated operation at PI with the OHE, however, additional changes in valve positions would be necessary to allow complete closing of the FVV.

The objective of test No. 11.01 was to demonstrate PI operation with the FVV closed. The second OHE, S/N 001, was installed prior to this run. This OHE had more weld repairs on the core. A total of 94.9 seconds were accumulated at THI prior to a 124.6 second run period at PI. The transition was accomplished the same as for test 10.01. A fuel pump stall occurred when the control valve downstream of the FVV was completely closed. The CVV area had been reduced below the test 10.01 level to back pressure the fuel pump prior to closing the control valve. The stall was probably due to the low CVV area. This test demonstrated PI transition, but indicated that further changes in valve positions would be necessary to close the FVV without pump overspeed or stall.

The objective of test No. 12.01 was to demonstrate PI operation with the FVV closed. A total of 90.3 seconds were accumulated at THI prior to 71.3 seconds of run time at PI. Transition to PI was done as during test 11.01. The CVV area was increased above that used for test 11.01, however, a pump stall occurred when the flow from the FVV was terminated. This test indicated another valve position change was necessary to allow PI operation with the FVV closed.

The objective of test No. 13.01 was to demonstrate PI operation with the FVV closed. Prior to this run the damper volume downstream of the OHE was removed and replaced with a straight piece of tubing to check the effects of the volume on oscillation attenuation. A total of 79.01 seconds were accumulated at THI prior to 261.4 seconds of runtime at PI. The transition to PI was accomplished the same as during test 12.01. Following the transition to PI, the GOV was

opened to raise chamber pressure and reduce pump speed by backpressuring the turbine. The FVV was successfully closed after gradually reducing the overboard flow with the control valve. A fuel pump stall occurred while the CVV area was being reduced. The FVV remained closed until shutdown. This test demonstrated PI operation with the engine system closed, and allowed accurate performance measurements since all flow was directed through the engine.

The objective of test No. 14.01 was to accomplish start with gaseous propellants. The gaseous start was accomplished by cooling down the stand lines, then forcing the liquid out with purges and allowing the lines to warm up slightly. This technique provided liquid at the flowmeters to avoid damage due to overspeed from gas flow, while allowing the sections of line nearer the engine to contain gas. A successful start was made, however, a false flame detector abort occurred at 35.0 seconds. This test demonstrated that the engine would start and run with gaseous propellants as would be required during operation on a vehicle prior to complete propellant settling and duct cooldown.

The objective of test No. 15.01 was to evaluate operation at THI and PI. A total of 200.5 seconds were accumulated at THI during which time a mixture ratio excursion was performed. The transition to PI was accomplished as during test 13.01. A total of 334.8 seconds were accumulated at PI during which mixture ratio excursions were also performed. This test again demonstrated successful transition to PI and with the FVV closed provided data for performance evaluation at the engine of various mixture ratios.

APPENDIX D
TEST RESULTS AND DATA ANALYSIS

The following sections describe the results of the RL10-IIB breadboard engine test and the subsequent analysis of the data.

CHAMBER/NOZZLE HEAT TRANSFER

Chamber/nozzle heat transfer was measured at both THI and PI operating conditions. These measurements were compared to predicted values and the results are shown versus chamber pressure and mixture ratio in Figures D-1 and D-2. The percent predicted temperature rise does not correlate with chamber pressure but appears to correlate with mixture ratio. At a mixture ratio of 6.0, the measured heat transfer was within 5 percent of predicted but as mixture ratio decreased to 4.0, the heat transfer was as much as 40 percent above predicted. This could have been caused by the high flow (250 scfm) Rigimesh injector used. At lower mixture ratios the fuel flow is more critical and the high flow Rigimesh causes uneven flow distribution producing hot spots and higher heat transfer rates. In addition, the momentum ratio of the oxygen to the hydrogen was high due to the 2-phase oxygen at the injector and the larger fuel injector flow area. This results in poorer mixing of the propellants, leading to hot spots.

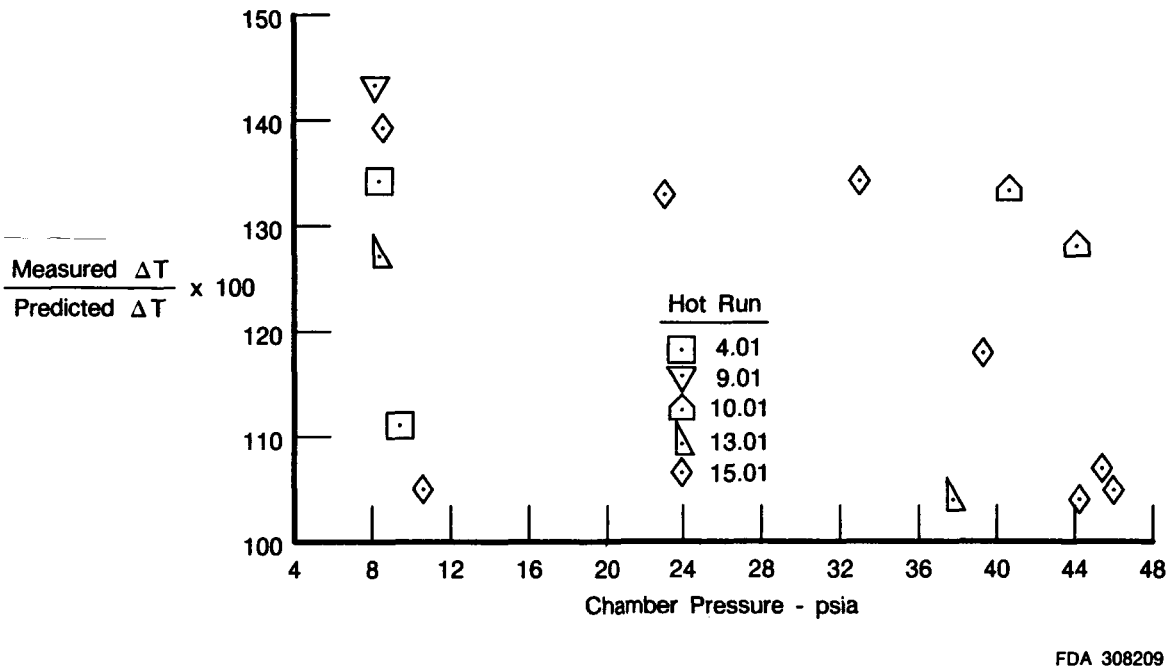

Figure D-1. Jacket Temperature vs Chamber Pressure

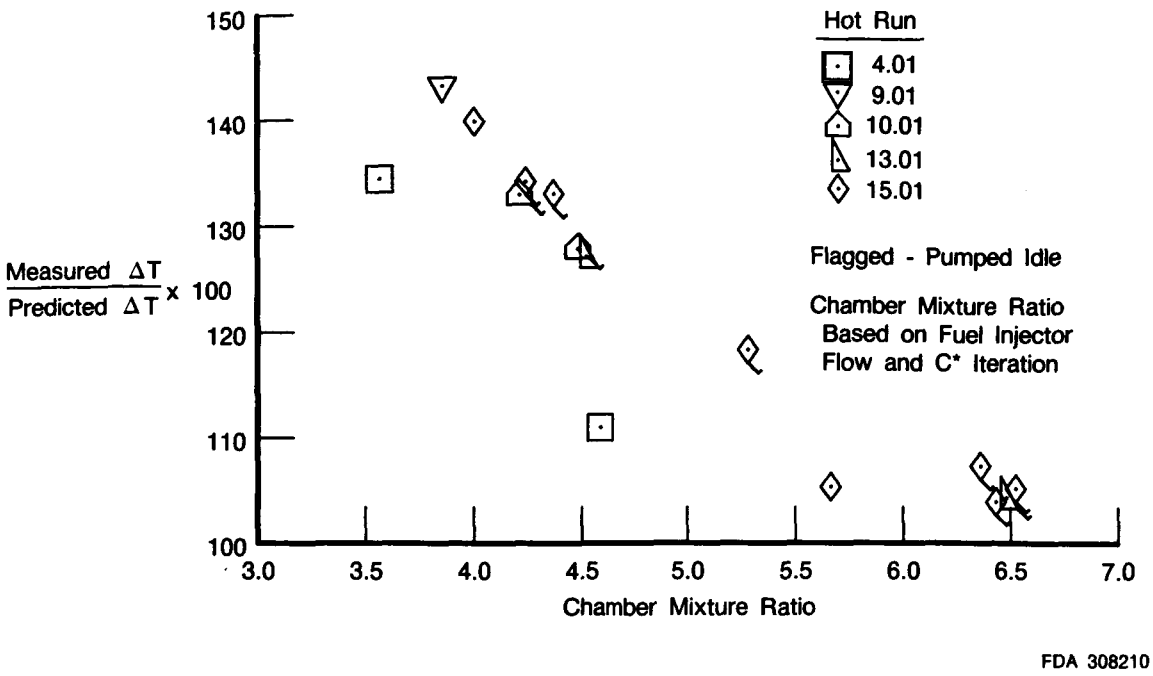

Figure D-2. Jacket Temperature vs Mixture Ratio

OXIDIZER HEAT EXCHANGER PERFORMANCE

Heat exchanger S/N 002 was used for the first ten tests, and heat exchanger S/N 001 was installed for runs 11.01 through 15.01. Heat transfer was lower than expected for both heat exchangers and is shown compared to that predicted versus chamber pressure and mixture ratio in Figures D-3 and D-4 respectively. The heat transfer calculated from measured parameters ranged from 10 percent to 50 percent of design values and does not correlate with either chamber pressure or mixture ratio. There was no significant difference in the heat transfer characteristics of the two heat exchangers. Figures D-5 through D-8 present pressure losses for each heat exchanger compared to predicted. Fuel side pressure losses were much worse than expected, from five to nine times predicted, and did not correlate with either chamber pressure or mixture ratio. Heat exchanger S/N 001 had lower fuel side pressure drop than heat exchanger S/N 002 at both THI and PI thrust levels. Oxidizer side pressure losses were approximately as predicted at THI, but increased to almost six times that of design at PI and correlated with chamber pressure due to the much higher oxidizer flow at the higher thrust level. Both heat exchangers had the same oxidizer side pressure loss characteristics and these losses would have been much higher had the predicted heat transfer levels been realized.

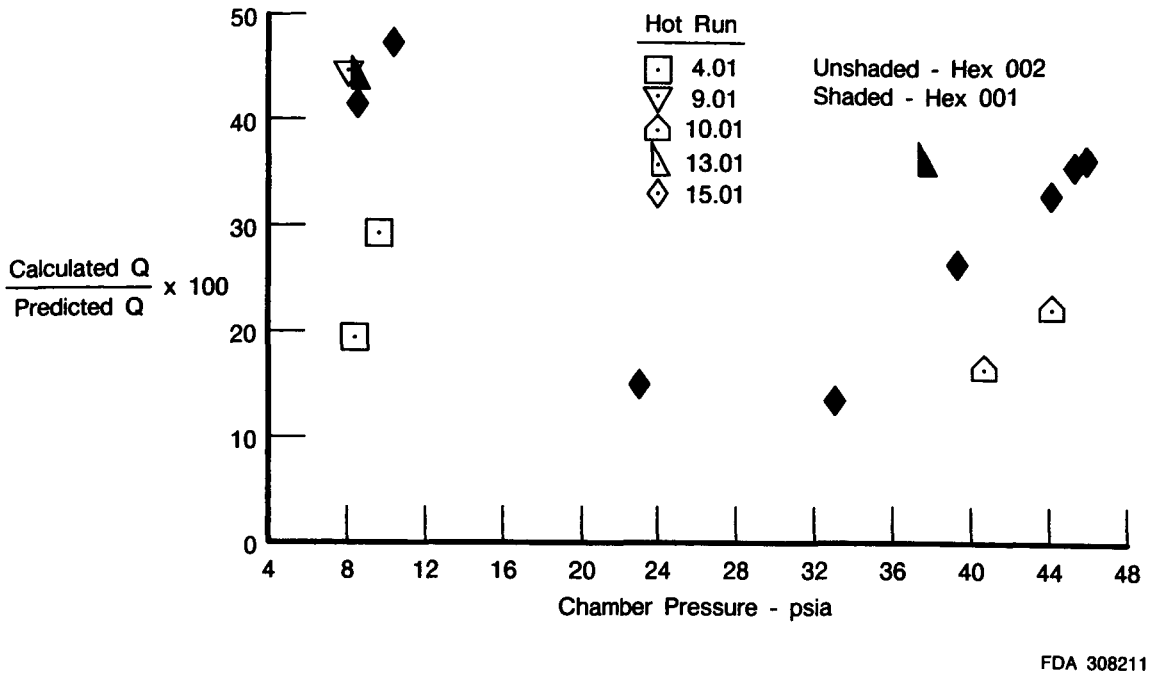

Figure D-3. OHE Heat Transfer vs Chamber Pressure

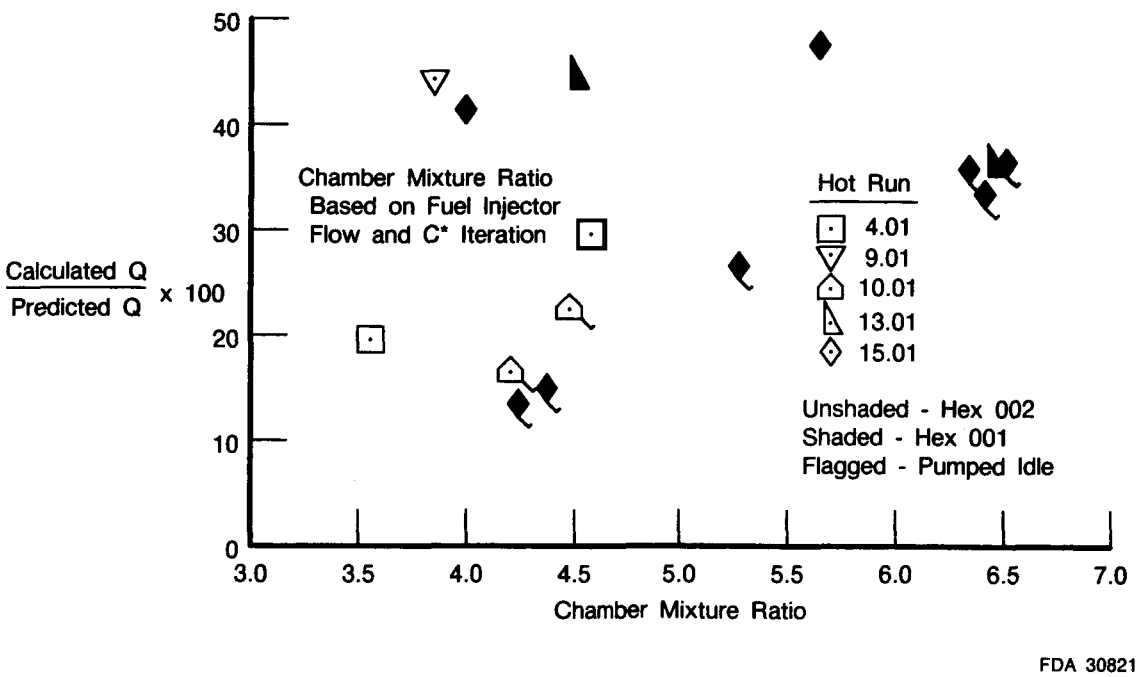

Figure D-4. OHE Heat Transfer vs Mixture Ratio

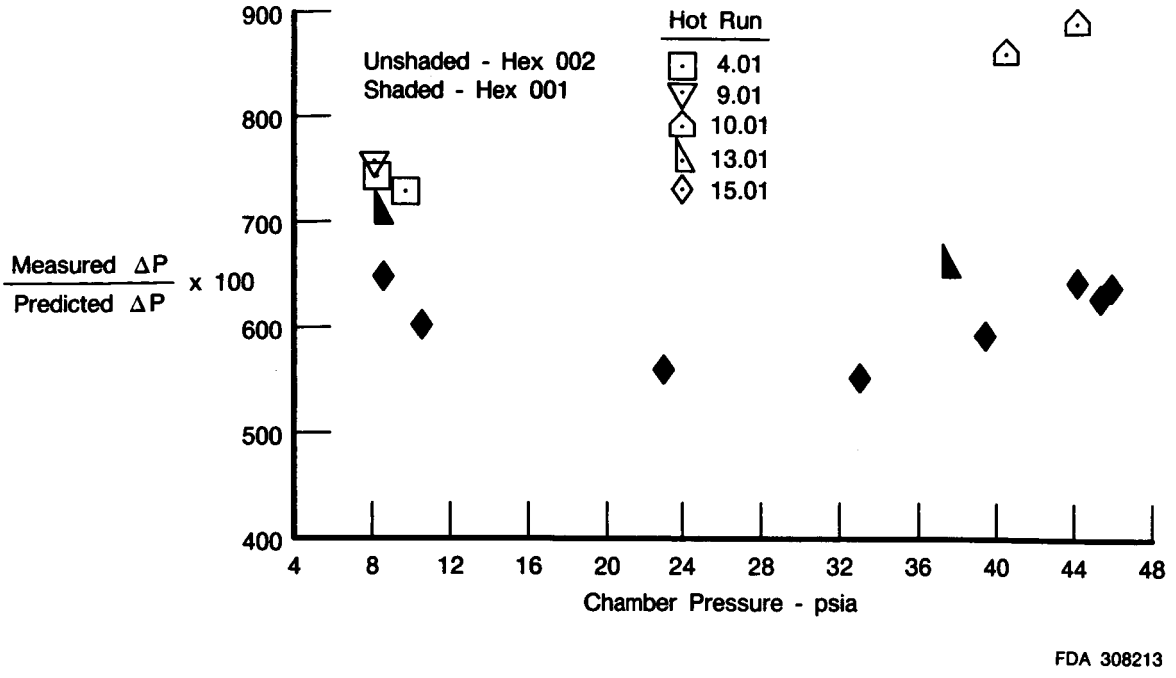

Figure D-5. OHE Fuel Side Pressure Loss vs Chamber Pressure

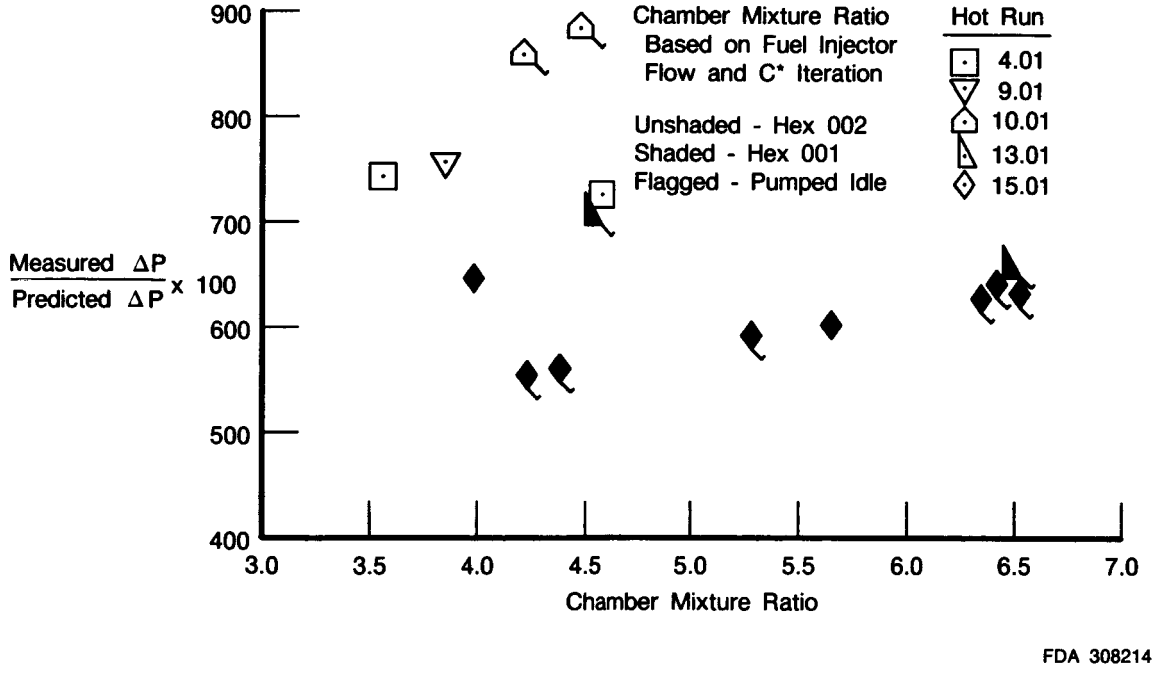

Figure D-6. OHE Fuel Side Pressure Loss vs Mixture Ratio

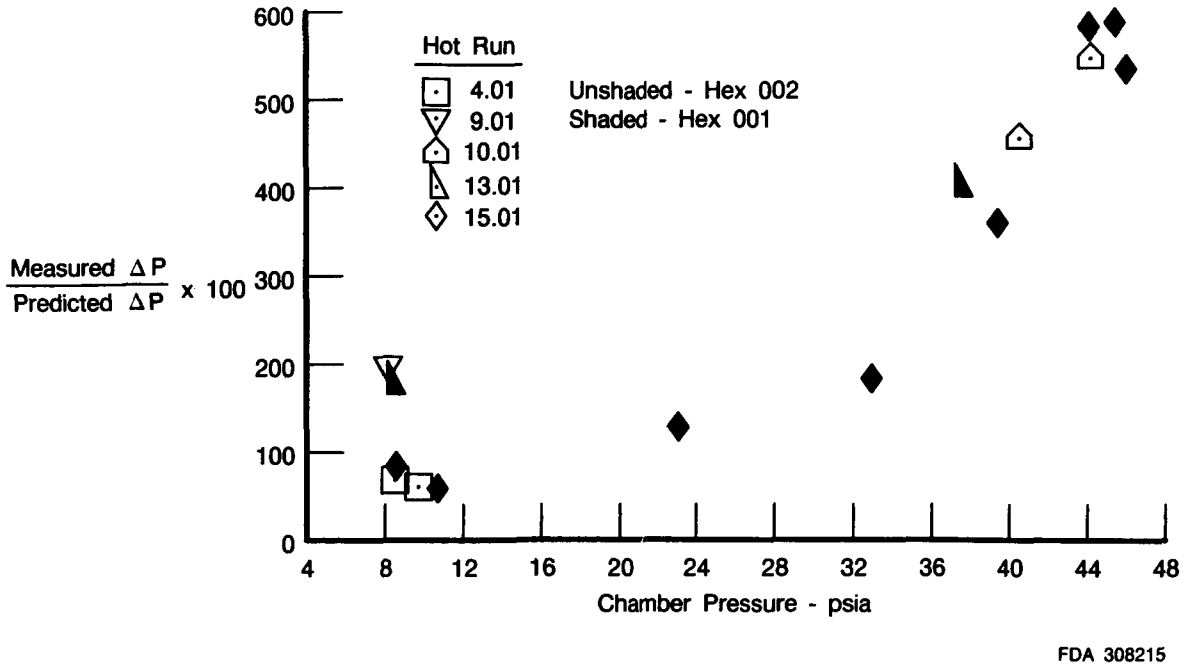

Figure D-7. OHE Oxidizer Side Pressure Loss vs Chamber Pressure

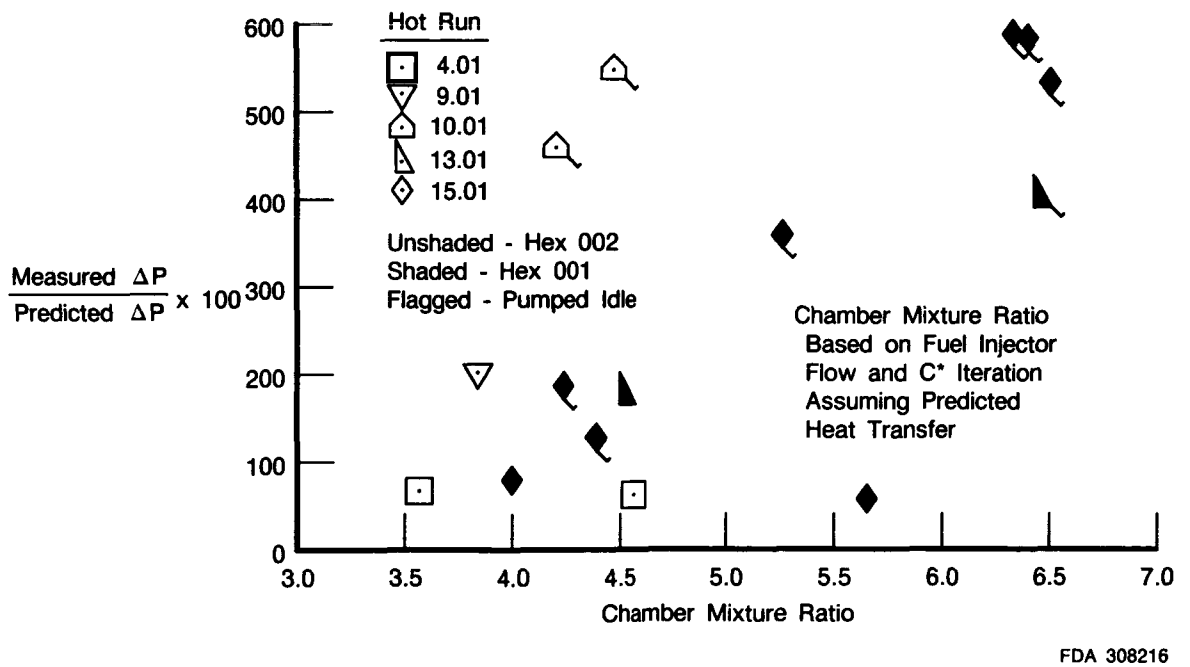

Figure D-8. OHE Oxidizer Side Pressure Loss vs Mixture Ratio

OXIDIZER FLOW OSCILLATIONS

Oxidizer flow oscillations, induced by unstable boiling within the OHE, were examined at both THI and PI thrust levels.

The oscillations which occurred during THI operation were of low enough amplitude to be insignificant to a vehicle system. Figure D-9 compares chamber pressure at THI steady state for each heat exchanger and indicates no major differences between the two. Mixture ratio effects on chamber pressure oscillations are shown in Figure D-10 for heat exchanger S/N 001 illustrating no significant correlation. The damper volume had little effect on system pressure and mixture ratio oscillations as shown in Figures D-11 and D-12, respectively.

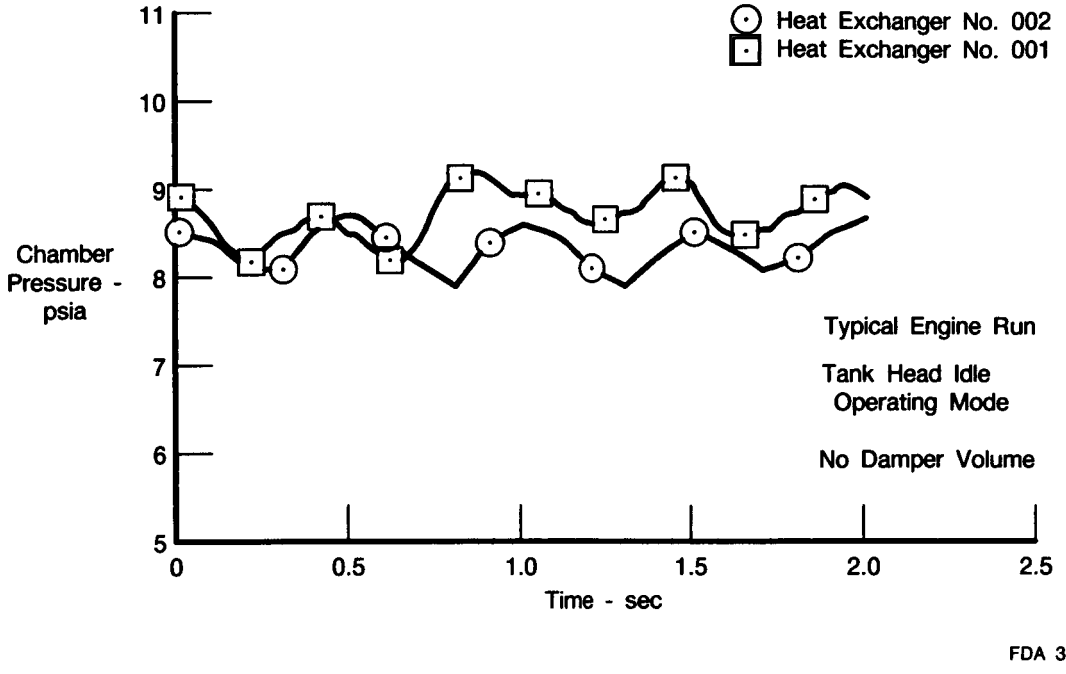

Figure D-9. Chamber Pressure Oscillations vs OHE Units

During pumped idle operation, the oxidizer flow oscillations were more significant. With the damper volume installed, the oscillations were intermittent and low in amplitude but after the volume was removed, they became regular and higher in amplitude. Figures D-13 and D-14 show several system pressure and chamber mixture ratio oscillations, respectively, and indicate that with the volume installed, chamber pressure varied approximately ± 2 psi while mixture ratio changed only about ± 0.25. With the volume removed, chamber pressure oscillation amplitude increased to ± 6 psi and frequency became regular at 3 cps. Mixture ratio variance also increased to ± 0.8. Mixture ratio effects on chamber pressure oscillations are presented in Figure D-15 which indicates, as expected, that with higher O/F, the oscillation frequency increases while amplitude decreases. This occurs because the nucleate boiling rate in the OHE increases with mixture ratio due to the increase in the hydrogen gas temperature. Figure D-16 compares chamber pressure at steady state PI operation for each heat exchanger and shows that with the volume installed, a more stable chamber pressure was obtained.

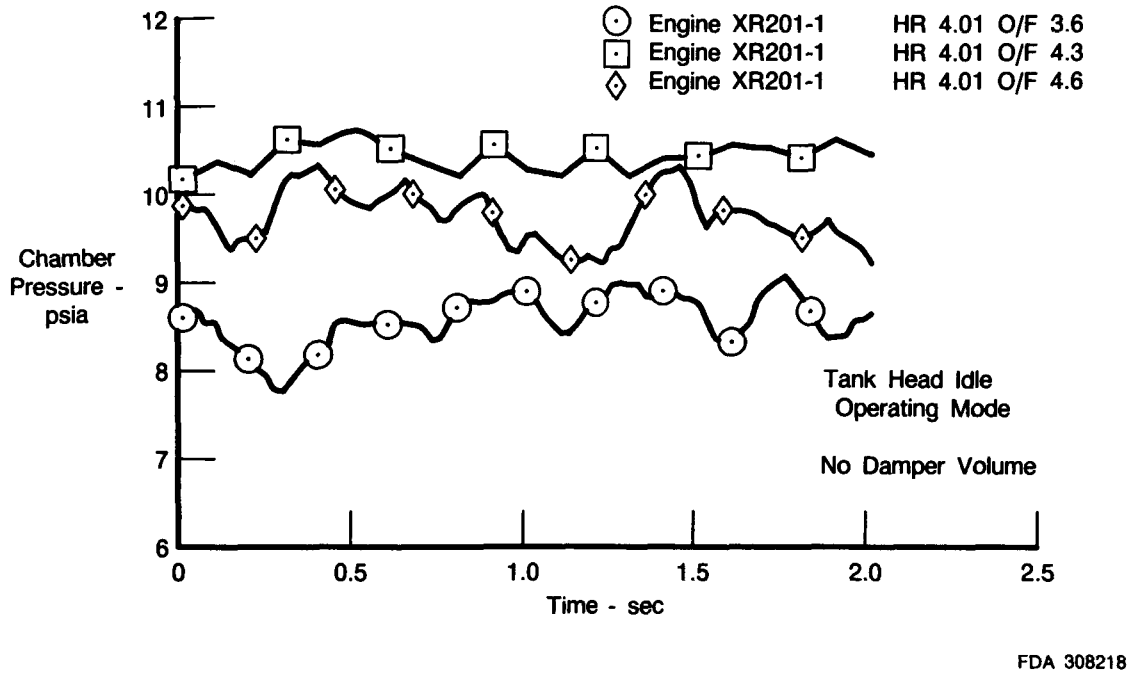

Figure D-10. Mixture Ratio Effects on Chamber Pressure Oscillations in Tank Head Idle Operating Mode

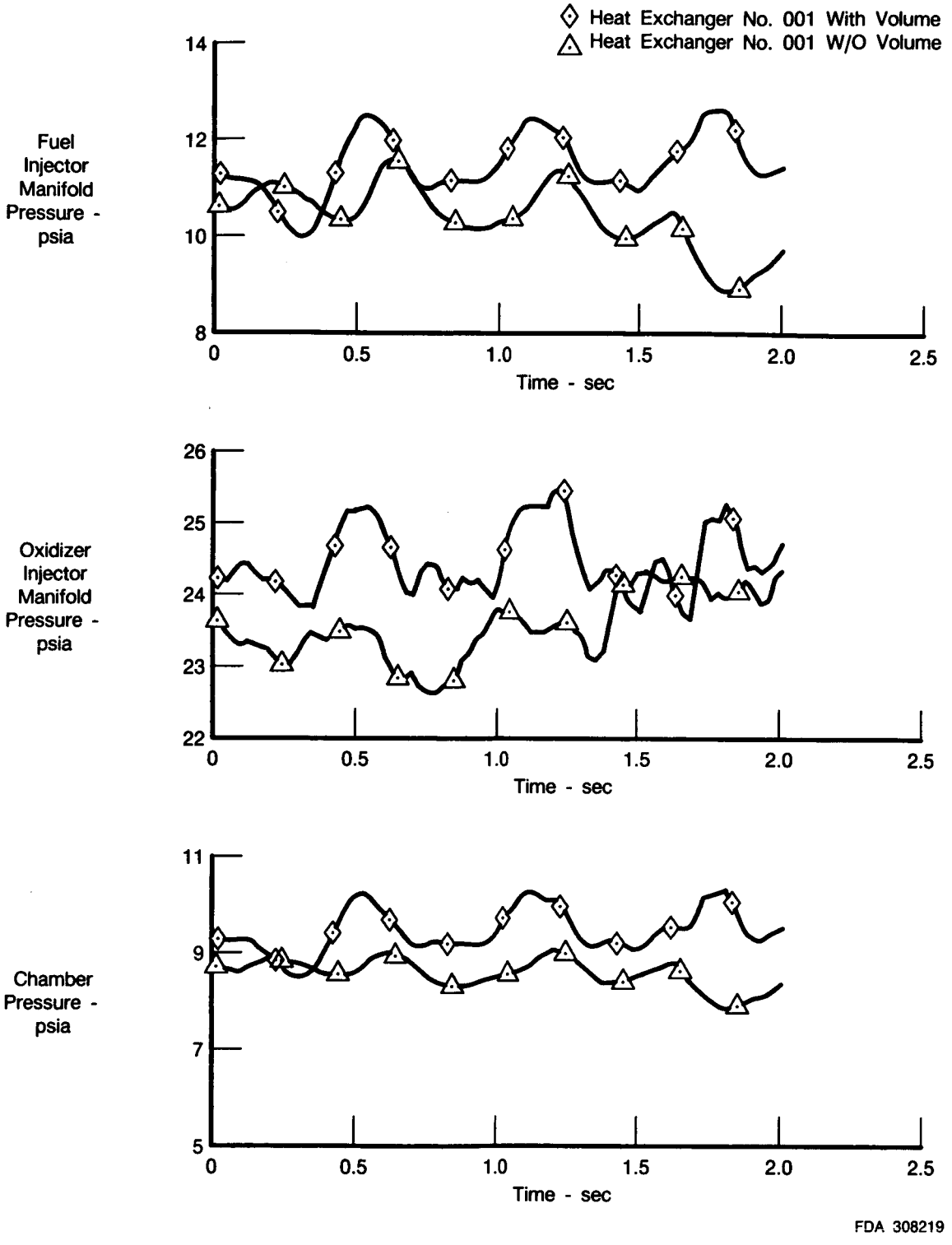

Figure D-11. Damper Volume Effects on Presure Oscillations in Tank Head Idle Operating Mode

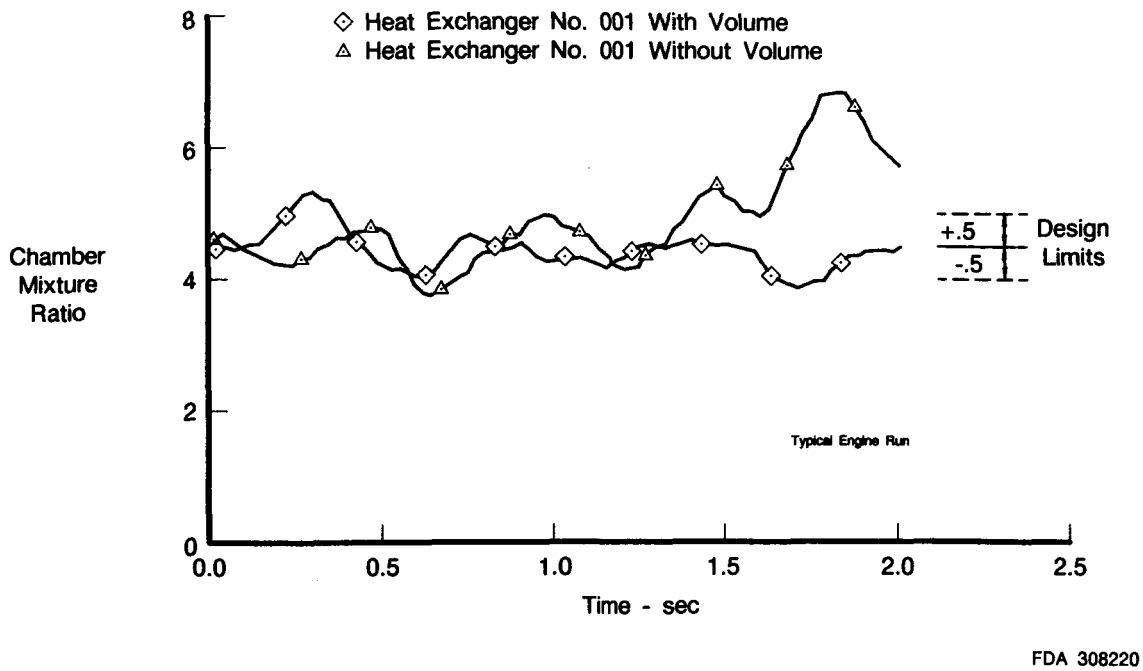

Figure D-12. Damper Volume Effects on Mixture Ratio Variation in Tank Head Idle Operating Mode

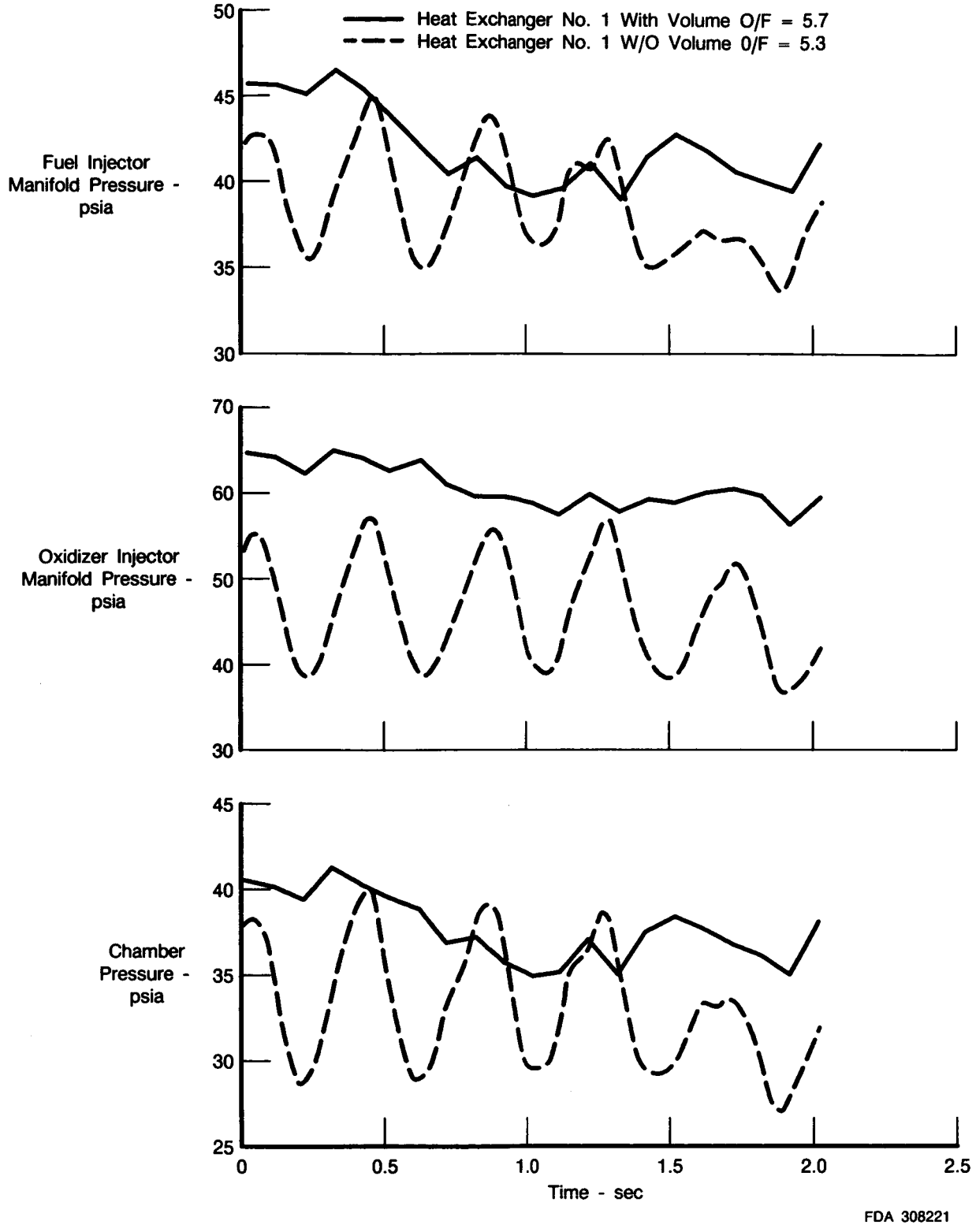

Figure D-13. Damper Volume Effect on Pressure Oscillations in Pumped Idle Operating Mode

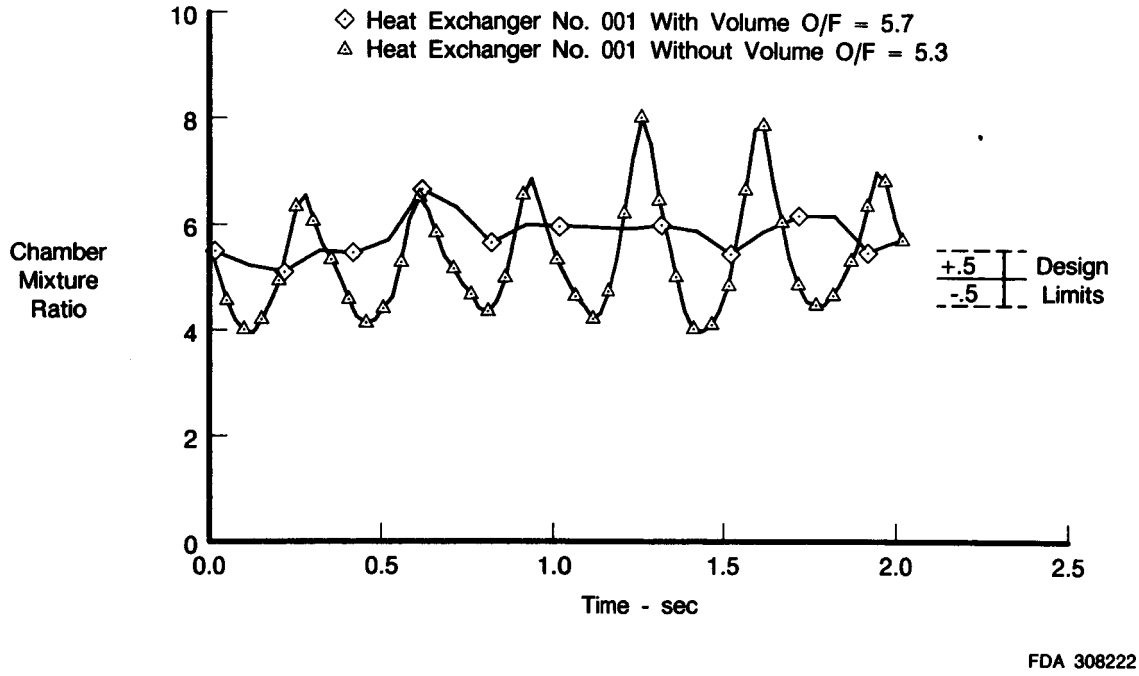

Figure D-14. Damper Volume Effect on Mixture Ratio Variation in Pumped Idle Operating Mode

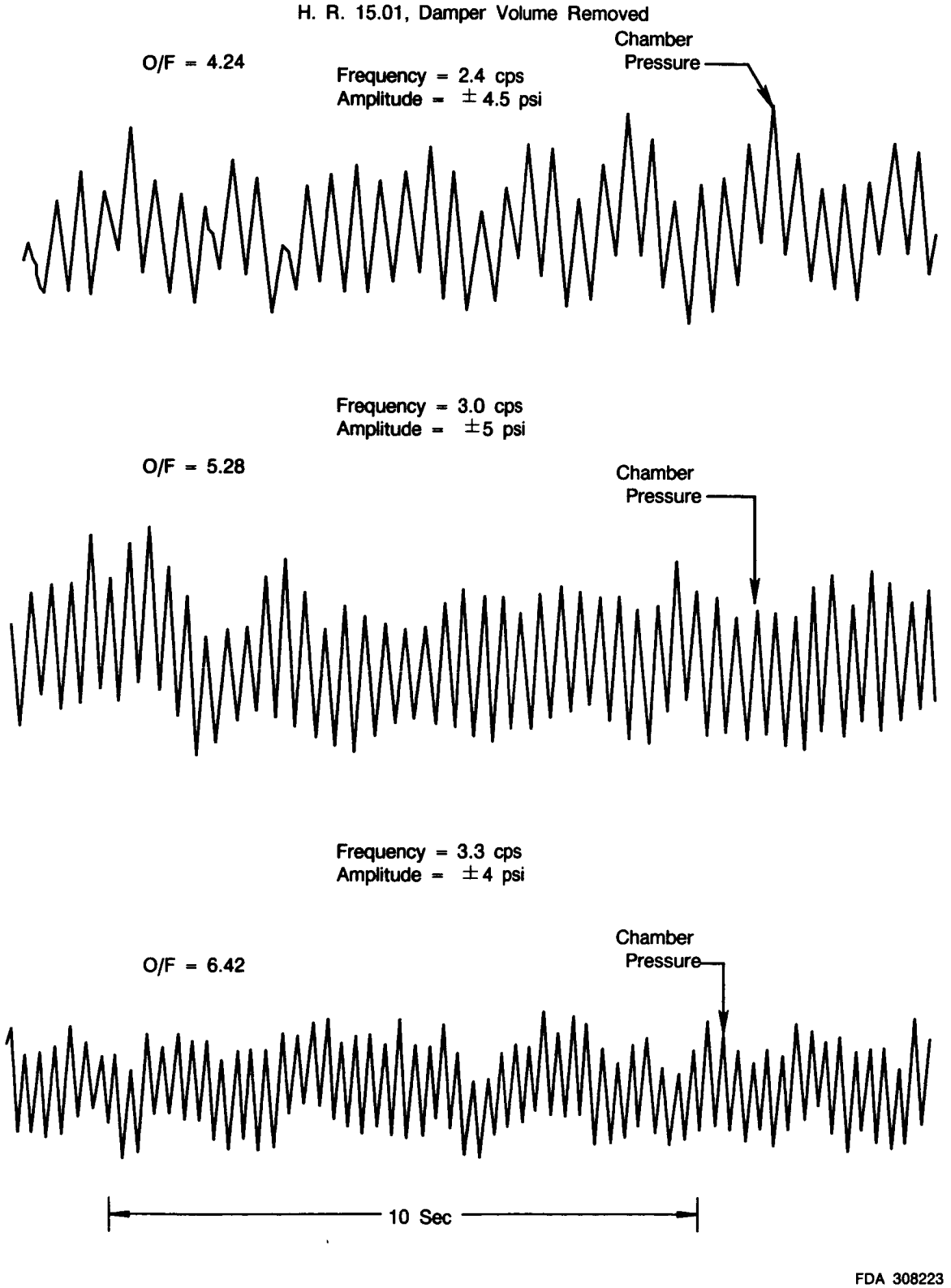

Figure D-15. Mixture Ratio Effects on Chamber Pressure Oscillations in Pumped Idle Operating Mode

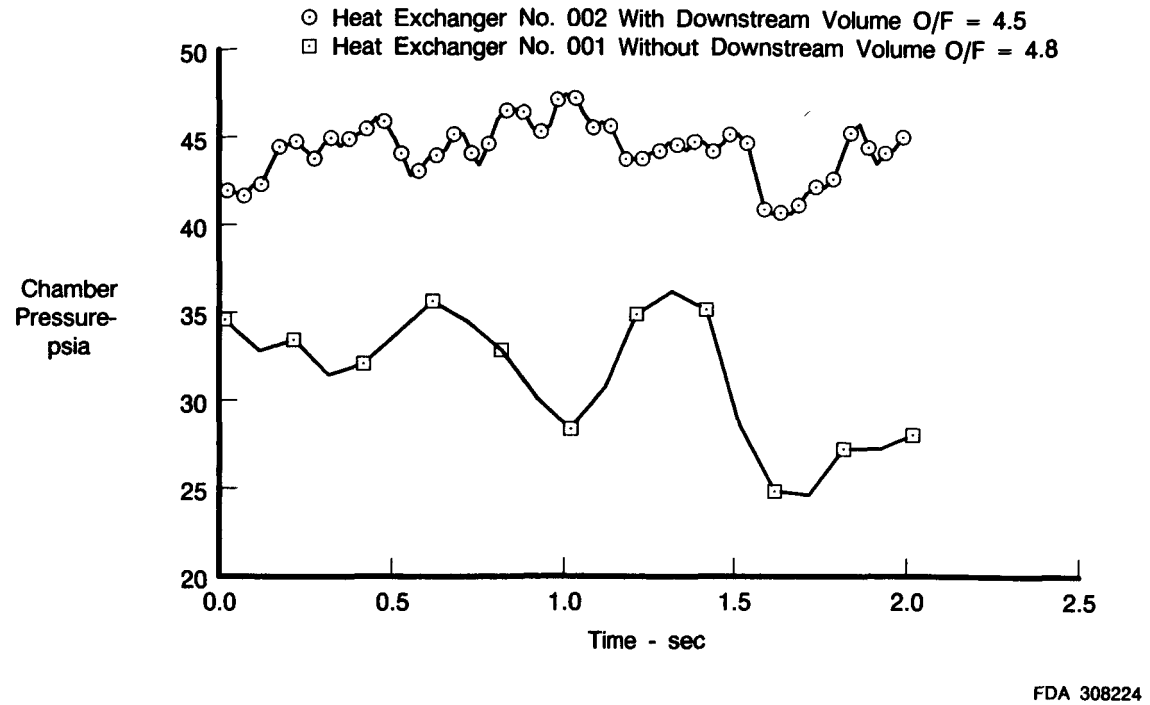

Figure D-16. Damper Volume Effect on Chamber Pressure Oscillations in Pumped Idle Operating Mode

THI PERFORMANCE

Without the Mylar blanket installed to isolate the turbopumps from the capsule environment, THI transients (pump cooldowns) were much slower than predicted. When the GOV area was decreased following start to reduce the mixture ratio, oxidizer pump cooldown with liquid at the inlet required 100 seconds, as shown in Figure D-17. However, when the GOV area was increased after start, oxidizer pump cooldown took 50 seconds, as shown in Figure D-18. This was still twice as long as predicted as shown in Figure D-19. Figure D-20 shows that as expected gas-gas inlet conditions decreased the pump cooldown rate even more when compared to a liquid-liquid inlet start. Hot run 14.01 was the only test with a gas-gas start and it aborted after 35 seconds due to a false flame detector abort. No other gas-gas inlet condition test data is available.

Hot run 3.01 was started with the GOV area at 0.20 $in.^2$ to reduce mixture ratio during THI. The test aborted after three seconds due to high diffuser pressure but a look at chamber pressure revealed a very late and soft ignition due to lower oxidizer flow and chamber pressure. Each following test had a starting GOV area of 0.30 $in.^2$ and no ignition problems occurred.

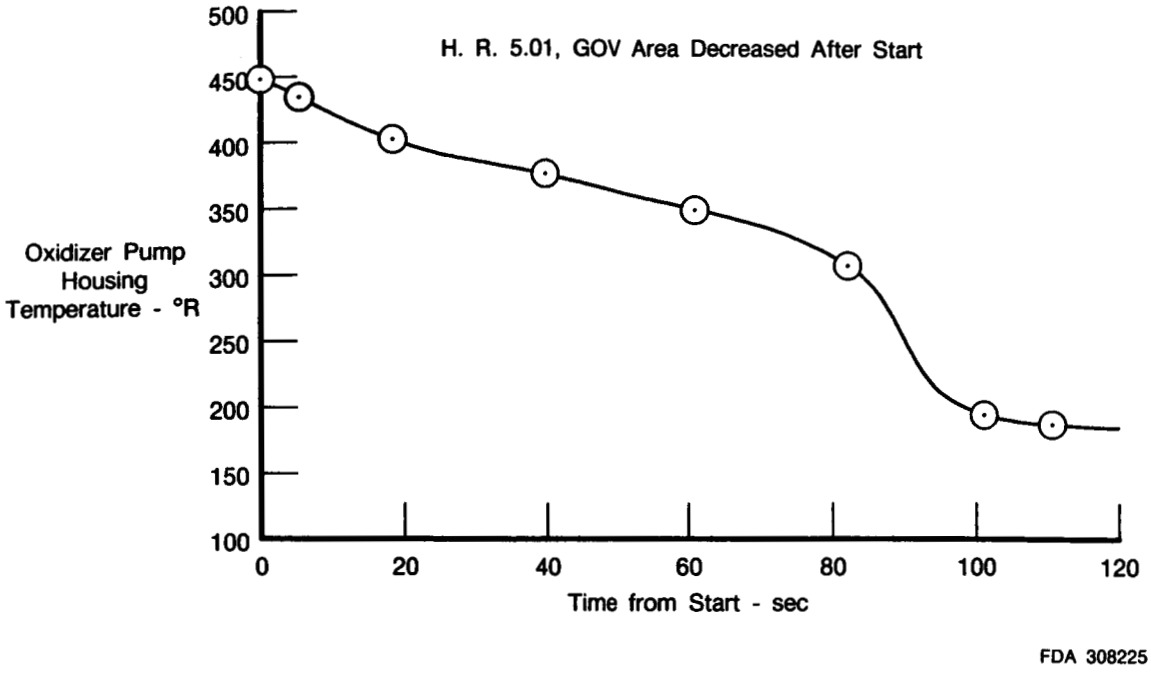

Figure D-17. Oxidizer Pump Cooldown With Decreased GOV Flow Area

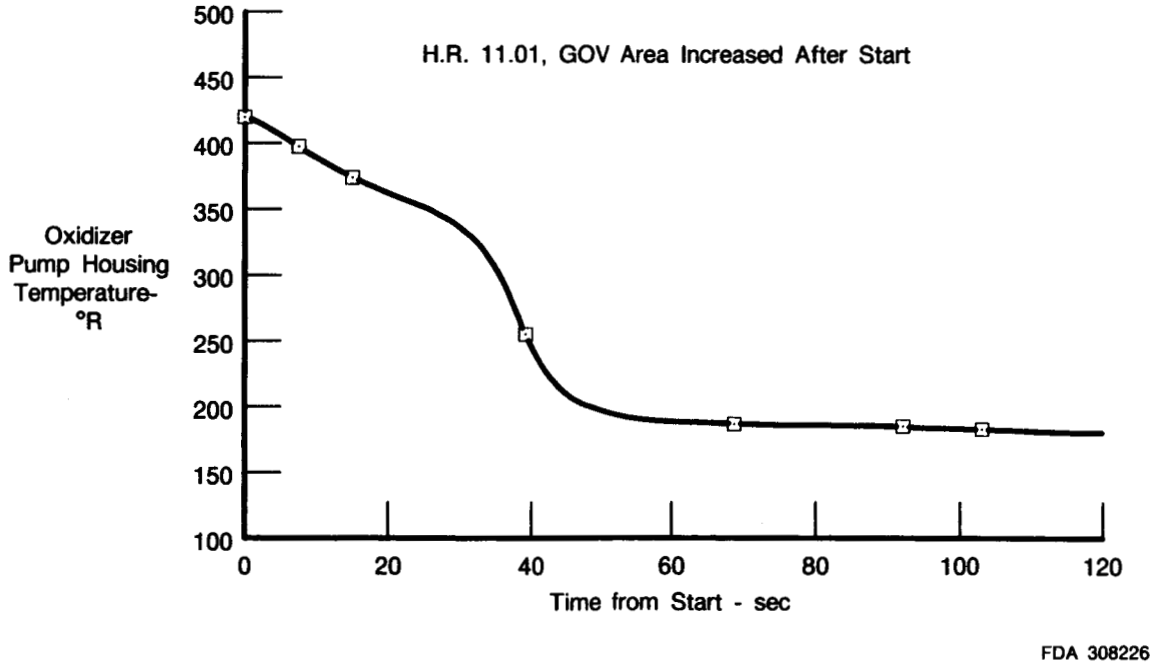

Figure D-18. Oxidizer Pump Cooldown With Increased GOV Flow Area

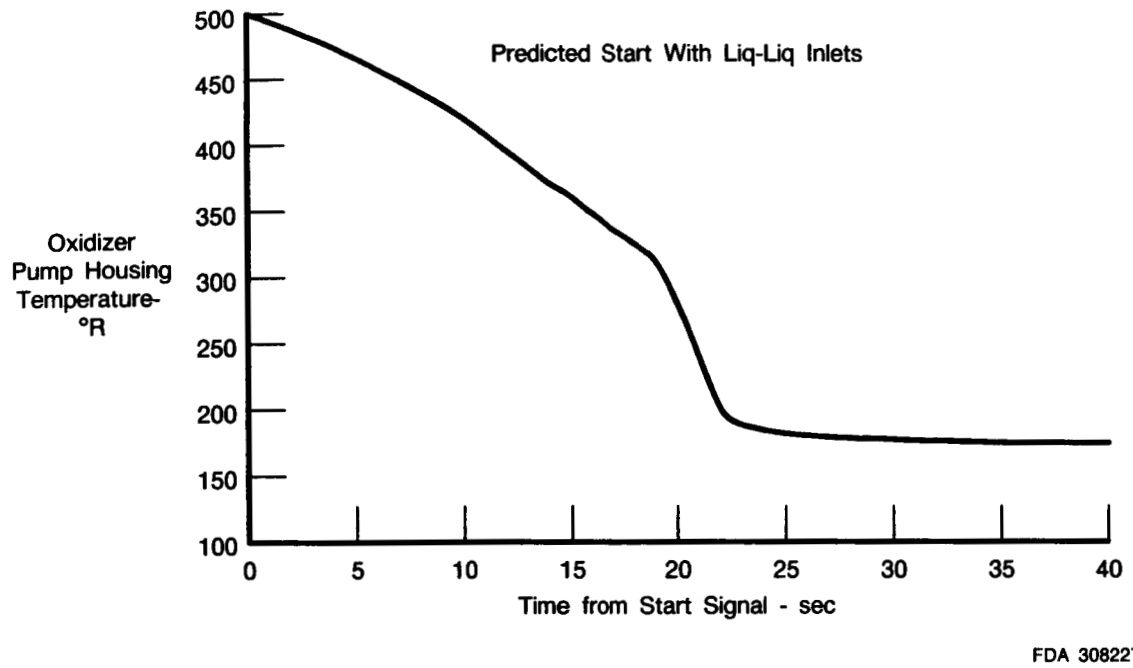

Figure D-19. Predicted Oxidizer Pump Cooldown

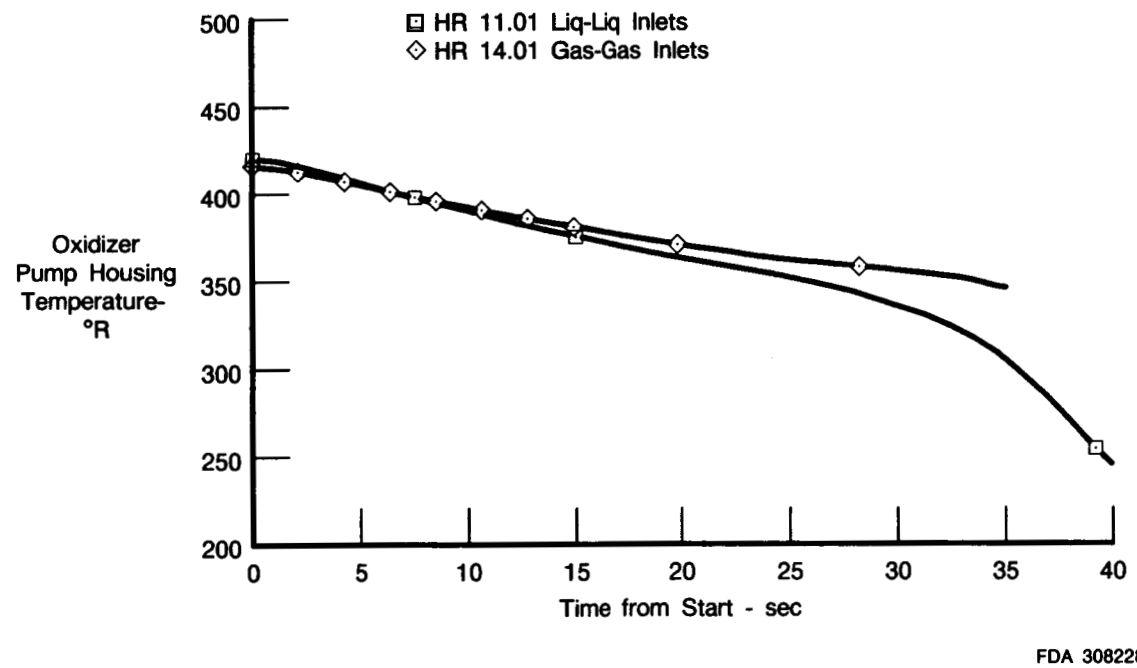

Figure D-20. Effects of Inlet Conditions on Oxidizer Pump Cooldown

TRANSIENT INTO PI

Predicted characteristics of the transient to Pumped Idle are presented in Figure D-21 with the valve sequencing used for the transition shown in Figure D-22. When this valve schedule was used on XR201-1, pump speed increased rapidly and the test aborted due to high heat exchanger

inlet pressure. Subsequent sequencing of the TBV, listed in Table D-1, resulted in the same abort. The pressure losses in the heat exchanger were so much higher than predicted that when the turbine shutoff valve was opened, the pressure ratio created across the turbine was great enough to overcome the pump breakaway torque without the expected need to close the TBV. Also, the breakaway torque of the cold turbopumps may be lower than the measured torque of ambient turbopumps used in the prediction model. Finally, for the hot run 8.01 PI transient, the TBV was left in the open position and the Fuel Vent Valve (FVV) was sequenced open allowing more flow through the fuel pump, thereby loading it and preventing it from overspeeding. Figure D-23 presents the pumped idle transient chamber pressure characteristics for hot run 11.01.

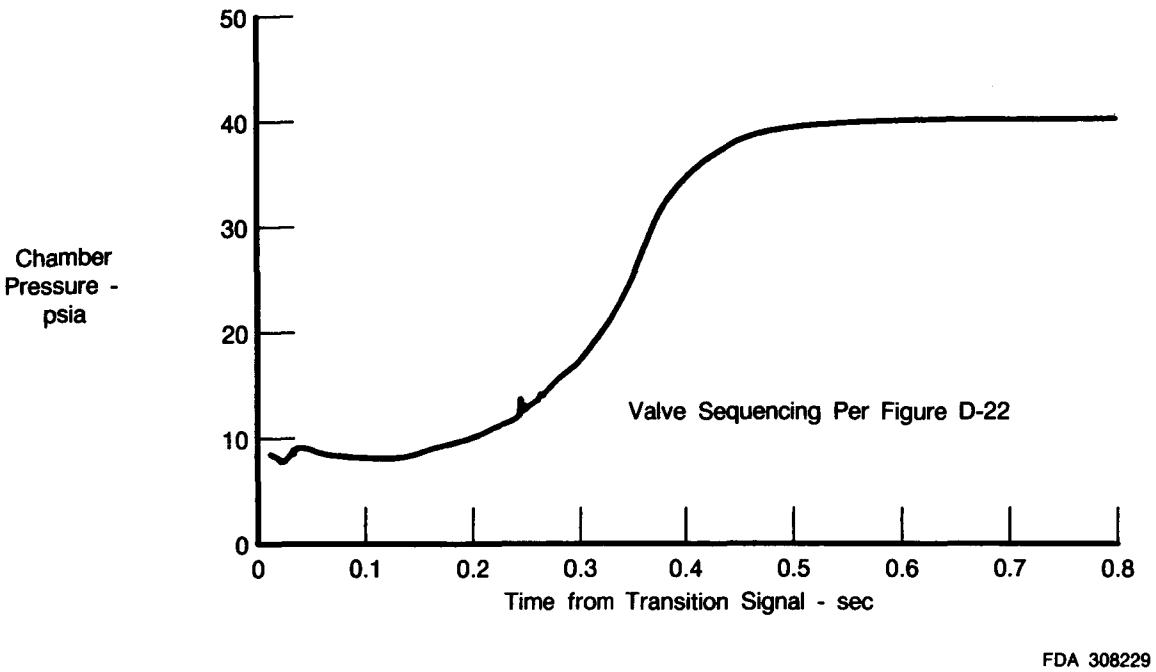

Figure D-21. Predicted Transient to Pumped Idle

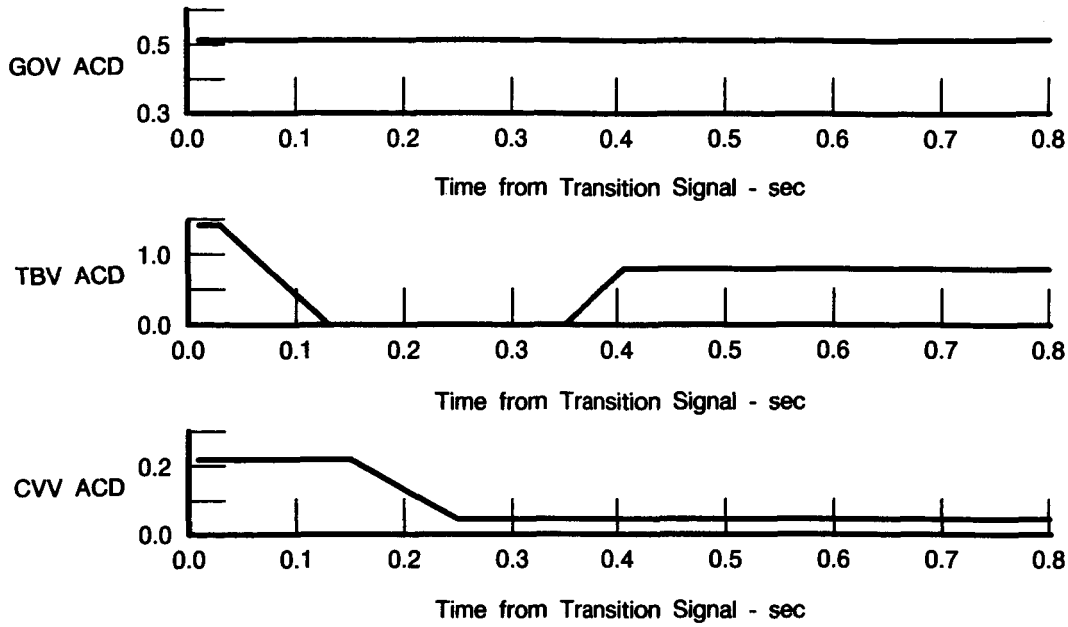

Figure D-22. Valve Sequencing for Tank Head Idle to Pumped Idle Transition Prediction

Table D-1. *PI Transient Valve Sequencing*

Run No.	*GOV Position % of full open*	*FVV Position % of full open*	*CVV Sequencing*	*TBV Sequencing*	*Test Result*
5.01	19	0	100% open ramped to 20% open at +100 msec.	95% open ramped to closed position at signal. Dwell time at close 250 msec and ramped to 95% open.	Test abort due to pump overspeed.
6.01	30	N/C	N/C	Dwell time at close decreased to 150 msec.	Test abort due to pump overspeed.
7.01	N/C	N/C	N/C	Valve ramped to 30% open and ramped back to 95% open immediately.	Test abort due to pump overspeed.
8.01	N/C	100	N/C	Remained at 95% open.	Successful transition to PI operation.

N/C - No change from previous run

6083M

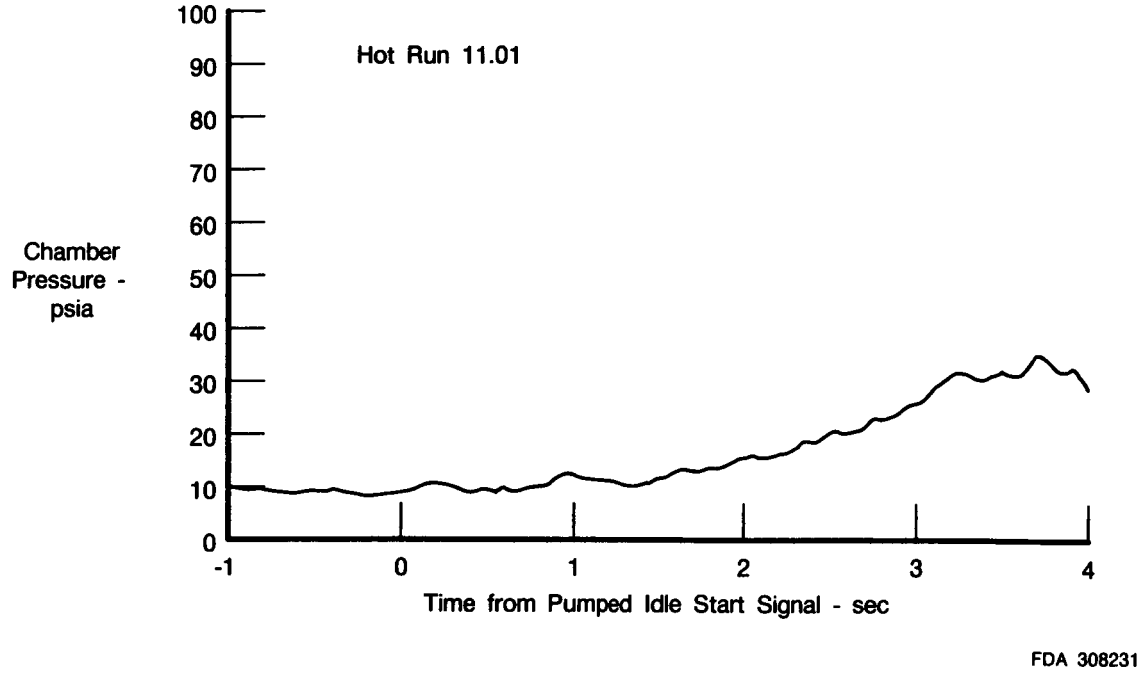

Figure D-23. XR201-1 Transient to Pumped Idle

PUMPED IDLE PERFORMANCE

Engine performance calculations were restricted to PI operation due to the inaccuracy of the thrust measurements at very low levels. Hot run 15.01 was chosen to evaluate engine performance because all the test stand dumps and the FVV were closed, making the flow going through the flowmeters, the pumps and the chamber the same. A comparison of methods to calculate flowrates was done to obtain the best procedure to use in evaluating engine performance. Oxidizer flow at the injector could not be calculated because it was 2-phase throughout PI operation and density could not be determined. Table D-2 lists the different methods used and the flowrates calculated while Table D-3 shows the corresponding mixture ratios and specific impulse values. The specific impulse versus mixture ratios relationships are presented in Figure D-24. The high mixture ratios indicated by the metered flows are not representative of the thrust chamber heat transfer obtained. Also, the specific impulse calculated with the metered flows curves down at the low mixture ratio while a higher value was expected. The fuel metered flows agree closely with injector flows and the mixture ratio and specific impulse values obtained using these flows and a C* iteration as described in Appendix F are reasonable. It was decided then, that the oxidizer metered flow was in error and all engine performance parameters were calculated using the fuel injector flowrate and a C* iteration.

Table D-2. *RL10-IIB Breadboard Demonstrator Engine XR201-1 Flowrate Calculation Methodology HR 15.01*

EDR Time*	Fuel Flow		Oxidizer Flow		
	Meter	Injector	Meter	Fuel Meter Flow and C* Iteration	Fuel Injector Flow and C* Iteration
	(lb/sec)	(lb/sec)	(lb/sec)	(lb/sec)	(lb/sec)
399	0.513	0.560	4.225	3.765	3.555
431	0.515	0.558	4.271	3.837	3.638
474	0.523	0.545	3.141	2.951	2.876
507	0.510	0.524	2.665	2.257	2.220
573	0.504	0.541	3.963	3.645	3.473

*Recording System Time for Reference Only

6083M

Table D-3. *RL10-IIB Breadboard Demonstrator Engine XR201-1 Flow and O/F Calculation Methodology Comparison HR 15.01*

EDR Time* (sec)	O/F			I sp (sec)		
	Meter Flows	Fuel Meter and C* Iter	Fuel Inj. and C* Iter	Meter Flows	Fuel Meter and C* Iter	Fuel Inj. and C* Iter
399	8.236	7.339	6.348	370.4	410.2	426.5
431	8.293	7.450	6.520	371.7	408.8	424.0
474	6.006	5.642	5.277	403.2	425.2	431.8
507	5.226	4.425	4.237	376.9	432.5	436.1
573	7.864	7.232	6.420	379.5	408.6	422.3

*Recording System Time for Reference Only

6083M

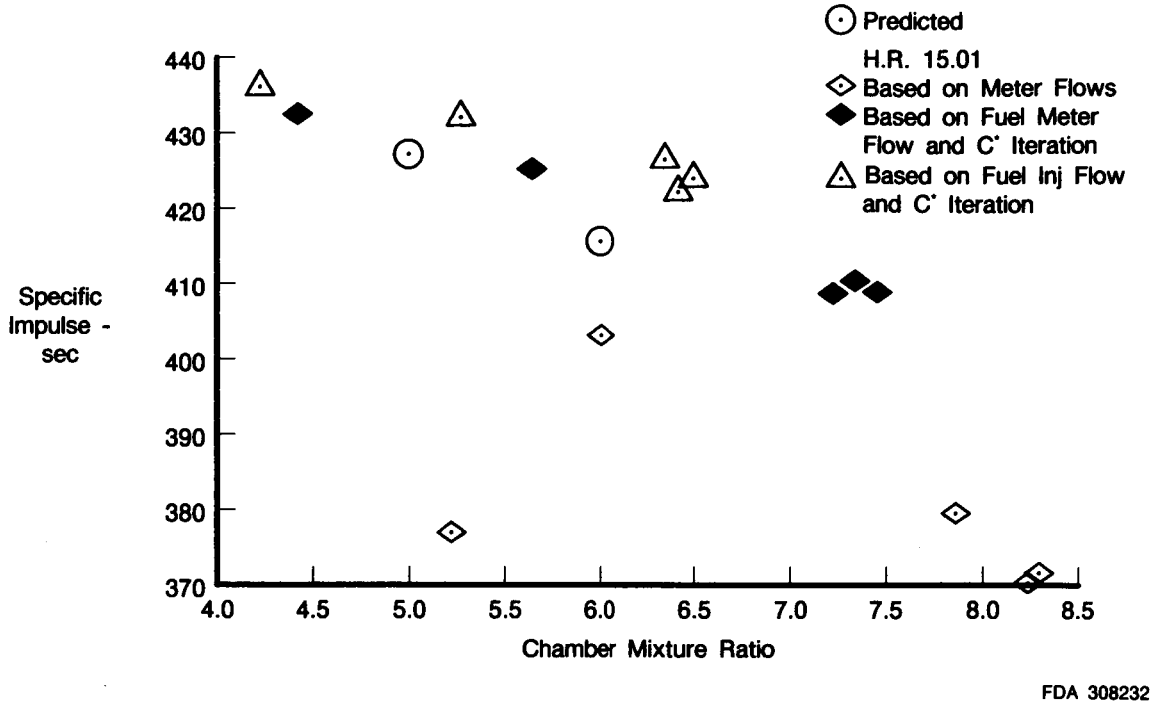

Figure D-24. Pumped Idle Operating Mode — Specific Impulse vs Mixture Ratio

PUMP OPERATION

Fuel pump operation at pumped idle thrust level is shown in Figure D-25 while Figure D-26 presents the oxidizer pump characteristics. The test data is compared to predicted values as well as test data from engine FX141-45 which ran the earlier low thrust tests in 1967 and 1968. The effects of the heat exchanger induced oscillations in the fuel flow can be seen in Figure D-25 as flowrate oscillations between 0.43 and 0.5 lb/sec and pump pressure rise oscillations between 81 and 92 psid. Figure D-26 shows oxidizer oscillations varying between 2.2 and 4 lb/sec and pump pressure rise oscillations between 35 and 78 psid. Neither pump stalled due to the oscillations but moved up and down the operating line as shown in the figures. In an attempt to go to a higher mixture ratio during test 13.01, the fuel flow was reduced using the CVV resulting in a fuel pump stall. This point is shown on Figure D-25 in relationship to the predicted stall line.

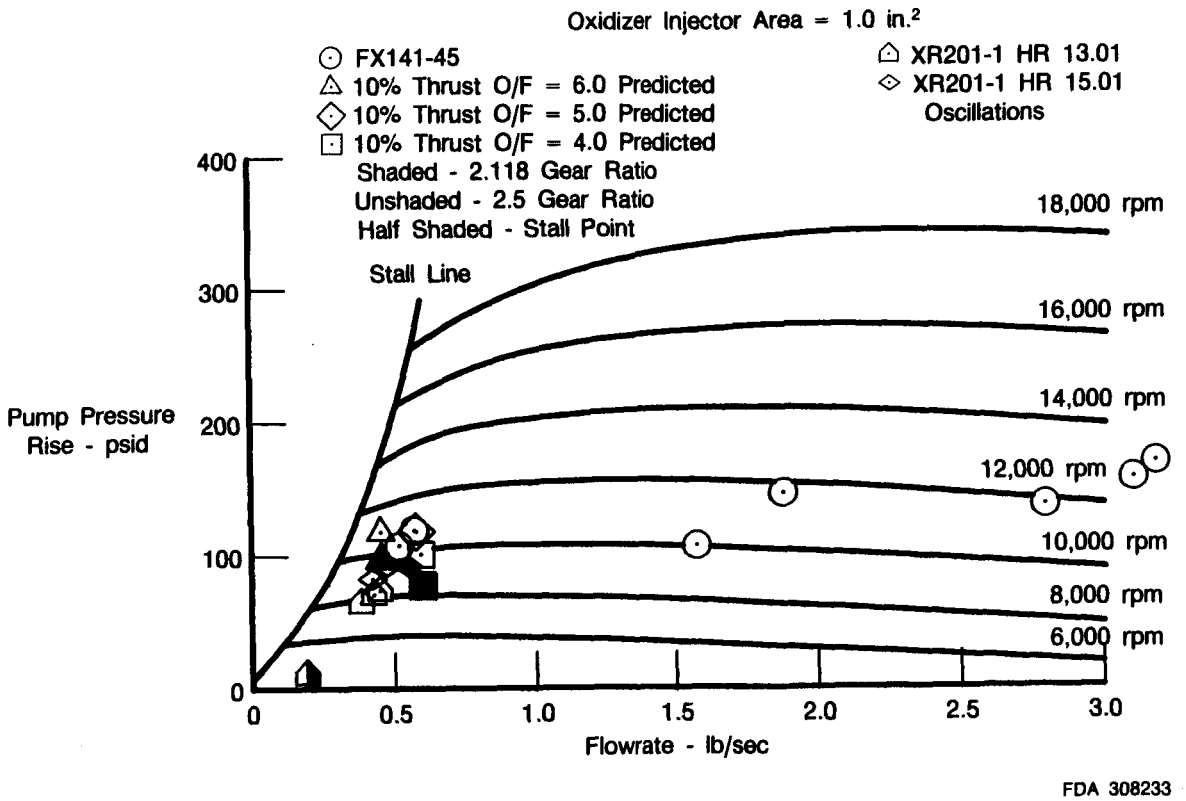

Figure D-25. Fuel Pump Operation Characteristics

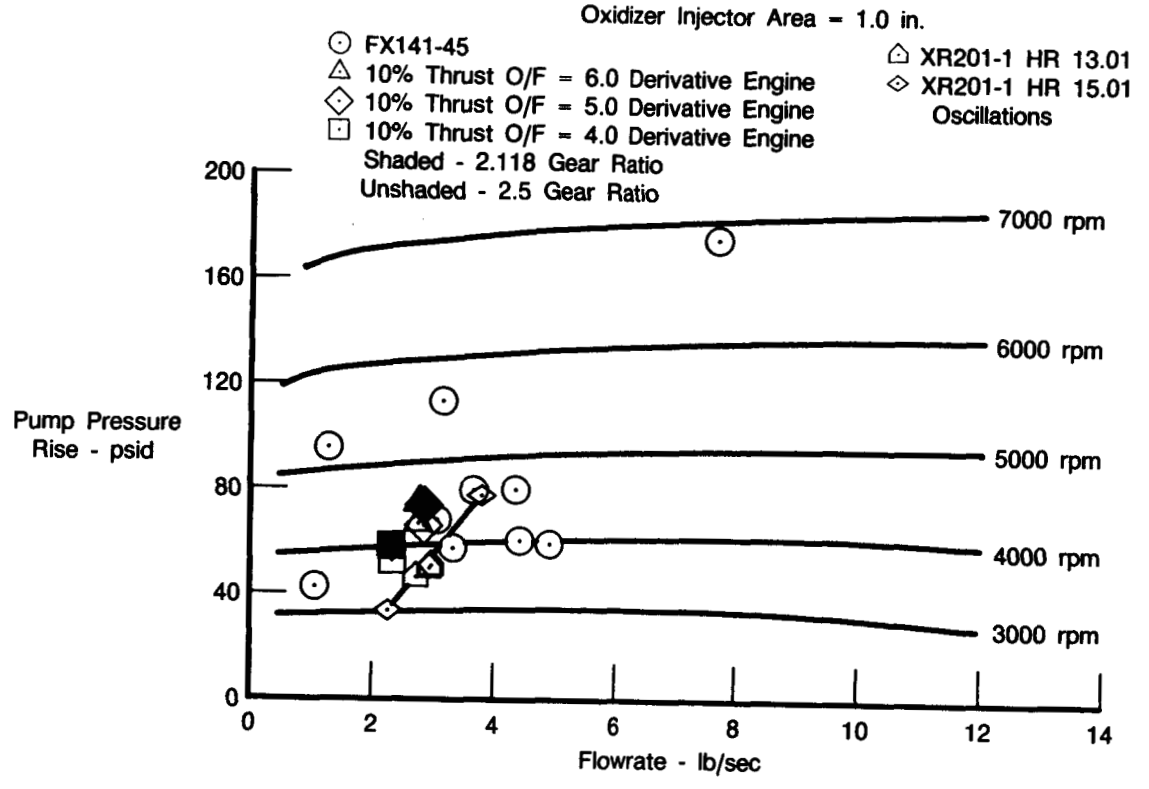

Figure D-26. Oxidizer Pump Operation Characteristics

APPENDIX E
COMPUTER SIMULATION ANALYSIS

PRE-TEST

The steady-state computer simulation described in Reference 1, was changed to reflect the initial test series configuration. RL10A-3-3A thrust chamber/nozzle heat transfer and pressure loss characteristics were incorporated into the deck. This data was obtained from low thrust testing carried out in 1967 and 1968. The three-stage oxidizer heat exchanger was replaced with the predicted operating characteristics of the Stage 3 only. Steady state points at both the THI and PI thrust levels were run with the different expected inlet conditions. Figures E-1 and E-2 present the cycle sheet for each predicted operating point. A computer program was written using a method derived from Reference 2 to calculate the heat exchanger oxidizer side discharge pressure oscillations. The predicted frequencies and amplitudes for the Stage 3 OHE are listed in Table E-1 for each thrust level. From these predictions, it was recommended that a volume be installed in the oxidizer line downstream of the heat exchanger. This recommendation was based on a computer simulation showing that oscillations, with a high frequency and a low amplitude, could be effectively damped with a downstream damper volume (Figures E-3 to E-7). Figure E-3 shows oxidizer flow exiting from the OHE oscillating with a predicted frequency of 31 cps and a predicted amplitude of ± 0.2 lb/sec. Figure E-4 illustrates how the flow out of the volume is effectively damped (± 0.04 lb/sec). In Figure E-5, the flow leaving the gaseous oxygen control valve and entering the injector is almost entirely damped out so that there are no apparent oscillations in chamber pressure (Figure E-6) and mixture ratio (Figure E-7).

Test Series No. 1 RL10A-3-3 Thrust Chamber PC 8.55 psia O/F 3.3

Inlet Conditions			
Fuel		LOX	
Pressure	25.85	Pressure	34.86
Temp	38.9	Temp	172.2
NPSP	4.50	NPSP	10.00
Flow	0.16	Flow	0.54

Jacket	
Flow	0.16
Inlet P	25.37
Inlet T	38.9
Delta PJ	5.987
Delta TJ	400.038

Leakage and Bleed	
WLeak	0.0
TLC	0.0
ODCL	0.0

RM Control Vlv	
Delta P	12.37
Acd	0.5017
K Factor	4.9692

Turb Byp Valve	
Delta P	6.15
Acd	1.4000
P/P	1.5078

Engine Station Conditions

Station	Pressure	Temp	Density	Enthalpy
Fuel System Conditions				
Inlet	25.85	38.86	4.3267	−98.77
Jacket Inlet	25.37	38.87	4.3261	−98.77
Jacket Dis	19.38	438.91	0.0083	1442.81
Turb Inlet	18.55	438.91	0.0083	1442.81
Valve Inlet	18.25	438.91	0.0083	1442.81
Valve Disch	12.10	438.91	0.0053	1442.81
HEX Inlet	11.74	438.91	0.0053	1442.81
HEX Dis	10.76	337.46	0.0060	1059.96
Inject Inlet	10.76	337.46	0.0060	1059.96
Oxidizer System Conditions				
Inlet	34.86	172.18	69.5069	65.11
HEX Inlet	34.86	172.18	69.5069	65.11
HEX Dis	34.35	293.87	0.3535	181.12
Valve Inlet	34.16	293.87	0.3535	181.12
Valve Disch	21.79	292.62	0.2242	181.12
Injet Inlet	20.86	292.52	0.0	181.12

Chamber	
PC (Inj Face)	8.550
Impulse (Chamber)	406.017
Impulse (Delivered)	406.017
Mixture Ratio (Inlet)	3.300
Mixture Ratio (Chamber)	3.299
CS	0.914
Eta C*	1.000
Area Ratio	57.000

Fuel Injector	
Delta P	2.21
Inlet P	10.76
Inlet T	337.5
Acd	2.414
MV	1.839

LOX Injector	
Delta P	12.47
Inlet P	20.86
Inlet T	293.9
Acd	0.800
Rho	0.215
MV	1.686

Mixture Ratio	3.299
Thrust	285.
Impulse	406.02
Chamber Pressure	8.55

Figure E-1. RL10-IIB Engine Cycle Sheet — Tank Head Idle

FD 308235

Test Series No. 1 RL10A-3-3 Thrust Chamber

PC 40 psia O/F 6.0 DPVEN 69

Inlet Conditions

Fuel		LOX	
Pressure	25.00	Pressure	33.00
Temp	38.6	Temp	170.7
NPSP	4.50	NPSP	10.00
Flow	0.52	Flow	3.12

Jacket

Flow	0.50
Inlet P	85.20
Inlet T	49.1
Delta PJ	23.371
Delta TJ	561.211

GOX Control Vlv

Delta P	44.99
Acs	0.5017
K Factor	12.1076

Leakage and Bleed

WLeak	0.021
WT/P-Fuel	0.0
WT/P-LOX	0.0
TOXP	212.327
POXP	130.985
PFP	46.334
TFP	461.610

RM Control Vlv

Delta P	0.0
Acd	0.0
K Factor	0.0

Turb Byp Valve

Acd	0.8020
WTBY/WF	41.354
WTBY	0.207
P/P	1.215

Fuel Turbine

Flow	0.293
Power	29.25
Eff	0.4538
Inlet P	61.21
Inlet T	610.3
Dis P(S)	47.00
Delh Act	70.6
M. Vel R	0.147
Acd	0.979
TDIS Mix	590.37
HP Trans	5.1
P/P	1.302

Fuel Pump (Main)

Speed	11256.
SS Speed	1912.
Flow	0.520
Inlet GPM	52.7

1st Stage

Power	12.97
Eff	0.1722
Inlet P	25.00
Disch P	91.87
Disch T	44.596
Rho In	4.339
Rho Out	4.094

2nd Stage

Power	11.17
Eff	0.2055
Inlet P	91.87
Disch P	154.29
Disch T	49.1
Rho Out	3.889

LOX Pump (Main)

Speed	5314.
SS Speed	2460.
Flow	3.123
Power	5.11
Eff	0.2283
Inlet P	33.0
Inlet T	170.7
Disch P	131.97
Disch T	173.1
Rho In	69.768
Rho Out	69.457
Inlet GPM	20.1

System Pressure Losses

OB/P Dis Line	0.0
FB/P Dis Line	0.0
Pump Intr Stg	0.0
Pump Dis Line	0.032
GOX Heat Exr	15.747
Jac In Line	0.062
Jac Dis Line	0.0
Fuel Turb In	0.0
Inj In Line	0.829

Chamber

PC (Inj Face)	40.014
Impulse (Chamber)	411.644
Impulse (Delivered)	411.265
Mixture Ratio (Inlet)	6.000
Mixture Ratio (Chamber)	6.252
CS	0.964
Eta C*	1.000
Area Ratio	57.000

Engine Station Conditions

Station	Pressure	Temp	Density	Enthalpy	Entropy
Fuel System Conditions					
Inlet	25.00	38.58	4.339	−99.47	0.0
Interstage	91.87	44.60	4.094	−81.54	0.0
Pump Dis	154.29	49.13	3.889	−66.02	0.0
Jacket Inlet	85.20	49.13	3.787	−66.71	0.0
Jacket Dis	61.83	610.34	0.019	2058.37	0.0
Turbin Inlet	61.21	610.34	0.019	2058.37	0.0
Turbine Dis	47.16	590.37	0.015	1987.76	0.0
BP Vlv Inlet	58.21	610.34	0.019	2058.37	0.0
BP Vlv Exit	47.91	610.34	0.019	2058.37	0.0
GOX HX Inlet	47.78	610.34	0.019	2058.37	0.0
GOX HX Exit	46.08	288.96	0.030	872.23	0.0
Inject Inlet	46.33	461.61	0.019	1526.44	0.0
Oxidizer System Conditions					
Inlet	33.00	170.66	69.768	64.47	0.0
Pump Dis	131.97	173.11	69.457	65.63	0.0
GOX Hx Exit	130.99	212.33	2.624	144.09	0.0
GOX Vlv Inlt	129.70	212.33	2.624	144.09	0.0
GOX Vlv Exit	84.70	200.04	1.701	144.09	0.0
Inject Inlet	78.26	197.94	1.572	144.09	0.0

Fuel Injector

Delta P	6.32
Inlet P	46.33
Inlet T	461.6
Acd	2.348
MV	5.644

LOX Injector

Delta P	38.25
Inlet P	78.26
Inlet T	197.9
Acs	0.770
Rho	1.572
MV	8.057

Mixture Ratio	6.000
Thrust	1498.
Impulse	411.26
Chamber Pressure	40.01

Figure E-2. RL10-IIB Engine Cycle Sheet — Pumped Idle

FD 308236

Table E-1. *Heat Exchanger Oxidizer Side Discharge Pressure Oscillations*

	Tank Head Idle	*Pumped Idle*
Frequency (cps)	16.5	31.7
Amplitude (psi)	±1.0	±2.3

6083M

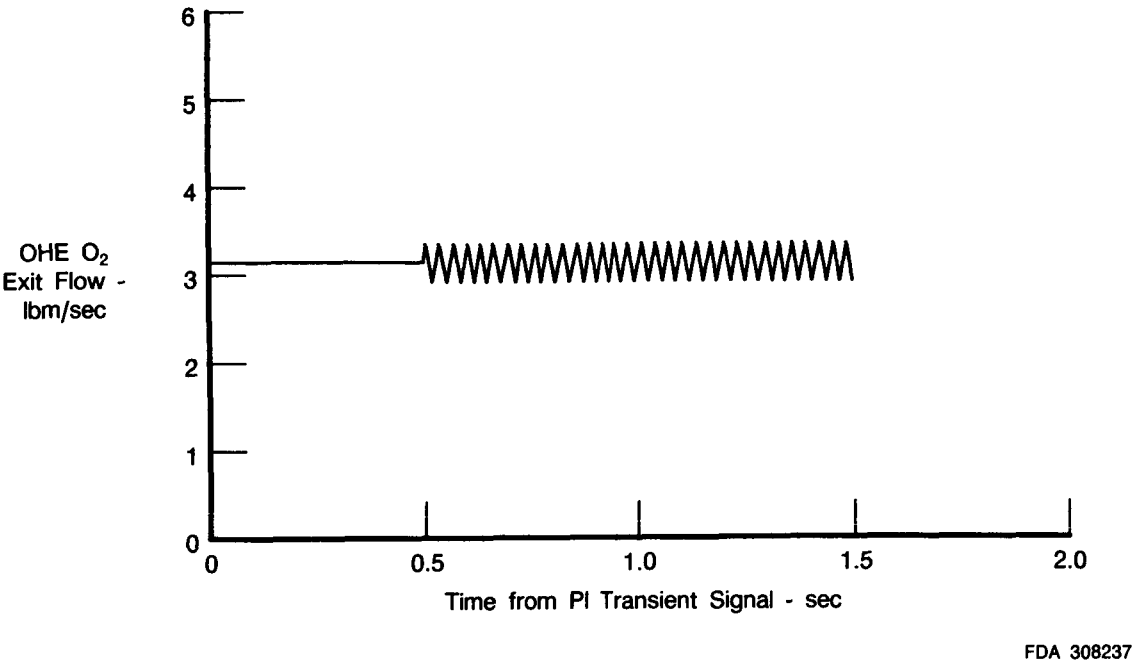

Figure E-3. Predicted OHE Exit Oxidizer Flow Oscillations — Pumped Idle

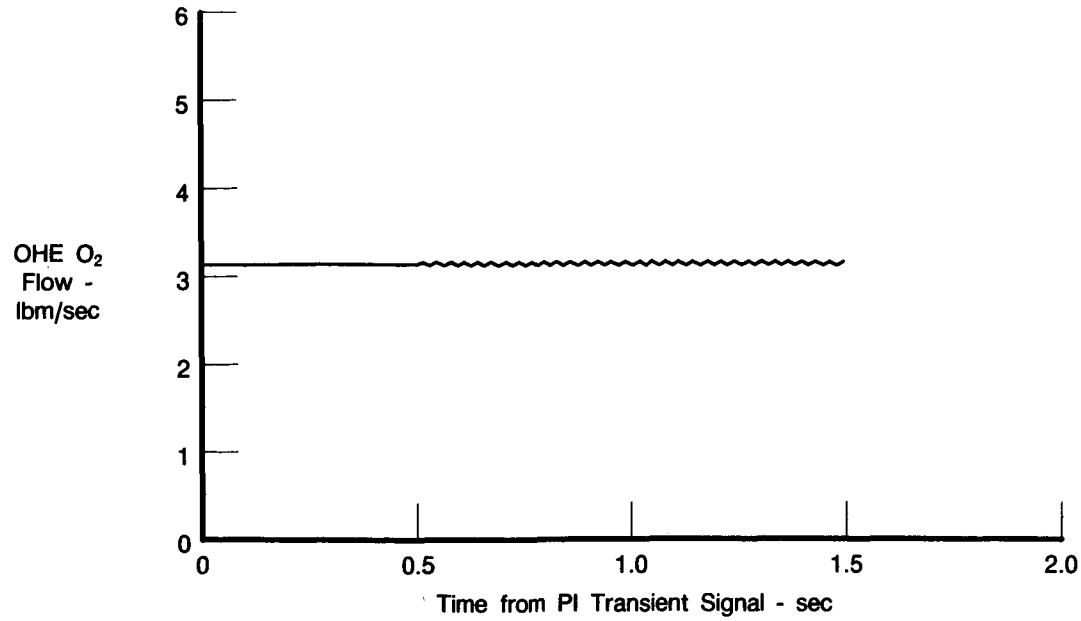

Figure E-4. Predicted Damper Volume Exit Oxidizer Flow Oscillations — Pumped Idle

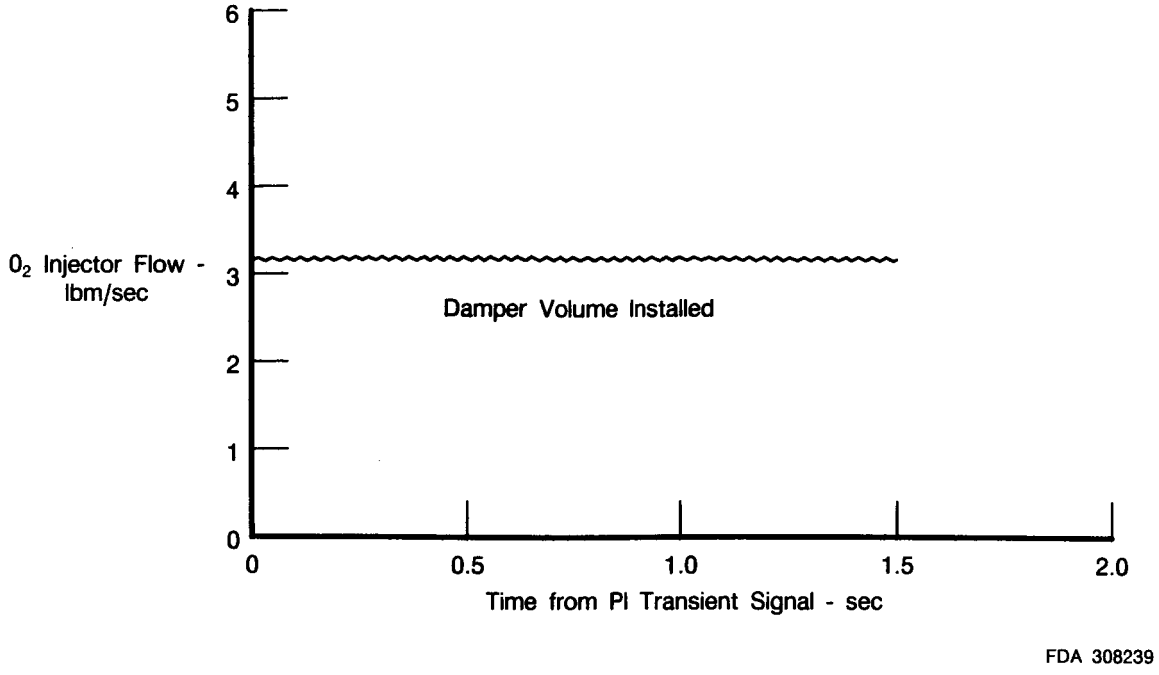

Figure E-5. Predicted Oxidizer Injector Flow Oscillations — Pumped Idle

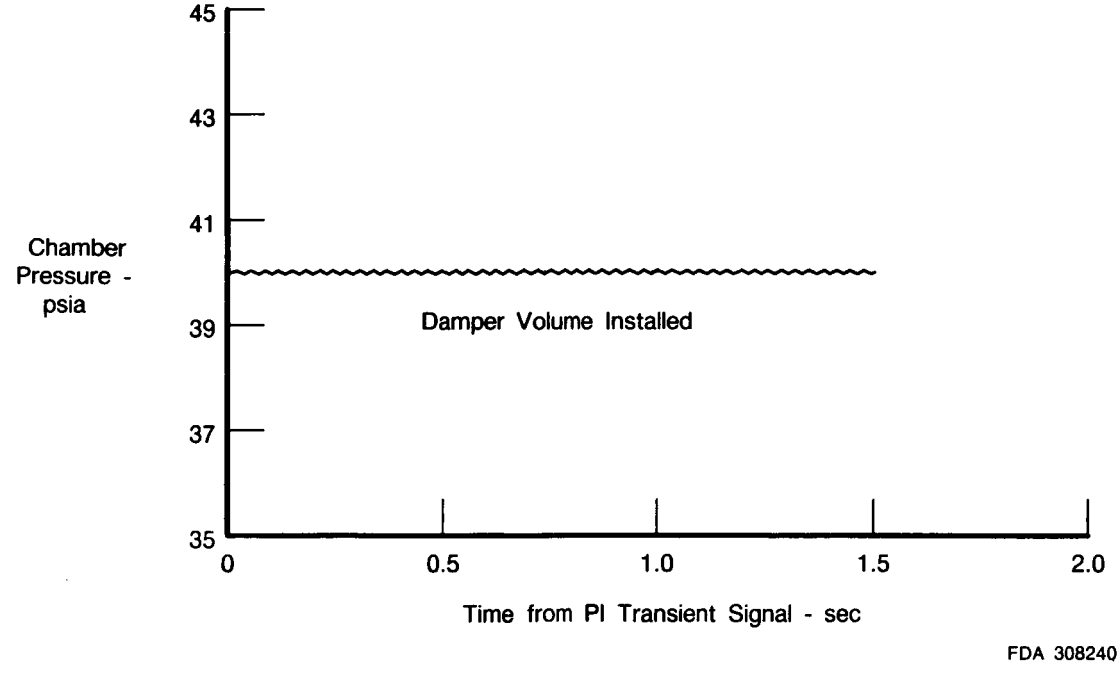

Figure E-6. Predicted Chamber Pressure Oscillations — Pumped Idle

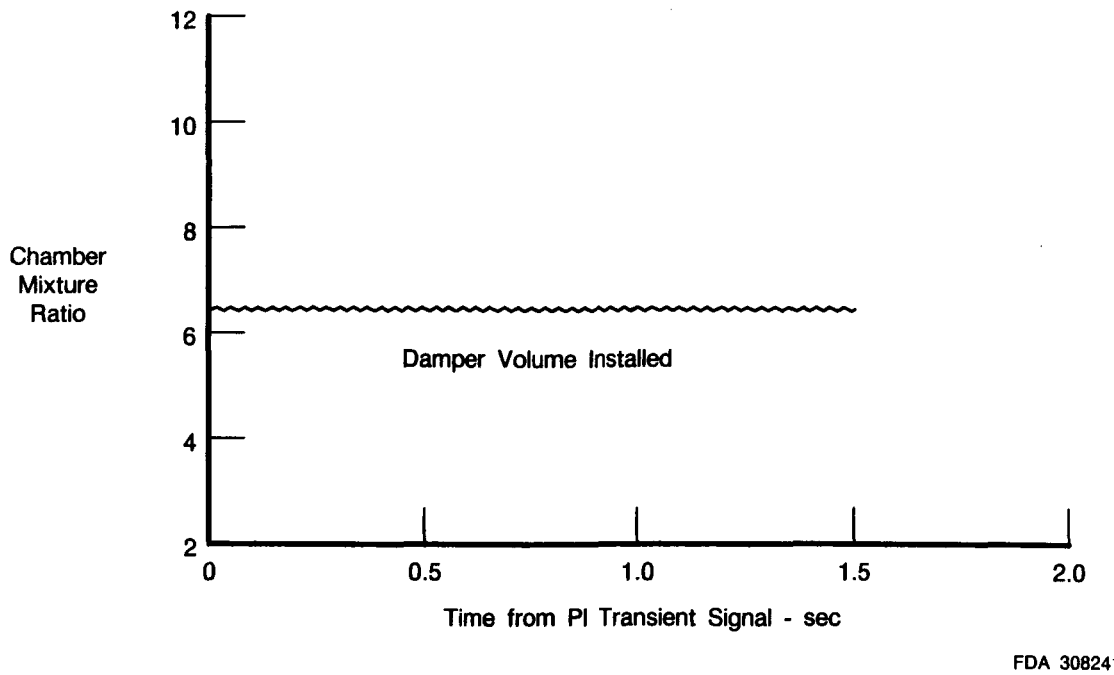

Figure E-7. Predicted Mixture Ratio Oscillations — Pumped Idle

The transient computer simulation was also modified to the first test series configuration. Engine transient from start to THI was predicted using the expected test inlet conditions, ambient temperature pumps, and the control valves steady state positions. Figures E-8 to E-14 present selected predicted engine parameters during start and into the THI period. The transient from THI to PI was also simulated and is shown in Figures E-15 through E-19. Figure E-20 presents the valve sequencing used in the predictions to get an acceptable fuel pump acceleration with the anticipated OHE characteristics.

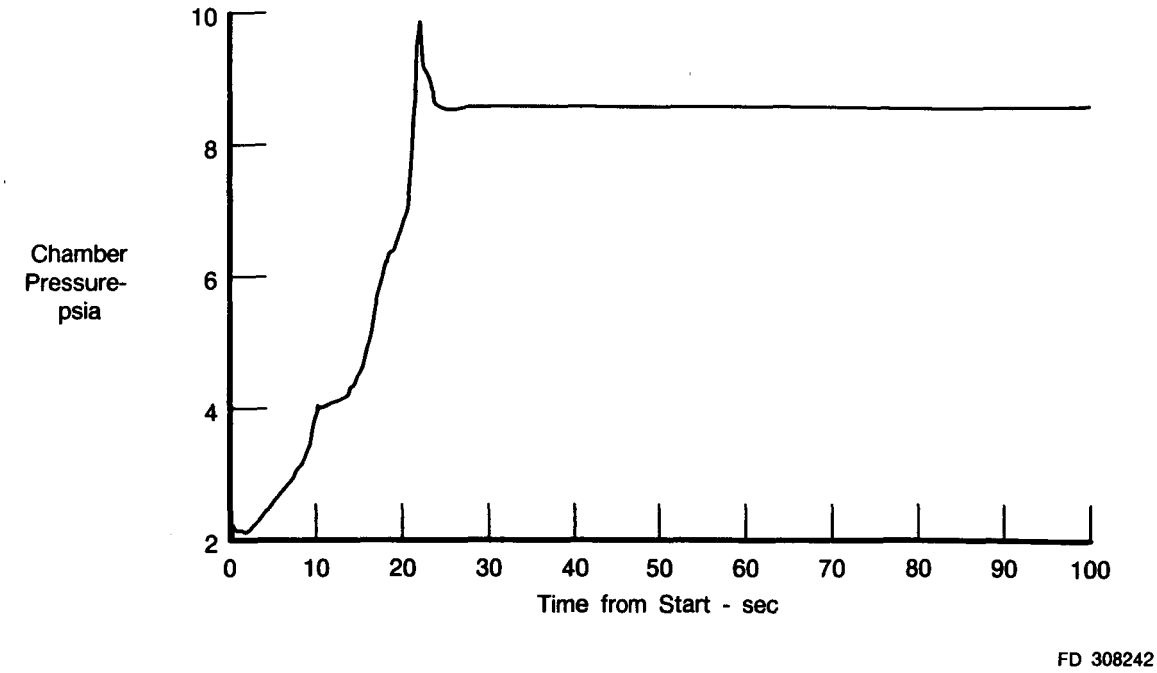

Figure E-8. Predicted Chamber Pressure During Engine Start Transient and Tank Head Idle

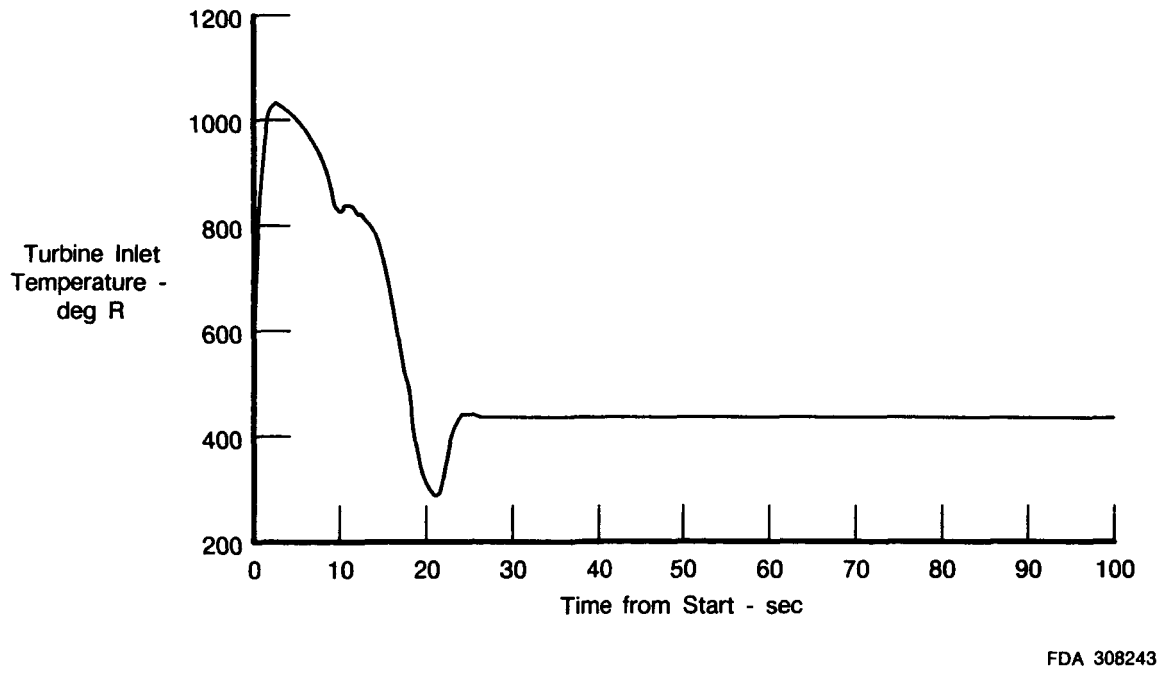

Figure E-9. Predicted Turbine Inlet Temperature During Engine Start Transient and Tank Head Idle

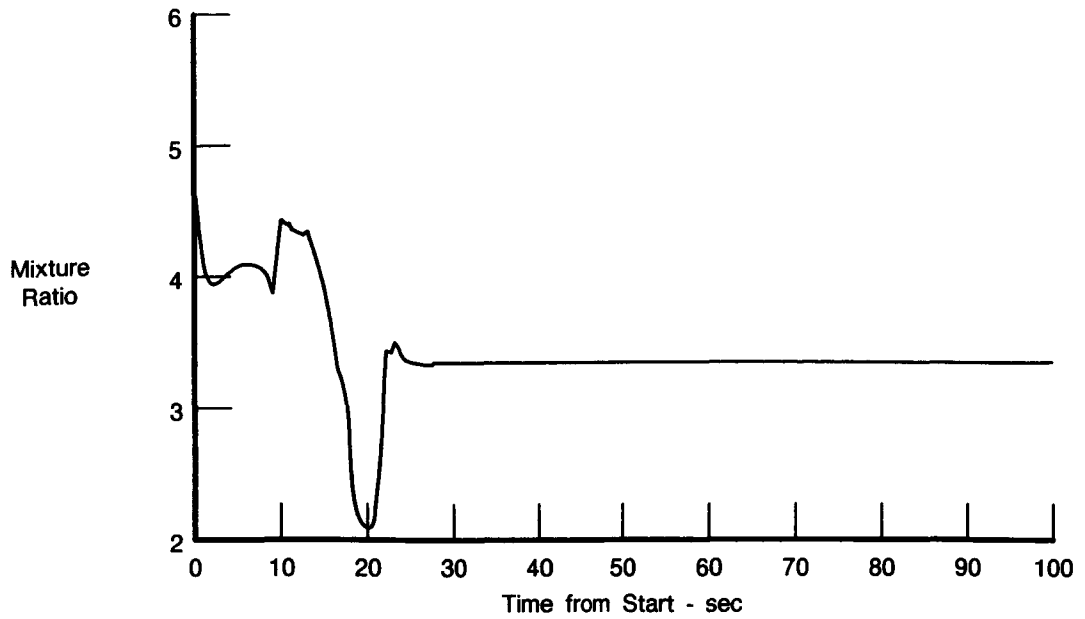

Figure E-10. Predicted Mixture Ratio During Engine Start Transient and Tank Head Idle

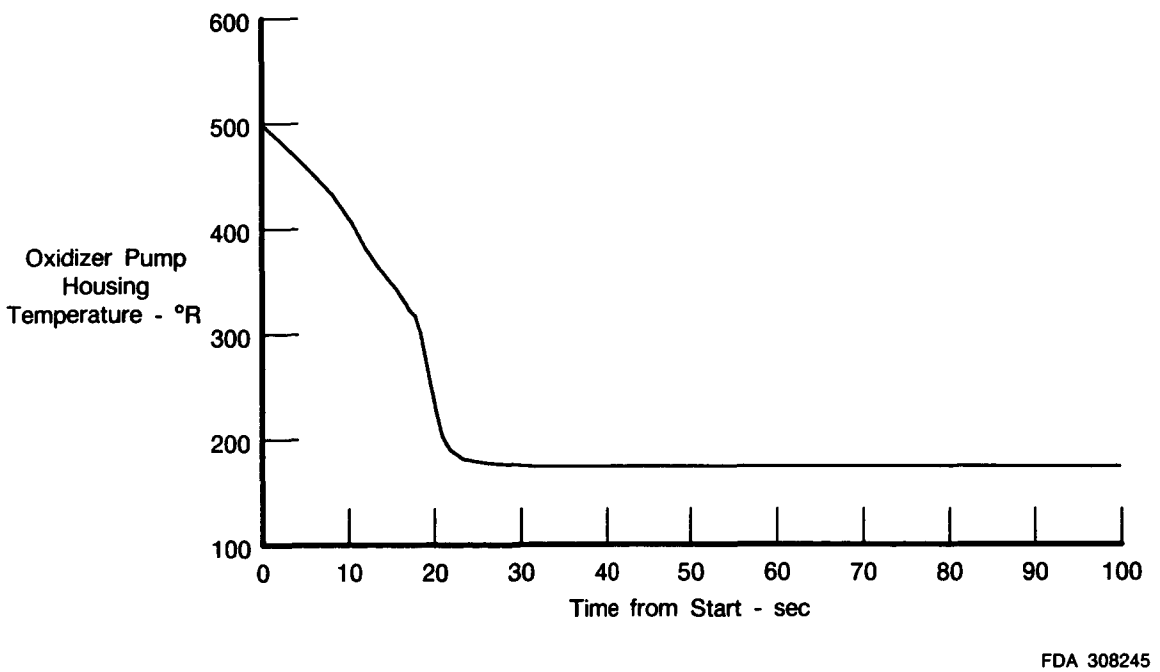

Figure E-11. Predicted Oxidizer Pump Housing Temperature During Engine Start Transient and Tank Head Idle

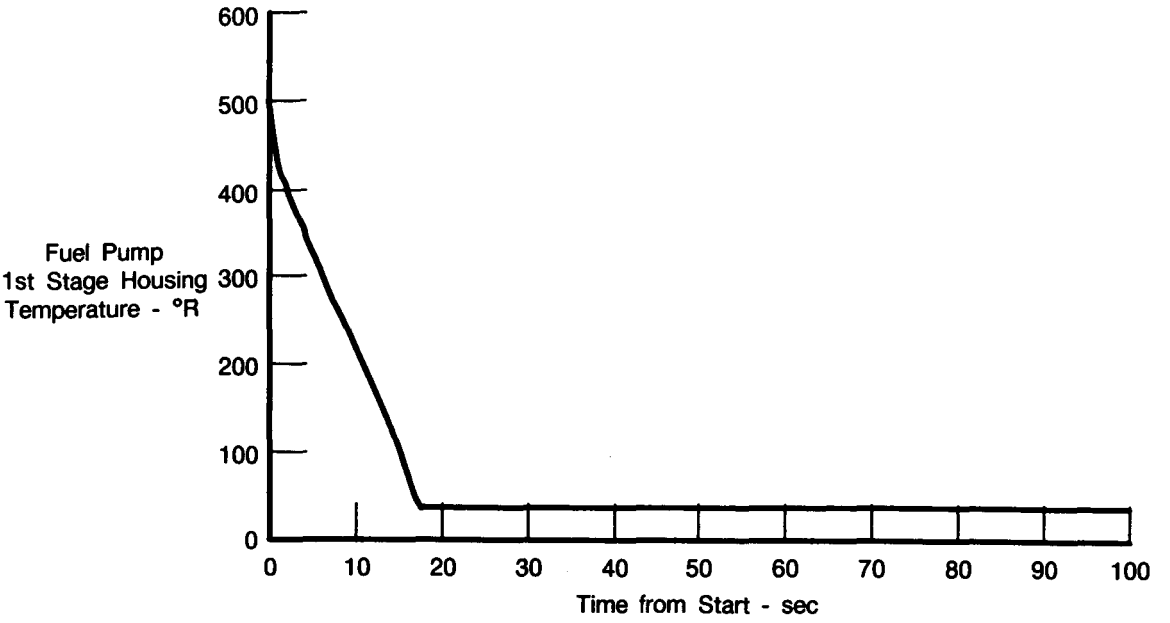

Figure E-12. Predicted Fuel Pump 1st-Stage Housing Temperature During Engine Start Transient and Tank Head Idle

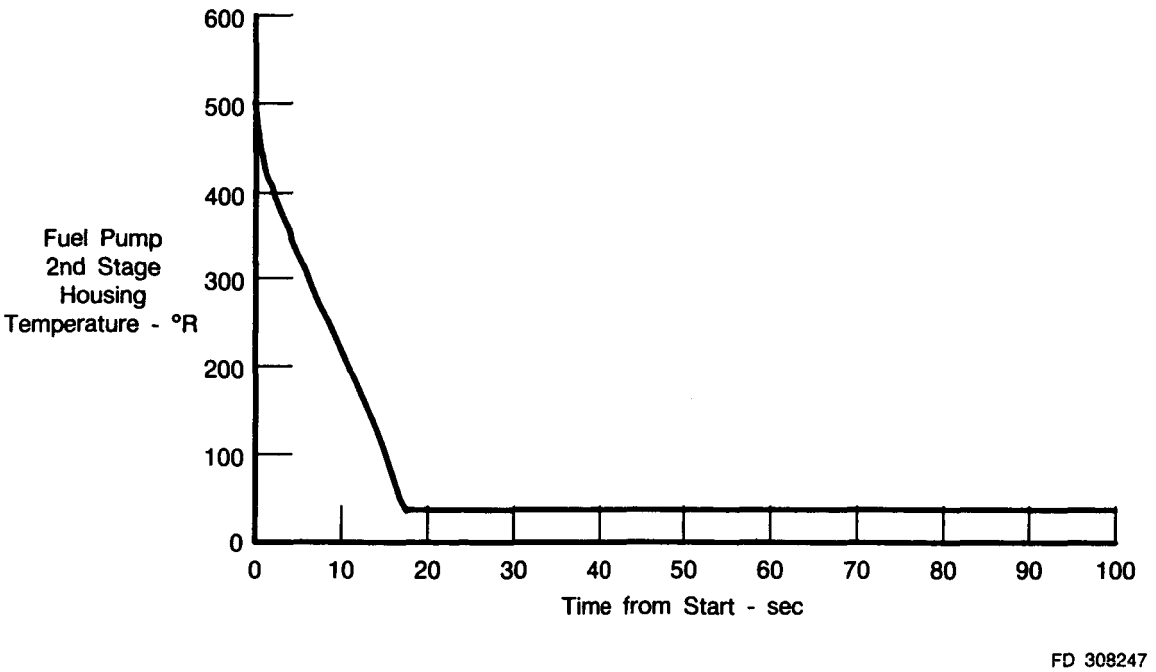

Figure E-13. Predicted Fuel Pump 2nd-Stage Housing Temperature During Engine Start Transient and Tank Head Idle

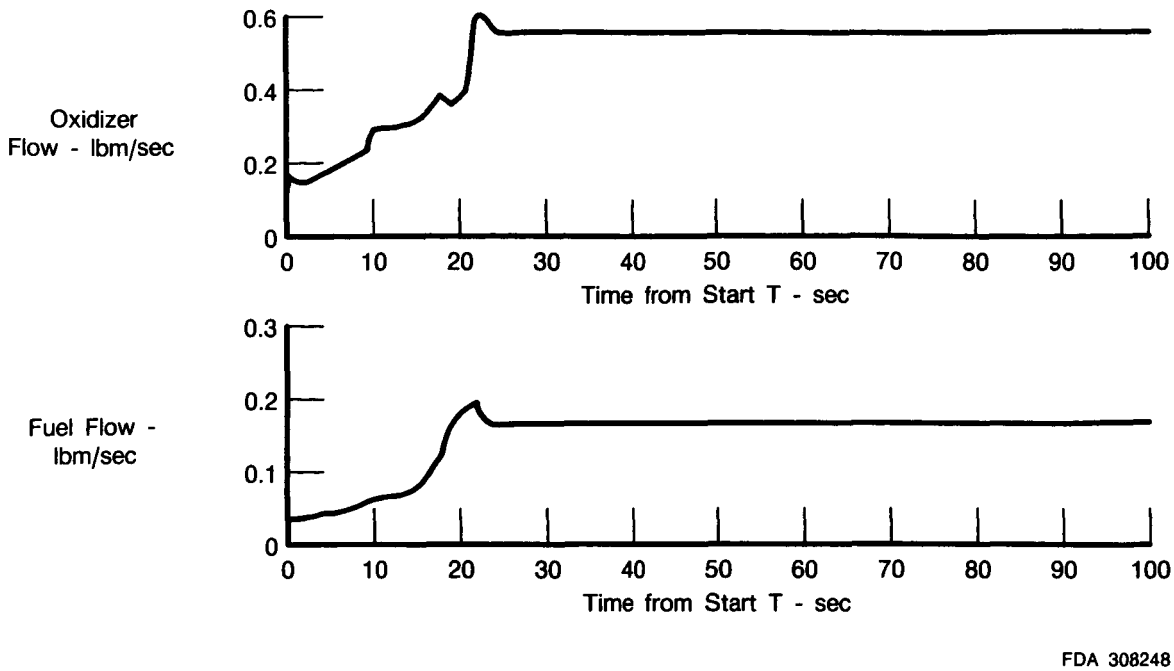

Figure E-14. Predicted Propellant Flow During Engine Start Transient and Tank Head Idle

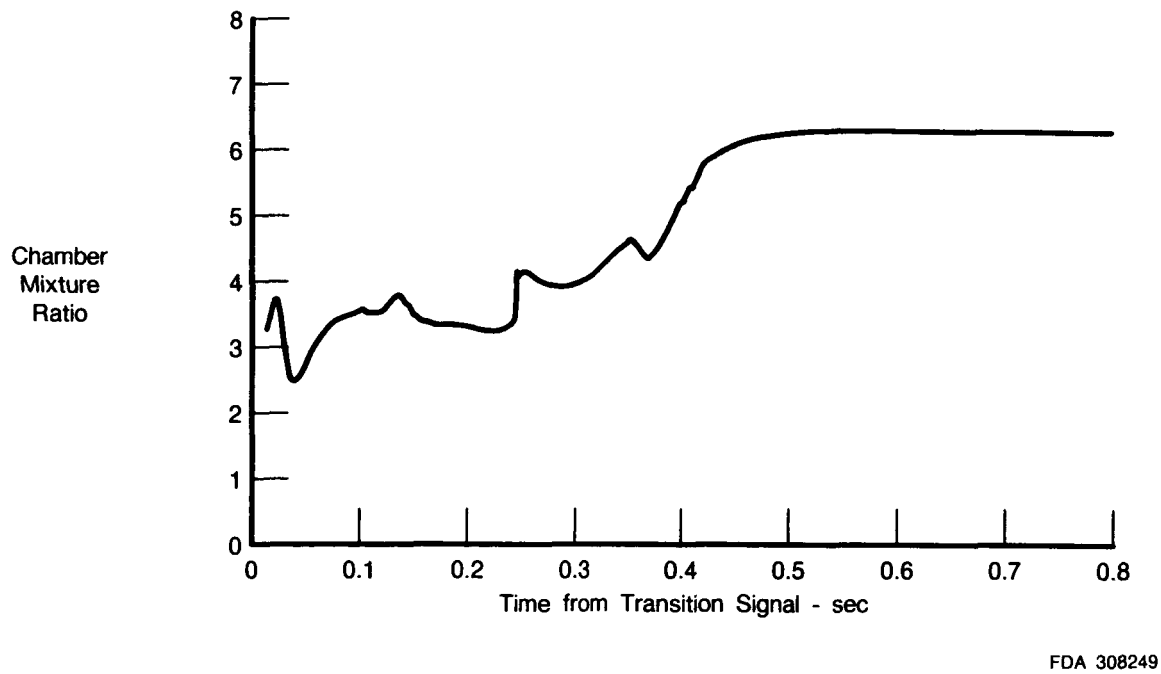

Figure E-15. Predicted Mixture Ratio During Tank Head Idle to Pumped Idle Transient

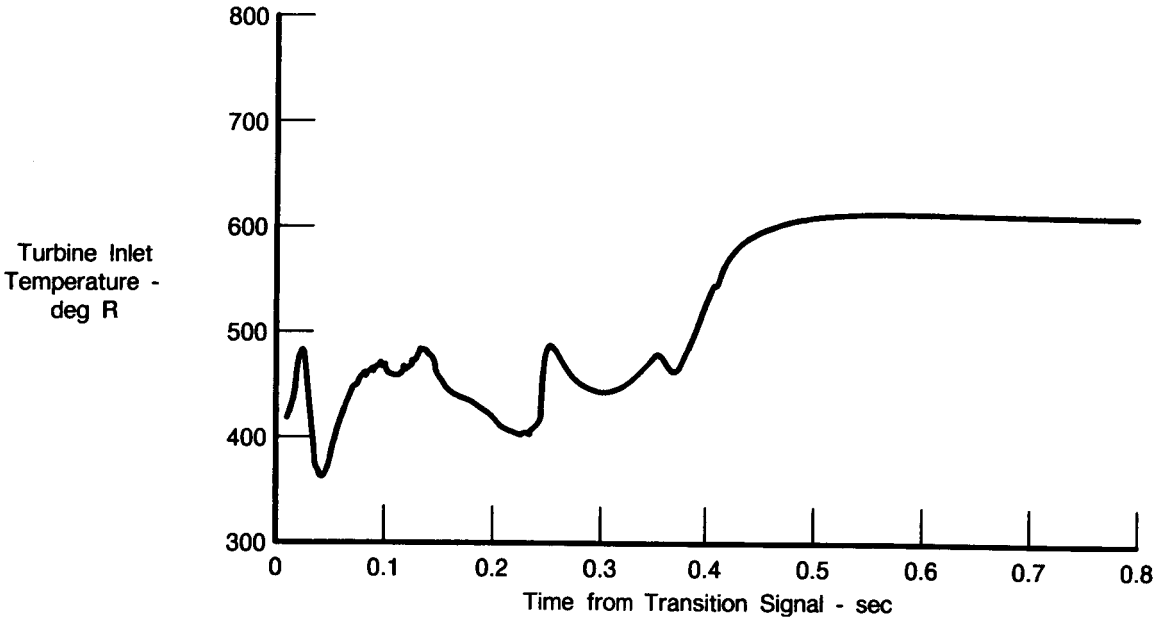

Figure E-16. Predicted Turbine Inlet Temperature During Tank Head Idle to Pumped Idle Transient

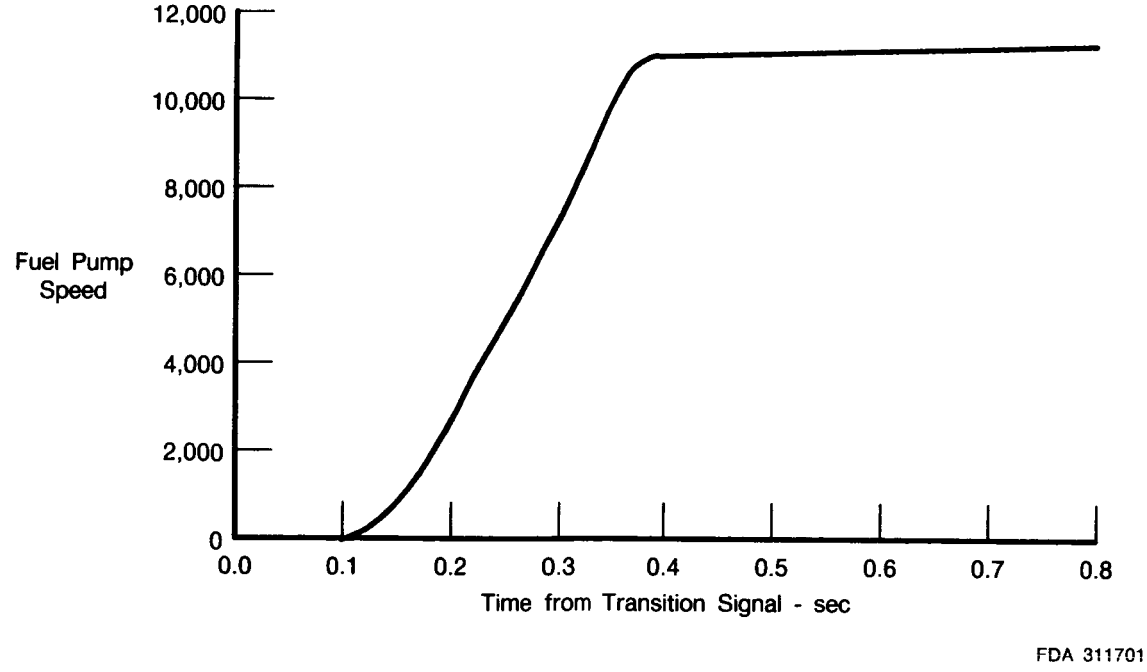

Figure E-17. Predicted Fuel Pump Speed During Tank Head Idle to Pumped Idle Transient

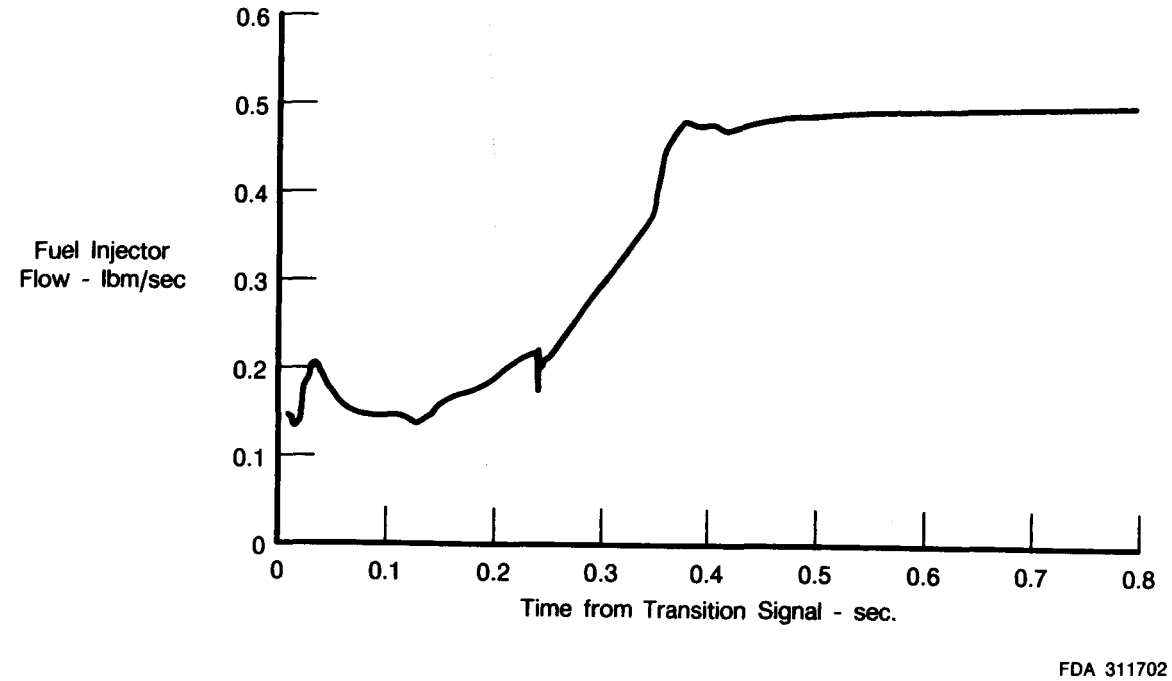

Figure E-18. Predicted Fuel Injector Flow During Tank Head Idle to Pumped Idle Transient

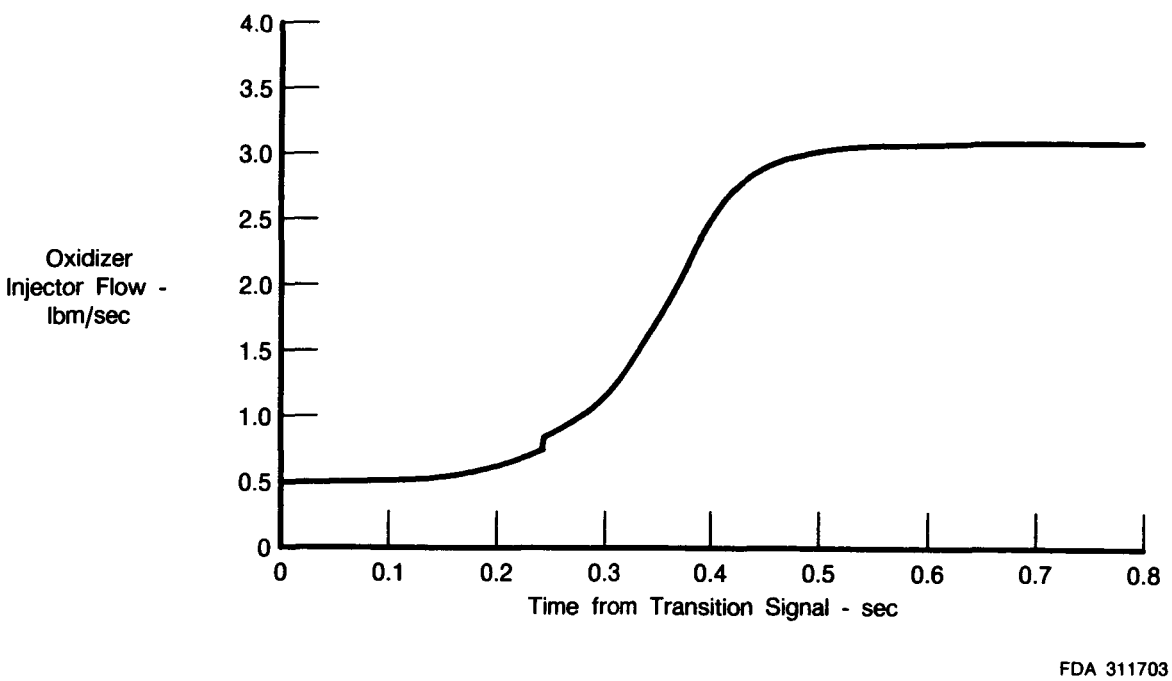

Figure E-19. Predicted Oxidizer Injector Flow During Tank Head Idle to Pumped Idle Transient

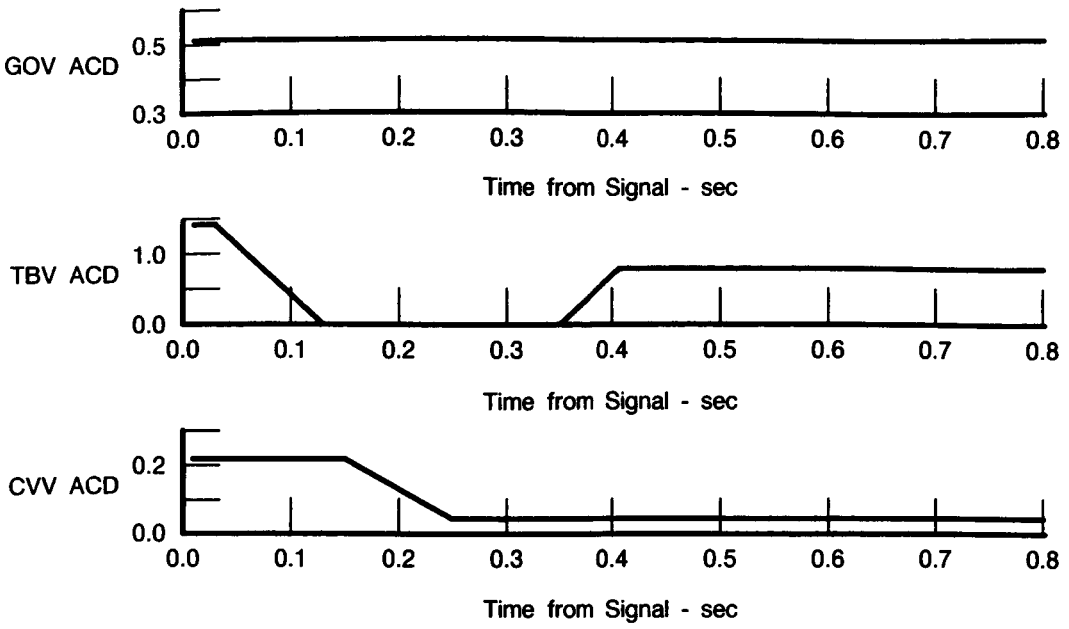

Figure E-20. Valve Sequencing for Predicted Tank Head Idle to Pumped Idle Transient

POST-TEST

Several modifications were made to the computer simulation as a result of the XR201-1 testing. Chamber/nozzle heat transfer characteristics at low thrust were correlated with mixture ratio while the Stage 3 oxidizer heat exchanger heat transfer was correlated as a function of both mixture ratio, which has a strong effect on the driving fluid initial temperature, and oxidizer mass flowrate because of its relation to the convective heat transfer coefficient. Oxidizer side pressure loss on the OHE was matched as a function of chamber pressure while fuel mass flowrate was used to correlate the OHE fuel side pressure losses since pressure loss is a direct function of flowrate for a gas. The effective flow areas of both injectors were adjusted in each computer deck to correspond to test data results. Line loss K-factors, especially important for tank head idle operation, were matched to the test results. The effective area of the test turbine was calculated for use in the transient simulation.

The steady state computer simulation was modified with the XR201-1 test results and cycle points were generated to compare with selected set points. Table E-2 shows pertinent measured and calculated parameters for two tank head idle points from HR 15.01, with mixture ratios of 4.0 and 5.7 for variance. Valve areas were set and the decks were balanced to chamber pressure and mixture ratio. The agreement between test data and cycle deck is considered good. Pumped idle operation was also simulated and three test points from HR 15.01 are presented in Table E-3 for a mixture ratio range of 4.2 to 6.3. Test inlet conditions were input and the cycle deck balanced to chamber pressure and mixture ratio with set valve areas. The fuel side agrees closely with the test data while the oxidizer side appears to be slightly different in some areas.

Table E-2. *Steady State Cycle Deck Match With XR201-1 Test Data*
Hot Run 15.01
Tank Head Idle Thrust

	Test Data	*Cycle Deck*	*Test Data*	*Cycle Deck*
EDR Time, (sec)*	118.0	—	191.0	—
Chamber Pressure, psia	8.6	8.6	10.6	10.6
Chamber Mixture Ratio	3.984	3.983	5.659	5.693
Inlet Fuel Flow, lbm/sec	0.143	0.143	0.143	0.142
Inlet Oxidizer Flow, lbm/sec	0.570	0.571	0.809	0.807
Fuel Inlet Pressure, psia	31.7	31.1	31.5	31.8
Fuel Inlet Temperature, R	37.7	37.7	37.5	37.5
Coolant Jacket Inlet Pressure, psia	29.9	29.4	30.2	30.1
Coolant Jacket Temperature Rise, R	689.0	690.0	708.0	703.0
Turbine Inlet Pressure, psia	24.4	23.9	24.7	24.4
Fuel Hex Inlet Pressure, psia	17.7	18.0	18.2	18.7
Fuel Hex Pressure Loss, psi	5.8	5.3	5.1	5.7
Hex Heat Transfer, Btu/sec	46.1	47.9	69.6	66.4
Fuel Injector Manifold Pressure, psia	10.8	10.6	12.3	12.1
Oxidizer Inlet Pressure, psia	35.8	33.2	35.9	35.1
Oxidizer Inlet Temperature, R	173.2	173.2	173.2	173.2
Oxidizer Hex Inlet Pressure, psia	34.8	33.0	35.5	34.7
Oxidizer Hex Pressure Loss, psi	0.74	0.71	0.76	0.55
GOV Pressure Loss, psi	10.7	10.6	2.5	2.1

*Recording system time for reference only.

6083M

The computer simulation describing the transient to THI was also modified with the test data results. The Oxidizer Pump Housing Temperature from start for HR 5.01 was simulated and is shown in Figure E-21. This compares poorly with the actual test data shown in Figure E-22 due to the heat input to the pumps because the Mylar blanket was not installed. The difficulty of simulating an unmeasured heat input into the pump precluded any attempt to do so. The computer simulation, however, would be useful for predicting pump cooldown with the Mylar blanket installed.

To evaluate the control valve effectiveness with a low heat transfer OHE, THI transients were simulated at the inlet pressure (20 psia) expected for future tests and a combination of either saturated liquid or saturated vapor propellants. The simulation employed the lower heat transfer characteristics experienced during the testing, but had the predicted low pressure losses. Figure E-23 presents the range of mixture ratios encountered with the various inlet conditions. With a GOV area of 0.3 $in.^2$, the mixture ratios are in an acceptable (2.0:1 to 3.0:1) range with saturated liquid at the oxidizer inlet. However, they become unacceptably low with saturated vapor at the oxidizer inlet. Increasing the GOV area to 0.5 $in.^2$ raises the low mixture ratios into a more acceptable range.

Table E-3. *Steady State Cycle Deck Match With XR201-1 Test Data*
Hot Run 15.01
Pumped Idle Thrust

	Test Data	*Cycle Deck*	*Test Data*	*Cycle Deck*	*Test Data*	*Cycle Deck*
EDR Time, sec*	400.0	—	474.0	—	507.0	—
Chamber Pressure, psia	45.4	45.4	39.4	39.4	32.9	32.9
Chamber Mixture Ratio	6.348	6.345	5.277	5.274	4.237	4.234
Thrust, lb	1754.8	1756.0	1477.2	1477.0	1196.7	1198.0
Specific Impulse, sec	424.0	424.0	429.2	428.7	433.3	433.3
Injector Fuel Flow, lbm/sec	0.560	0.560	0.545	0.546	0.524	0.524
Inlet Oxidizer Flow, lbm/sec	3.555	3.553	2.876	2.880	2.220	2.219
Fuel Bypass Flow, lbm/sec	0.262	0.263	0.258	0.258	0.249	0.249
Fuel Inlet Pressure, psia	33.8	33.8	33.9	33.9	33.8	33.8
Fuel Inlet Temperature, R	39.4	39.4	39.6	39.6	39.4	39.4
Fuel Pump Discharge Pressure, psia	123.6	124.7	121.7	122.4	118.1	119.3
Coolant Jacket Inlet Pressure, psia	89.2	90.4	82.9	83.5	75.0	76.1
Coolant Jacket Temperature Rise, R	593.0	598.0	564.0	555.0	536.0	536.0
Turbine Inlet Pressure, psia	62.5	60.8	57.0	54.9	50.8	47.7
Fuel Hex Inlet Pressure, psia	56.7	55.1	51.1	49.7	44.9	43.7
Fuel Hex Pressure Loss, psi	4.1	4.8	4.0	3.8	3.7	5.0
Hex Heat Transfer, Btu/sec	106.3	100.6	67.0	63.0	26.6	47.2
Fuel Injector Manifold Pressure, psia	50.3	50.3	44.6	44.9	38.6	38.8
Oxidizer Inlet Pressure, psia	39.0	39.0	41.1	41.1	40.9	40.9
Oxidizer Inlet Temperature, R	173.7	173.7	173.7	173.7	174.0	174.0
Oxidizer Hex Inlet Pressure, psia	102.5	107.0	98.3	106.8	99.6	103.6
Oxidizer Hex Pressure Loss, psi	8.7	9.4	4.3	6.3	1.7	3.9
GOV Pressure Loss, psi	13.0	25.5	31.6	42.5	50.3	53.9

*Recording system time for reference only

6083M

When the transient from tank head idle to pumped idle was simulated using the valve schedule shown in Figure E-24 from HR 5.01, the pump began to rotate as soon as the turbine shutoff valve started to open, thus duplicating the actual test results. This indicated that the unanticipated breakaway ease of the turbopump during the pumped idle transient was caused by the high pressure loss of the heat exchanger and not lower than predicted breakaway torque levels. The transient from tank head idle to pumped idle for HR 11.01 was then simulated and is shown in Figures E-25 to E-27. The GOV and TBV were held constant while the CVV was actuated as it was during the test (Figure E-28). The FVV downstream of the pump was simulated to open during the start to load down the pump, preventing it from overspeeding. This resulted in a transient that is comparable to the actual test data shown in Figure E-29.

The current computer program is an effective tool in the prediction of steady state operation at THI and PI thrust levels for a RL10-IIB engine with a RL10A-3-3A thrust chamber/nozzle and a Stage 3 OHE. The computer program will prove useful in the accurate prediction of key engine parameters such as mixture ratio and chamber pressure for THI operation and combustion stability at PI. The transient simulation also proved effective although additional work is needed to accurately predict heat absorbed by uninsulated pumps during THI. The computer simulation model was used to evaluate the control valve effectiveness with a heat exchanger having a low heat transfer characteristic. The simulation indicated that acceptable mixture ratios are attainable with a constant GOV setting across the range of propellant inlet conditions. Further, it was determined, using the computer simulation, that the breakaway of the

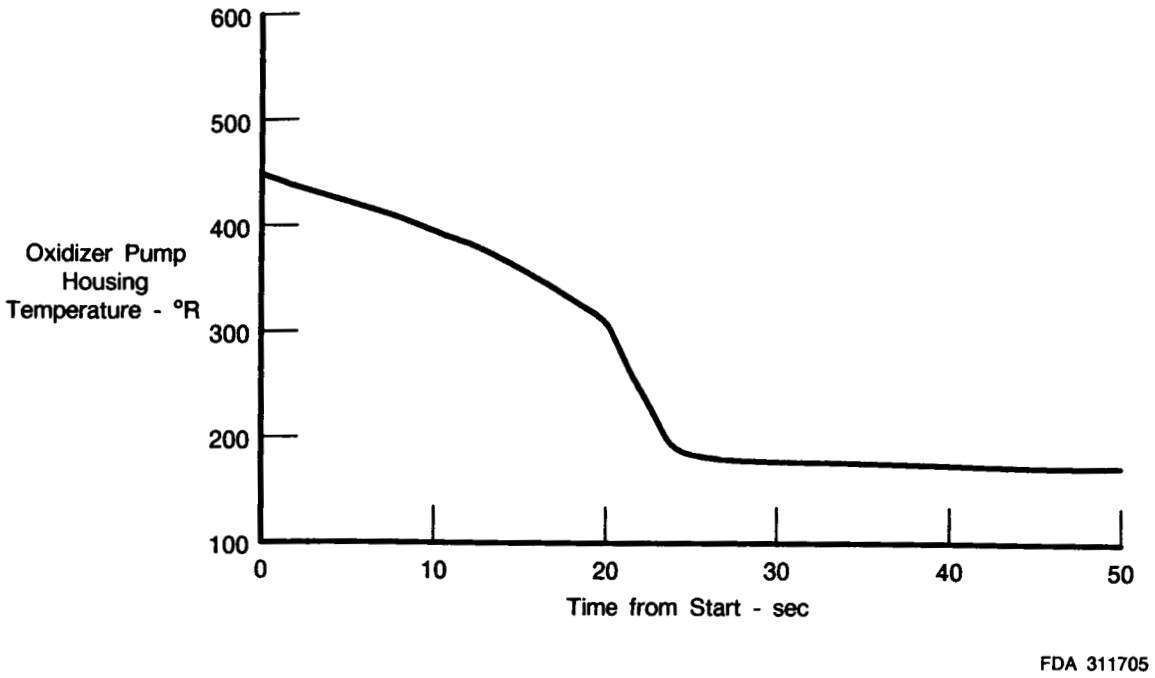

Figure E-21. Predicted Oxidizer Pump Housing Temperature During THI

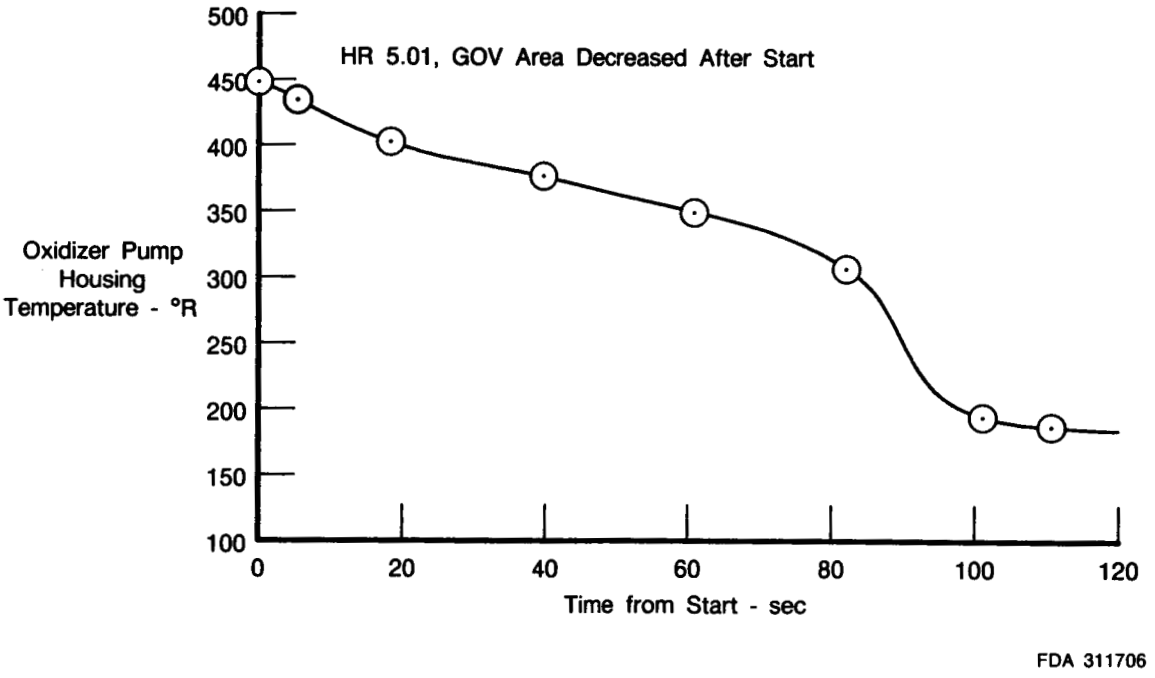

Figure E-22. XR201-1 Oxidizer Pump Housing Temperature During THI

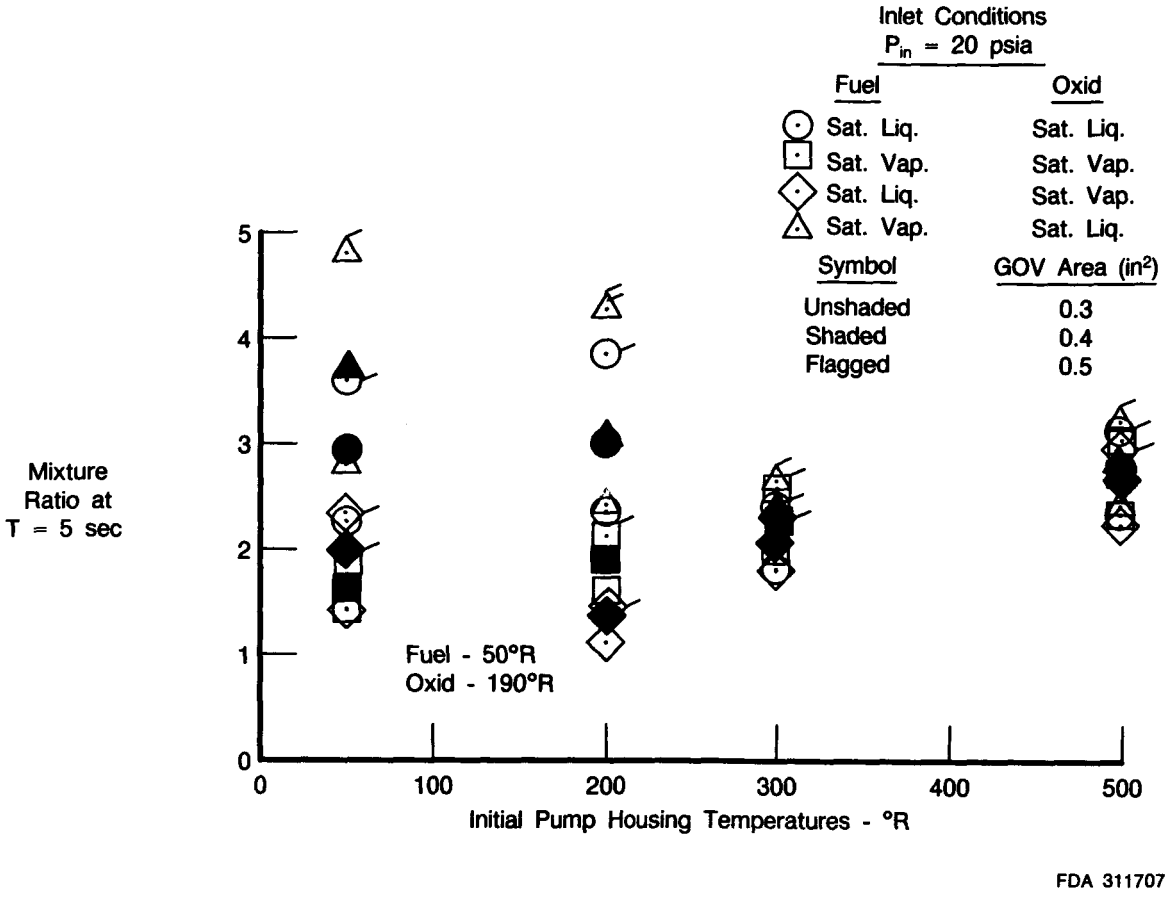

Figure E-23. Predicted Mixture Ratio Variations

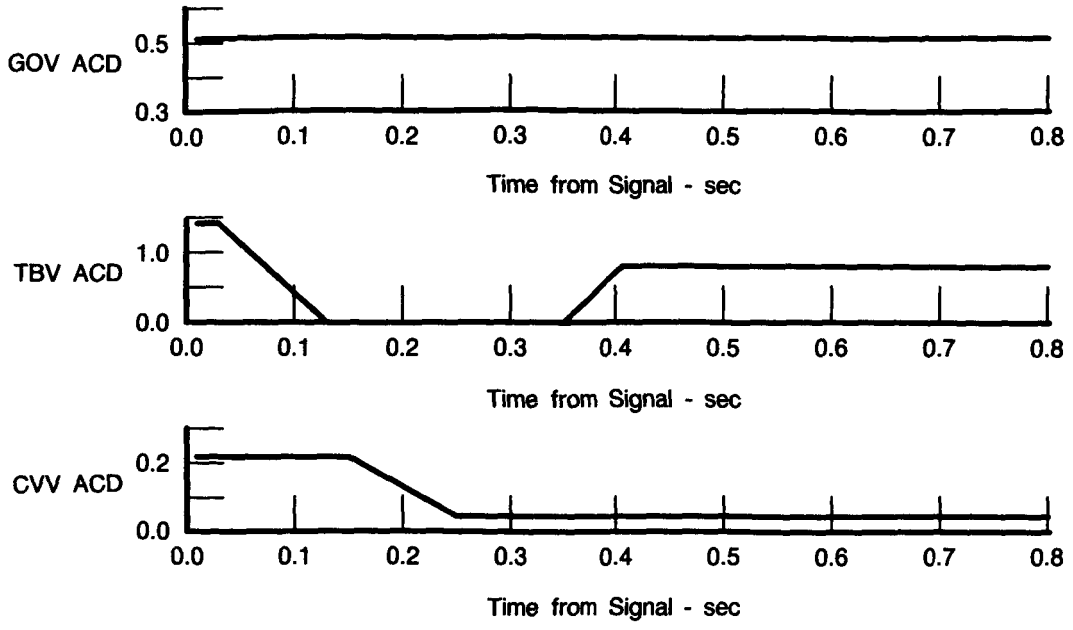

Figure E-24. Valve Sequencing During Tank Head Idle to Pumped Idle Transient (Run 5.01 Simulation)

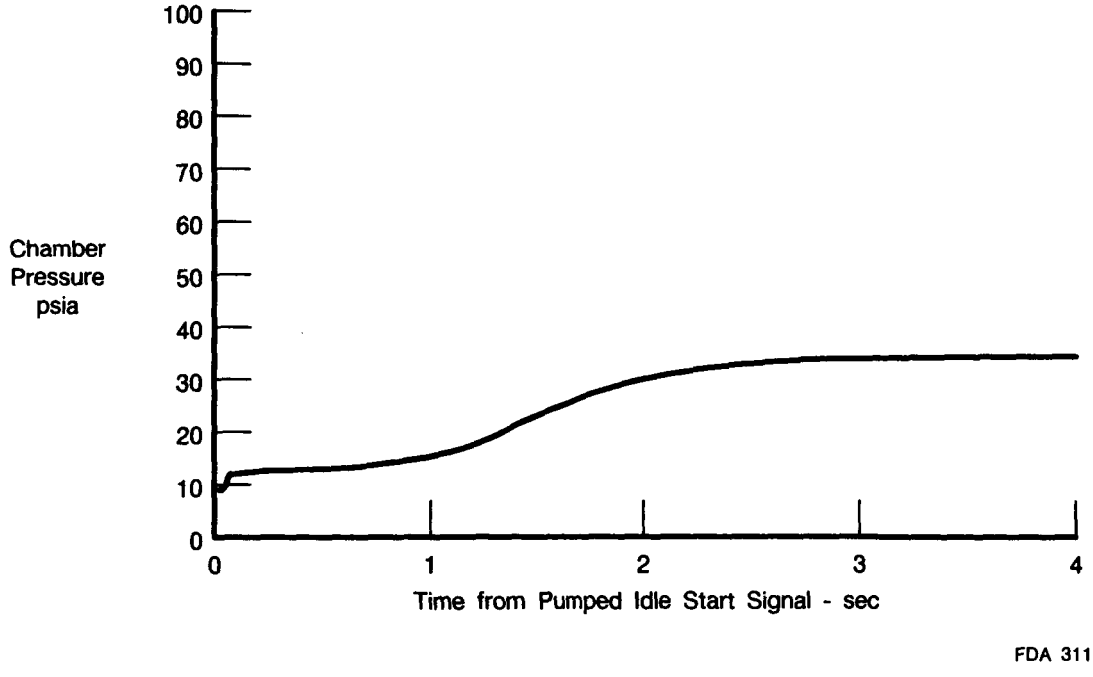

Figure E-25. Predicted Chamber Pressure During Pumped Idle Transient (Run 11.01 Simulation)

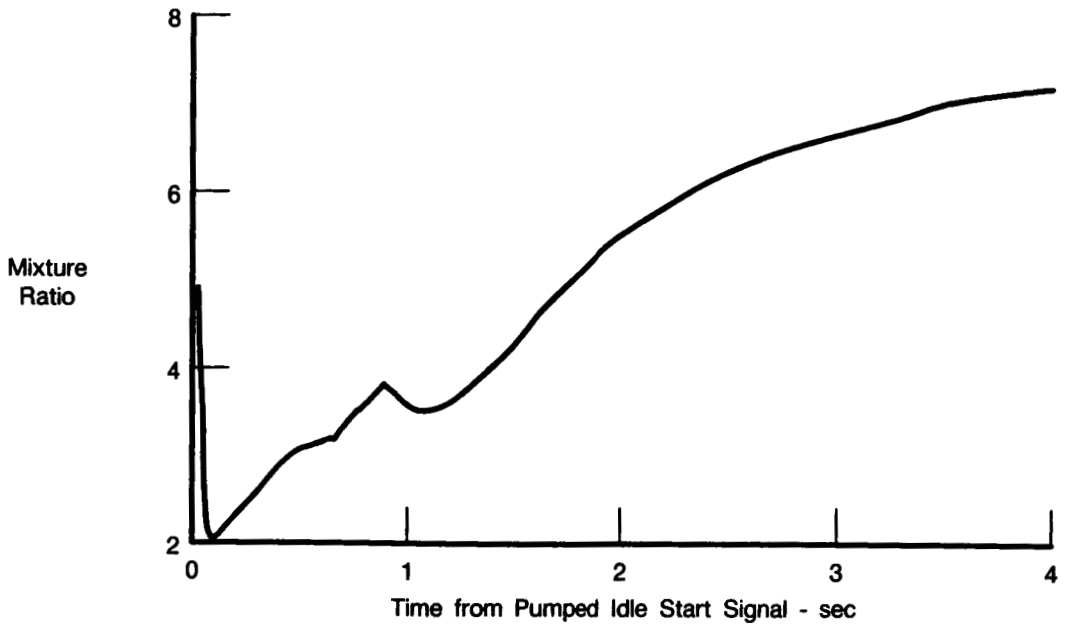

Figure E-26. Predicted Mixture Ratio During Pumped Idle Transient (Run 11.01 Simulation)

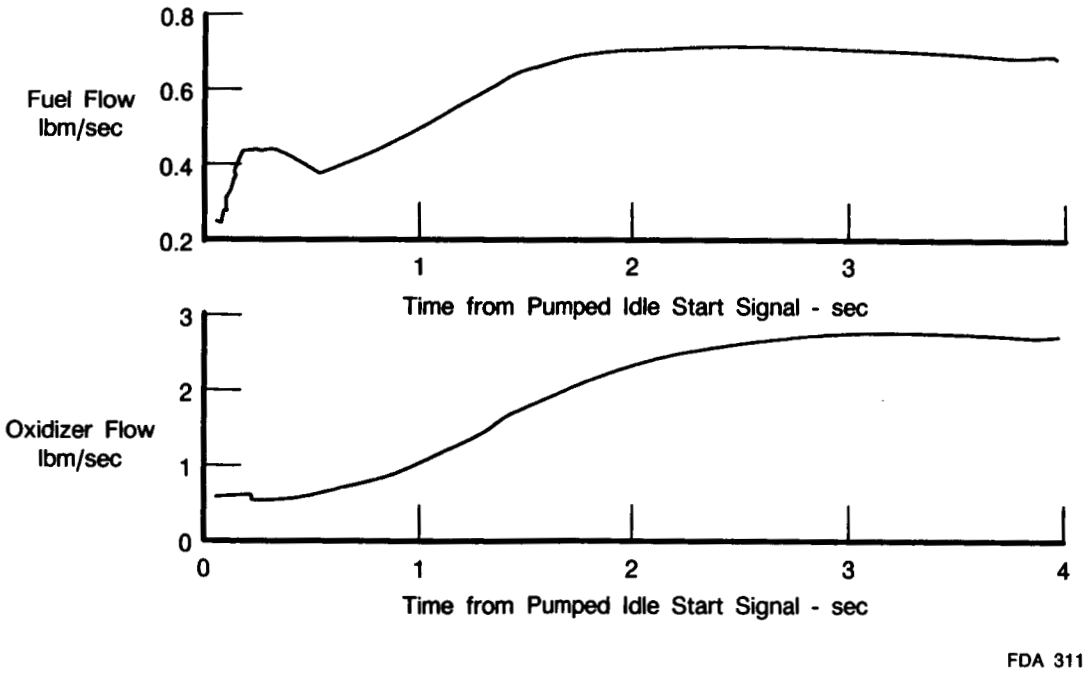

Figure E-27. Predicted Propellant Flow During Pumped Idle Transient (Run 11.01 Simulation)

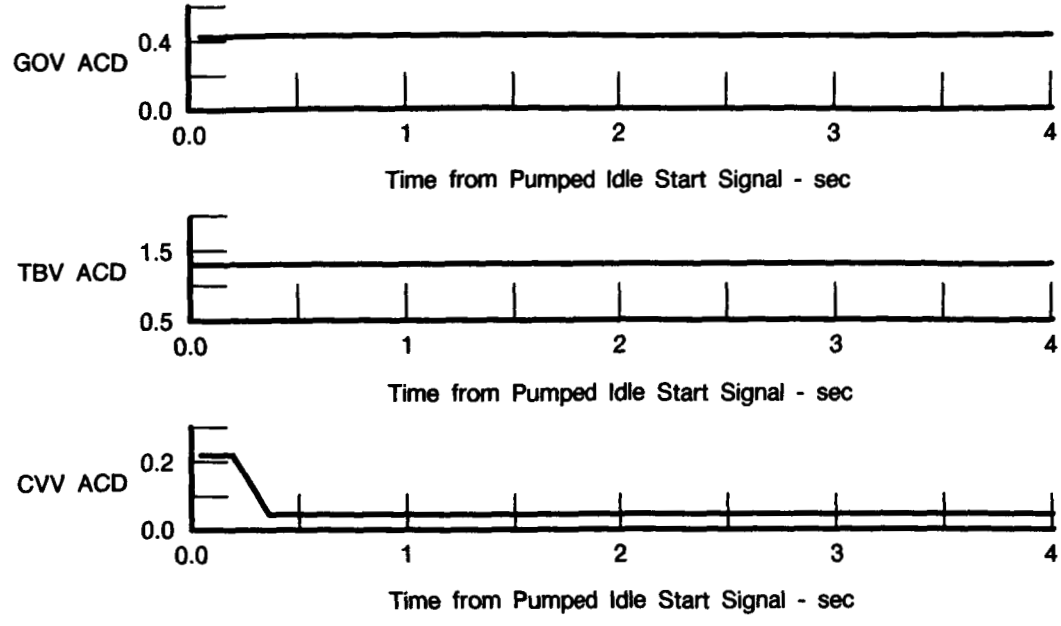

Figure E-28. Valve Sequencing During Pumped Idle Transient (Run 11.01 Simulation)

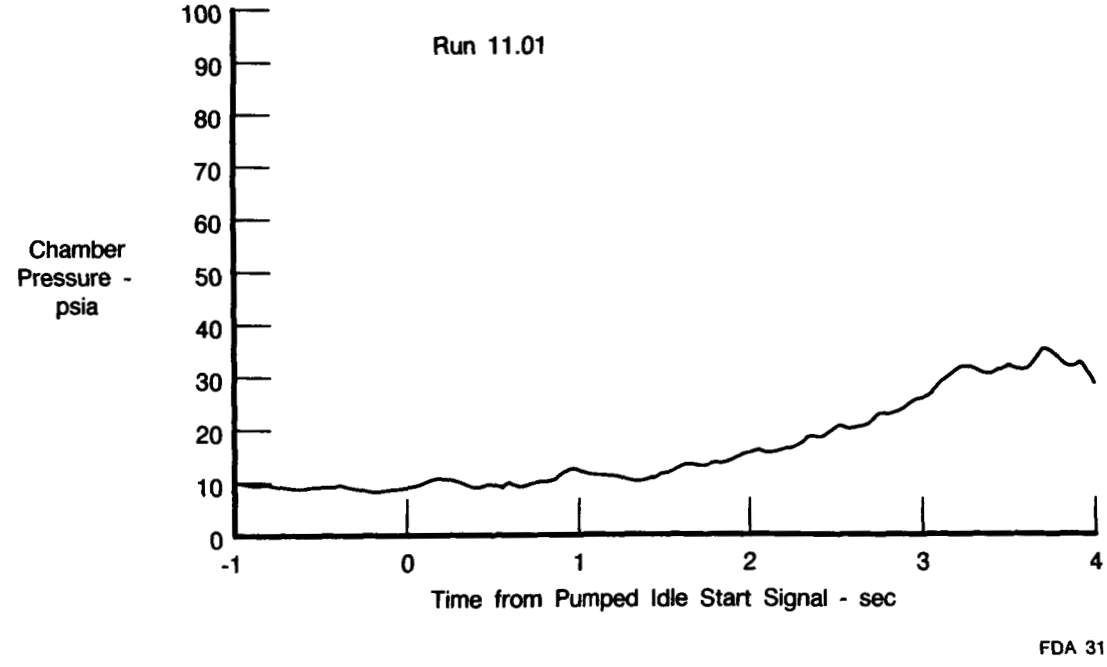

Figure E-29. XR201-1 Chamber Pressure During Pumped Idle Transient

PRESSURE OSCILLATION PREDICTION

Prior to testing, a method to calculate the heat exchanger oxidizer side discharge pressure oscillations was derived from Reference 2. Using anticipated test conditions, this method predicted pressure oscillations at PI with a high frequency (31.7 cps) and a low amplitude

(±2.3 psi). During testing, however, the oscillations experienced were low in frequency (2-4 cps) and high in amplitude (12-22 psi). When the actual XR201-1 test conditions were used in the prediction program, along with the reduced flow area indicated by the high OHE pressure losses, frequencies and amplitudes closer to test values were calculated. These predicted numbers were compared to the actual test data and are presented in the form of ratios in Figure E-30. In addition, the computer program was run so that the predicted frequency matched the test frequency in order to examine the theoretical relationship between frequency and amplitude. The amplitude obtained, which is a function of the frequency, was then compared to XR201-1 test data and the results are also shown as ratios in Figure E-30. Figure E-31 shows the amplitude number versus the threshold boiling number and compares the relationship of XR201-1 test data to the pressure amplitude correlation used in the prediction method. As can be seen from the inserted plot, the XR201-1 test data falls within the scatter band of the test data used in Reference 2. The prediction technique could be modified to more correctly predict the oscillation characteristics for future testing. This could be done by taking into consideration the differences in test conditions between the original test setup (Reference 2) and the XR201-1 test series. The original setup included higher inlet pressures, constant heat input along the tubes, and integration to obtain the density changes axially within the heat exchanger. The computer simulation could be changed to include a density integration procedure as well as a more accurate heat transfer routine.

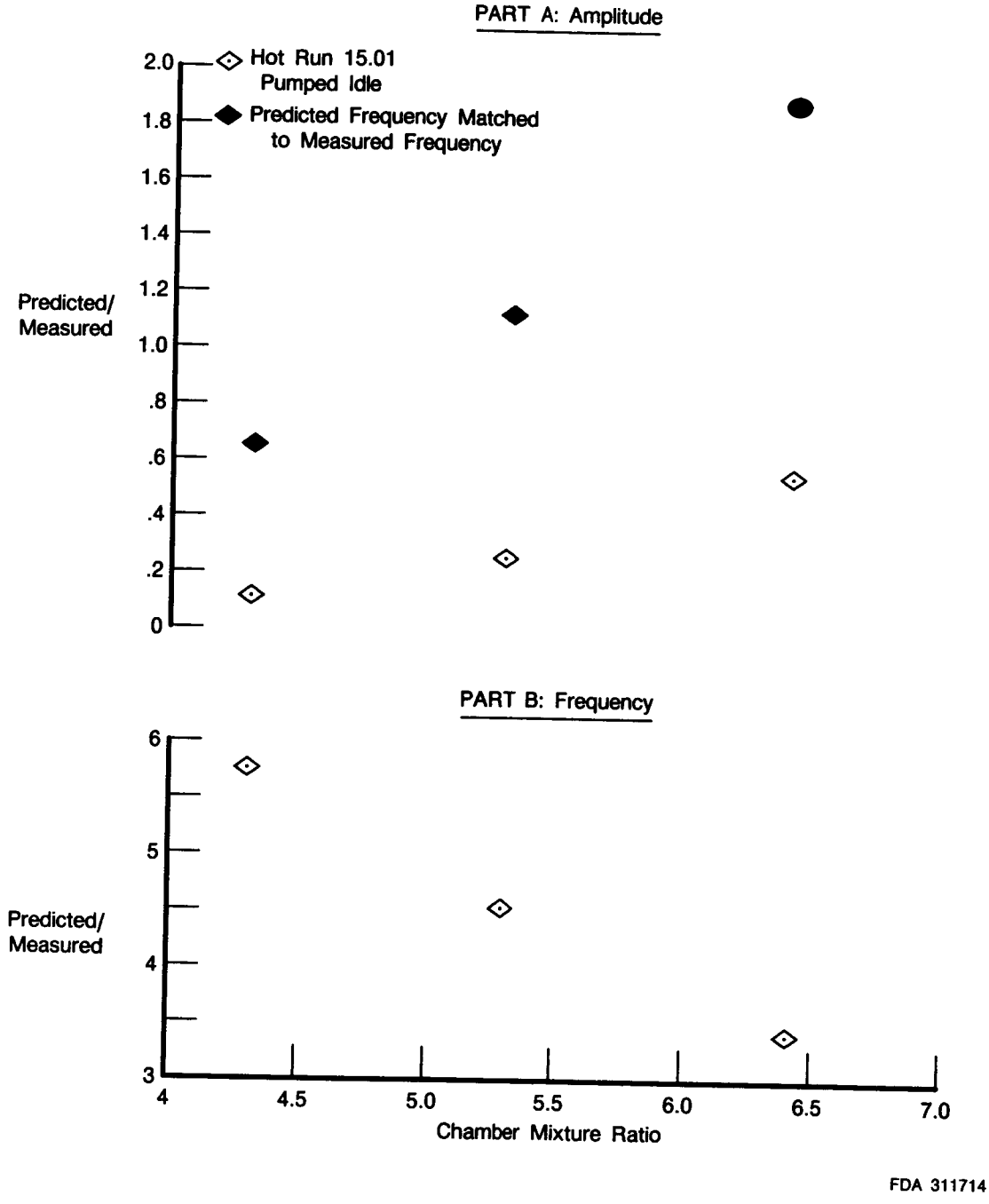

Figure E-30. Predicted Heat Exchanger Pressure Oscillations

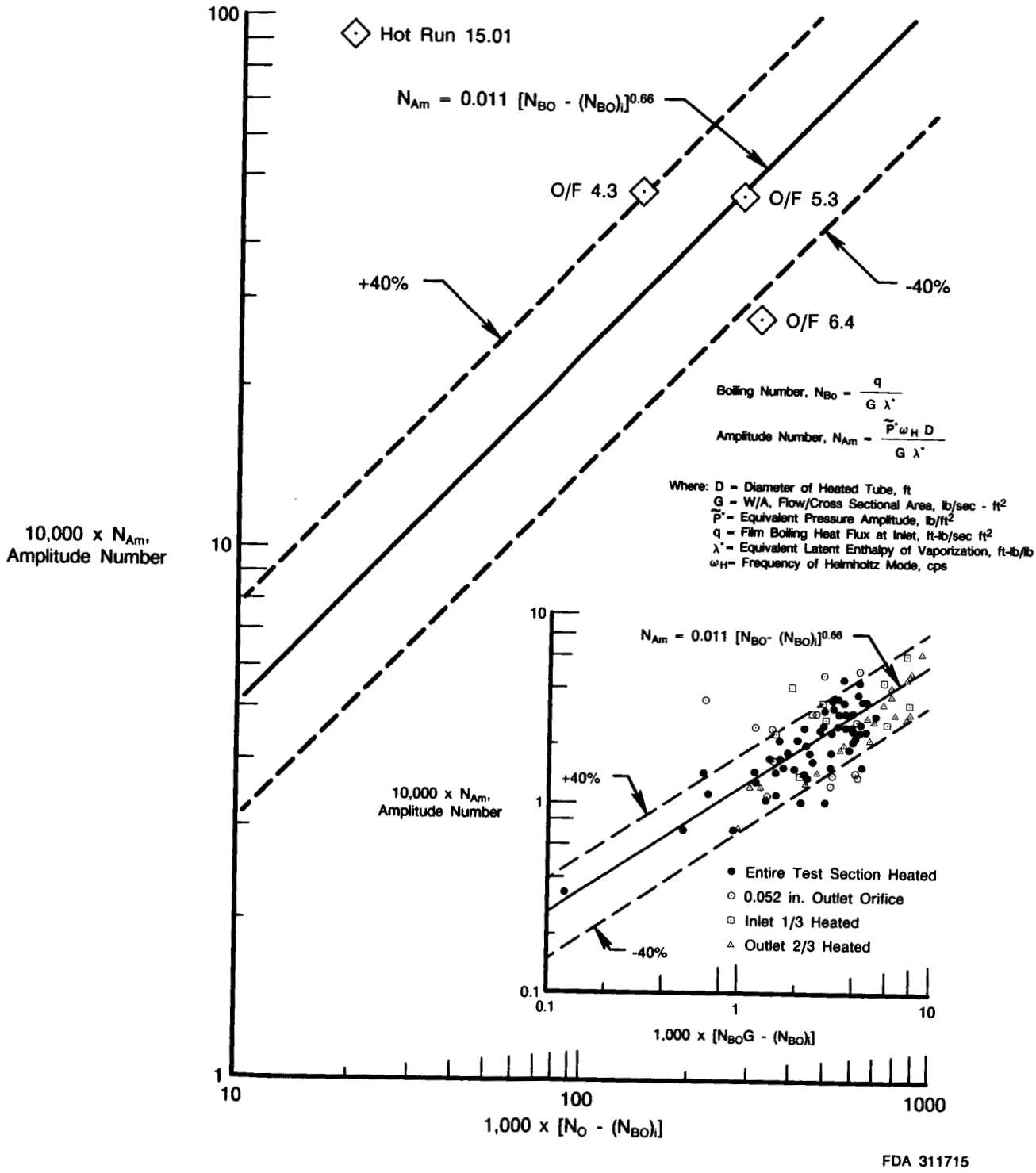

Figure E-31. Heat Exchanger Discharge Pressure Amplitude Number Correlation — Oxidizer Side

APPENDIX F
C* ITERATION MODEL FOR OXIDIZER FLOW CALCULATION

Step

1. Actual Characteristic Velocity Equation:

   (Characteristic Velocity Efficiency, eta*) (Ideal spc c*) =

   $$\frac{\text{(Pc Throat Total) (Chamber Throat Area) (Grav Accel Constant)}}{(\dot{\omega}_{o2} + \dot{\omega}_{Fuel})}$$

2. LOX Flowrate, $\dot{\omega}_{o2}$, As A Function Of C* Iteration:

   Assume $\dot{\omega}_{o2}$ = 30 lb/sec for first estimate and perform calculations (2a) through (2f) below. Compare $\dot{\omega}_{o2}$ assumed with $\dot{\omega}_{o2}$ C* from Step (2f). If $\dot{\omega}o_2$ assumed $\neq$ $\dot{\omega}_{o2}$ C*, repeat Steps (2a) through (2f), where applicable, with new $\dot{\omega}_{o2}$ assumed until values of $\dot{\omega}_{o2}$ assumed = $\dot{\omega}_{o2}$ C*.

   a. $\dot{\omega}_{Fuel}$, lb/sec = Metered Fuel Flow

   b. Mixture Ratio, Rm = $\dot{\omega}_{o2}/\dot{\omega}_{Fuel}$

   c. Pc Throat Total, psia = (Measured Pc) (0.977)

   d. ηc^* = 1.0 (For Pumped Idle Thrust Levels)

   e. Ideal C*, ft/sec = [f(Rm, Pc Throat Total) From Curve]

   f. $\dot{\omega}_{o2}$ c*, lb/sec = $\left[\frac{\text{(Pc Throat Total) (20.75) (32.174)}}{(\eta c^*)\,(\text{IdealC}^*)}\right] - \dot{\omega}_{Fuel}$

      Derived From Step No. 1.

APPENDIX G
LIST OF ACRONYMS

OHE Oxidizer Heat Exchanger

THI Tank Head Idle

PI Pumped Idle

GOV Gaseous Oxidizer Valve

OCV Oxidizer Control Valve

CVV Cavitating Venturi Valve

TBV Turbine Bypass Valve

FVV Fuel Vent Valve

B/M Bill-of-Materials

NAS3-22902 and NAS3-24238
Distribution List
FR 18683-2

		Copies
National Aeronautics & Space Administration Headquarters Washington, D.C. 20546		
Attn:	MSD/S. J. Cristofano	5
	MSD/H. J. Clark	1
	MS/J. B. Mahon	1
	MP/W. F. Dankhoff	1
	MPS/P. N. Herr	1
	MPE/J. B. Mulcahy	1
	MTT/L. K. Edwards	1
	RST/E. A. Gabris	1
	RST/F. W. Stephenson	1
	MV/J. A. Scheller	1
	MOL/C. H. Neubauer	1
	NXG/K. A. Bako	1
	Library	1
National Aeronautics & Space Administration Lewis Research Center 21000 Brookpark Rd. Cleveland, OH 44135		
Attn:	J. P. Couch/MS 500-107	1
	J. A. Burkhart/MS 500-107	5
	L. C. Gentile/MS 500-107	1
	T. P. Burke/MS 500-319	1
	L. A. Diehl/MS 500-200	1
	J. P. Wanhainen/MS 500-219	1
	C. A. Aukerman/MS 500-220	1
	R. L. DeWitt/MS 500-219	All Unassigned Copies
	R. Oeftering/MS 500-107	1
National Aeronautics & Space Administration George C. Marshall Space Flight Center Marshall Space Flight Center, AL 35812		
Attn:	ET01/W. Taylor	1
	EP23/R. H. Counts	1
	EP24/R. J. Richmond	1
	PD13/J. L. Sanders	1

	Copies
Pratt & Whitney Aircraft, GPD P. O. Box 109600 West Palm Beach, FL 33410-9600	
Attn: R. R. Foust	1
W. C. Shubert	1
W. C. Ring	1
P. G. Kanic	5
T. D. Kmiec	1
National Aeronautics & Space Administration Lyndon B. Johnson Space Center Houston, TX 77058	
Attn: EP8/C. Vaughan	1
EP/H. O. Pohl	1
Library	1
National Aeronautics & Space Administration National Space Technology Laboratories NSTL Station, MS 39529	
Attn: H. Guin	1
Jet Propulsion Laboratory Edwards Test Station Section 344 Edwards, CA 93523	
Attn: M. Guenther	1
Library	1
LA Air Force Station Air Force Space Division Dept. AF Los Angeles, CA 90009	
Attn: J. Kasper	1
Library	1
Arnold Engineering Development Center Arnold Air Force Station, TN 37389	
Attn: R. F. Austin	1
Library	1
AEDC/DOT Mail Stop 900 Arnold Air Force Station, TN 37389	
Attn: R. Roepke	2

	Copies
White Sands Test Facility P. O. Drawer MM Las Cruces, NM 88004	
Attn: R. R. Tillett	5
Rockwell International Space Division 12214 Lakewood Blvd. Downey, CA 90241	
Attn: Library	1
F. G. Etheridge/MS SK06	1
Air Force Rocket Propulsion Laboratory Edwards, CA 93523	
Attn: C. Hawk	1
M. V. Rogers	1
Library	1
Bell Aerospace Textron P. O. Box One Buffalo, NY 14240	
Attn: R. W. Riebling	1
L. Carey	1
Rockwell International Rocketdyne Division 6633 Canoga Ave. Canoga Park, CA 91304	
Attn: F. Kirby	1
A. T. Zachary	1
National Aeronautics & Space Administration Langley Research Center Hampton, VA 23365	
Attn: 365/C. H. Eldred	1
365/I. O. MacConochie	1
Library	1
AFAPL Wright Patterson AFB, OH 45433	
Attn: Library	1

	Copies
Aerojet TechSystems Co. P. O. Box 13222 Sacramento, CA 95813	
Attn: L. Schoenman	1
R. W. Michel	1
Library	1
Boeing Company Space Division P. O. Box 868 Seattle, WA 98124	
Attn: W. W. Smith	1
D. Andrews	1
Library	1
General Dynamics/Convair P. O. Box 80847 San Diego, CA 92138	
Attn: W. J. Ketchum	1
Library	1
Lockheed Missiles & Space Company P. O. Box 504 Sunnyvale, CA 94087	
Attn: C. C. Christman	1
Library	1
Marquardt Corporation 16555 Saticoy Street Box 2013 South Annex Van Nuys, CA 91409	
Attn: T. Hudson	1
Library	1
Martin Marietta Corp. P. O. Box 179 Denver, CO 80201	
Attn: J. Bunting	1
Library	1
McDonnell Douglas Astronautics 5301 Bosa Avenue Huntington Beach, CA 92647	
Attn: Library	1